

AMERICAN UNIVERSITY OF BEIRUT

DENTOALVEOLAR EFFECTS DURING MINIMALLY
INVASIVE SURGICALLY ASSISTED RAPID PALATAL
EXPANSION: A FINITE ELEMENT ANALYSIS

By

MARIANE MANSOUR KMEID

A thesis
submitted in partial fulfillment of the requirements
for the degree of Master of Science
to the Department of Dentofacial Medicine
of the Faculty of Medicine
at the American University of Beirut

Beirut, Lebanon
April 25, 2023

AMERICAN UNIVERSITY OF BEIRUT

DENTOALVEOLAR EFFECTS DURING MINIMALLY
INVASIVE SURGICALLY ASSISTED RAPID PALATAL
EXPANSION: A FINITE ELEMENT ANALYSIS

By

MARIANE MANSOUR KMEID

Approved by:



Dr. Joseph Ghafari, Professor and Head
Department of Dentofacial Medicine

Chief of Committee



Dr. Kinan Zeno, Assistant Professor
Department of Dentofacial Medicine

Advisor & Member of Committee



Dr. Samir Moustapha, Associate Professor
Department of Mechanical Engineering

Member of Committee



Dr. Elie Shamma, Associate Professor
Department of Mechanical Engineering

Member of Committee

Date of thesis defense: April 25, 2023

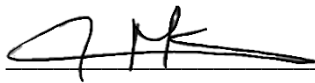
AMERICAN UNIVERSITY OF BEIRUT

THESIS RELEASE FORM

Student Name: Kmeid _____ Mariane _____ Mansour _____
Last First Middle

I authorize the American University of Beirut, to: (a) reproduce hard or electronic copies of my thesis; (b) include such copies in the archives and digital repositories of the University; and (c) make freely available such copies to third parties for research or educational purposes:

- As of the date of submission
- One year from the date of submission of my thesis.
- Two years from the date of submission of my thesis.
- Three years from the date of submission of my thesis.



8/5/2023

Signature

Date

ACKNOWLEDGMENTS

First and foremost, it is a genuine pleasure to express my deep sense of gratitude to Dr. Joseph Ghafari. Your dedication and keen interest, above all your kind approach to help your students had been solely and mainly responsible for completing my thesis. Your timely advice, meticulous scrutiny, and scientific basis allowed this project to flourish and to come to fruition. I am grateful for your invaluable expertise, immense knowledge, and endless patience.

I am also extremely thankful for Dr. Kinan Zeno for all your continuous help and generous advice that was influential in shaping this thesis and for guiding me to reach my full potential. Many thanks for your supervision, patience, and encouragement throughout my thesis.

Additionally, I would like to acknowledge the valuable feedback and advice of Dr. Samir Mustapha and Dr. Elie Shamma.

To Dr. Makram Ammouy, thank you for your time, effort and your essential insights to shape my work, and enrich it immeasurably.

I would also like to express my appreciation for Dr. Ingrid Karam and Dr. Samah Al Mohtar for their hard work and all their contributions in statistical analysis, and 3D modeling respectively, which allowed this research to blossom.

I would also like to express my gratitude to my orthodontic faculty, my fellow residents, in particular Cesar and Firas for their time and moral support.

Thank you, Chris and Perla for being true friends throughout this journey.

Finally, words are not sufficient to express my gratitude to my parents Mansour and Rosy for their support, tremendous understanding, and encouragement in the past few years.

ABSTRACT

OF THE THESIS OF

Mariane Mansour Kmeid

for

Master of Science

Major: Orthodontics

Title: Expansion and dental effects during minimally invasive surgically assisted rapid palatal expansion: a finite element analysis study

Introduction:

Maxillary transverse deficiency is a common problem in all types of malocclusion. The treatment differs relative to the age of the patient. In growing patients, the maxillary suture is not yet well inter-digitated; therefore, rapid palatal expansion is the treatment of choice and is usually associated with suture opening and correction of the deficiency. However, in adults, the suture opening and the expansion are less likely to occur, necessitating an adjunct surgical intervention. A minimally invasive surgical protocol has been introduced, yet the dental effects on the supporting dentition and amount of skeletal expansion are yet to be explored.

Aims:

1. Evaluate the stresses on the teeth and define the setup with the least amount of stress and greatest amount of expansion.
2. Evaluate the effects of adding brackets with different wire sizes on the amount of stress on the teeth and the amount of expansion at the level of the bone.
3. Investigate a potential pattern between amount of stress and expansion with respect to the bone thickness variations between the models.

Methods:

A 3-dimensional model of the maxilla was adapted, and a total expansion amount of 8 mm was applied on the anchor teeth of the tooth-borne expander namely, the first premolars and first molars, and on the 4 mini-screws of the bone-borne expander. Five different clinical setups of the maxilla were simulated: setup 1: control with only a tooth-borne expander, setup 2: tooth-borne expander with sagittal palatal osteotomy, setup 3: tooth-borne expander with sagittal palatal osteotomy and fixed appliances with 0.016*0.022 inch stainless steel arch wire, setup 4: tooth-borne expander with sagittal palatal osteotomy and fixed appliances with 0.019*0.025 inch stainless steel arch wire, and setup 5: bone-borne expander with sagittal palatal osteotomy. The data derived from 13 cadavers were incorporated into each of the setups to simulate individual variation of cortical bone thicknesses at different regions. The stresses on the teeth and the skeletal expansion were recorded and analyzed through finite element analysis. Statistical methods included t-tests, pairwise comparisons tests, and correlation tests for associations among variables.

Results:

The stress was observed in setups 1 and 2 only on the anchor teeth of the RPE. However, in setups 3 and 4, stress was observed on all the teeth, while in setup 5, no stress was observed on the teeth. Moreover, more expansion occurred posteriorly with setups 1, 2, 3, and 4 that decreased gradually towards the incisors. An opposite trend was observed in setup 5. Setup 3 and 4 showed the least amount of stresses at the anchor teeth and the highest amount of expansion posteriorly with only mean differences between the stresses on the central and lateral incisors were statistically significant among all variables. The expansion was statistically significant at the molars and premolars regions with all the setups compared to setup 1 except with setup 5 at the molars region.

In the setups with the tooth-borne expander included, the stresses at the first premolars were positively correlated to the stresses at the first molars with higher amount of stresses observed at the first premolars. The stresses on the teeth were negatively correlated to the expansion, while positively correlated to the cortical bone thicknesses. In addition, the expansion was negatively correlated to the cortical bone thicknesses, but no correlation was seen between these two variables in setup 5.

Conclusion:

The sagittal palatal osteotomy was minimally invasive and efficient in increasing the simulated expansion in a skeletally mature patient by decreasing the resistance to expansion at the mid-palatal suture. The bone-borne expander led to more bony expansion anteriorly rather than posteriorly, with absent stresses on the teeth. In contrast, the tooth-borne expanders resulted in more posterior than anterior expansion. As the cortical bone thickness increased, the expansion decreased and stresses on the teeth increased. As expansion increased, the stresses on the teeth decreased. The results suggest that the optimal posterior expansion would be achieved with a tooth-borne expander combined with a sagittal palatal osteotomy and fixed rectangular arch wires engaged in the maxillary teeth. The 0.016*0.022 inch stainless steel arch wire produced the same effect as the heavier wire (0.019*0.025 inch stainless steel). However, anterior expansion would be accomplished with a bone-bone expander combined with the sagittal palatal osteotomy.

Future research is needed in more diverse facial structures, such as hyper and hypo-divergent facial patterns with variable resistance to expansion from the buttressing bones. Also, time-dependent finite element modeling should better elucidate the progressive response to expansion.

TABLE OF CONTENTS

ACKNOWLEDGMENTS	1
ABSTRACT	2
ILLUSTRATIONS.....	7
TABLES.....	10
INTRODUCTION.....	11
1.1 Definition.....	11
1.2 Prevalence.....	12
LITERATURE REVIEW	13
2.1 Development of the Human Mid-palatal Suture.....	13
2.2 Transverse Maxillary Skeletal Growth.....	14
2.3 Transverse Growth of Maxillary Arches	16
2.4 Etiology	17
2.5 Methods of Assessment	18
2.5.1 Clinical evaluation.....	19
2.5.2 Dental Model analysis	20
2.5.3 Occlusal radiographs/occlusograms	22
2.5.4 Posteroanterior cephalograms.....	23
2.5.5 CBCT evaluation	24
2.6 Management of MTD	26
2.6.1 Age: a critical factor	26
2.6.2 Palatal Expansion in the Primary and Early Mixed Dentition....	28
2.6.3 Palatal Expansion in the Late Mixed Dentition.....	31
2.6.4 Rate of Expansion.....	31
2.6.4.1 Rapid Palatal Expansion	31
2.6.4.2 Slow Palatal Expansion.....	34
2.6.5 Mini-implant Assisted Rapid Palatal Expansion	35
2.6.6 Surgically Assisted Rapid Palatal Expansion	38
2.6.6.1 SARPE Indications	40
2.6.6.2 SARPE Conventional Approaches	41

2.6.6.3	SARPE Minimally Invasive Approaches.....	45
2.6.7	Other Adjunctive Treatment Approach to Facilitate Expansion	48
2.6.8	Structural Effects of Expansion.....	49
2.6.9	Functional Effects of Expansion.....	53
2.6.10	Envelope of Discrepancy: Limits for Dental Expansion	55
2.6.11	Adverse Effects of Expansion.....	56
2.6.11.1	Dental Effects.....	56
2.6.11.2	Periodontal Effects.....	58
2.7	Finite Element Analysis (FEA)	59
2.7.1	Principles and Applications of FEA	59
2.7.2	FEA in Orthodontics.....	60
2.7.3	FEA and Maxillary Expansion	61
2.8	Significance	64
2.9	Specific Objectives	65
MATERIALS AND METHODS.....		67
3.1	Materials	67
3.2	Methods	68
3.2.1	Expansion Setups.....	68
3.2.2	Meshing	73
3.2.3	Finite Element Analysis.....	74
3.2.4	Materials properties	74
3.2.5	Boundary Conditions.....	75
3.2.6	Application of expansion.....	76
3.2.7	Data collection and Export	78
3.3	Statistical Analysis	80
RESULTS.....		81
4.1	Descriptive Data	81
4.1.1	Stress on the teeth	81
4.1.2	Expansion within the different setups	85
4.1.3	Cortical bone thickness in different regions	89
4.2	Comparison of stresses between setups.....	90
4.3	Comparison of expansion between setups.....	90
4.4	Comparisons of stress, bone thickness, and expansion across setups	91
4.5	Correlations between variables within each setup.....	95
DISCUSSION		104

5.1	Strengths	104
5.1.1	Originality of the research	104
5.1.2	Individual variation.....	104
5.1.3	Complete 3D model.....	105
5.2	Model construction	105
5.2.1	Anatomical considerations	105
5.2.2	Variations in loading and expansion	106
5.3	Sagittal Palatal osteotomy	107
5.3.1	Designs	107
5.3.2	Surgical considerations.....	108
5.4	Results and clinical implications	109
5.4.1	Sagittal Palatal Osteotomy.....	109
5.4.2	Greater expansion and stresses	110
5.4.3	Tooth-borne vs bone-borne	111
5.4.4	Thickness	112
5.4.5	Regional differences	112
5.5	Comparison with Other Studies.....	113
5.6	Future Research Tracks and Recommendations.....	116
CONCLUSIONS		117
APPENDIX		119
REFERENCES		122

ILLUSTRATIONS

Figure

2.1. Scanning electron micrographs of mouse embryos (which are very similar to human embryos early in embryogenesis), showing the stages in facial development. A, Before the elevation of the palatal shelves. B, Shelves during elevation. C, Initial fusion of the shelves at a point about one third of the way back along their length. D, Secondary palate immediately after fusion (Proffit, Fields, Larson, & Sarver, 2018).....	14
2.2. Postero-anterior cephalogram showing the location of left Jugale and right Jugale and the corresponding distance between them (J-J).	16
2.3. Extra-oral (A,C) and intra-oral (B,D) photographs of a patient with MTD. Based on clinical evaluation: A, Dark buccal corridors upon smiling. B, Bilateral posterior crossbite. C, Paranasal hollowing. D, High and V-shaped palatal vault.	20
2.4. Determination of skeletal crossbite following removal of dental compensations based on dental casts. A, If transverse dental compensations, usually labial maxillary crown torque and lingual mandibular torque, are visualized as being removed, B, the transverse interarch relationship usually worsens when the discrepancy is of skeletal origin (Marshall et al., 2005).	22
2.5. A, Schematic drawing and B, Postero-anterior cephalogram of the landmarks used to measure the effective maxillary and mandibular widths (Vanarsdall Jr, 1999).	24
2.6. CBCT images of a 12 years 9 months girl. A, Pre-treatment radiograph showing transverse skeletal deficiency and significant dental compensations. B, In diagnosis and treatment planning, when maxillary and mandibular molars were decompensated, the molars resulted in posterior crossbite. C, Post-expansion radiograph showing corrected molar relationship. Patient was expanded with a TADs supported RPE. (Courtesy of Dr. Norman Boucher) (Chung, 2019).	25
2.7. Schematic drawing of the mid-palatal suture based on the degree of maturation. A, In the first stage the suture is short, broad, and Y shaped; B, the course is more sinuous; and C, the course is so heavy that a separation of the two halves of the maxilla would not be possible without fracturing the interdigitated processes (Melsen, 1975).	27
2.8. Schematic drawing of the maturation stages observed in the mid-palatal suture (Angelieri et al., 2013).	28
2.9. Intraoral photograph of the maxillary arch in occlusal view with a removable expander appliance.	29
2.10. Intra-oral photograph of the maxillary arch in occlusal view with a cemented quad-helix appliance used for expansion in a patient in the early mixed dentition.....	30
2.11. Intra-oral photographs of the maxillary arch. A, Haas-type expander and B, hyrax-type expander at the end of the active phase of RPE (Weissheimer et al., 2011).	33
2.12. Diagrammatic representation of the typical skeletal and dental response to rapid (A) versus slow (B) palatal expansion (Proffit et al., 2018).	35
2.13. Intra-oral photographs of the maxillary arch. A, Bone-borne MARPE supported by 4 mini-screws (Celenk-Koca et al., 2018) and B, tooth-bone- borne or hybrid MARPE supported by 2 anterior mini-screw.	37
2.14. Schematic representation of a 2-piece Le Fort 1 osteotomy with the maxillary segments in a widened transverse dimension (O. H. Junior et al., 2017).	40

2.15. Different human skull views: A, frontal view; B, lateral view and C, occlusal views. 1, anterior mid-cut; 2, bilateral cuts from the piriform rim to the pterygoid plate; 3, mid-palatal cut; 4, pterygomaxillary disjunction, and 5, 3-pieces segmental osteotomies (Adapted from (Sinelnikov, Sinelnikov, & Sinelnikov, 1996)).	43
2.16. Insertion of a 2 mm osteotome to perform the horizontal osteotomy line in the maxillary lateral wall; this technique eliminates the need to make a mucoperiosteal flap for exposing the underlying bone, unlike what is usually done in the traditional open technique. A, Sketch and B, Intraoperative view (Morselli, 1997).	46
2.17. Surgical field when the osteotomies have been completed (Hernandez-Alfaro et al., 2010).	47
2.18. Intra-oral photographs of the maxillary arch. A, corticotomy in the palate; B, a periodontal dressing was used to promote wound healing; C, Hyrax rapid maxillary expansion device was placed 1 week after surgery (Luxi et al., 2017).	48
2.19. Intra-oral photographs of the maxillary arch with the MARPE in place and minimally invasive surgical procedure to reduce suture resistance: A, day of installation; B, after corticopuncture procedure (Suzuki et al., 2018).	49
2.20. Occlusal view of maxillary expansion illustrating mid-palatal suture opening with greatest separation occurring anteriorly, lateral rotation of palatal halves, bony remodeling of maxillary elements, and lateral/ rotational movement of the maxillary teeth (Weissheimer et al., 2011).	50
2.21. Intra-oral photographs. A, frontal view prior expansion; B, frontal view after expansion and C, lateral view after expansion. Note the bite opening because of the premature dental contact at the first molar due to extrusion and buccal tipping.	52
2.22. Envelopes of discrepancy for the transverse dimension of the maxilla (A) and mandible (B). The inner circle establishes the limits of orthodontic treatment alone; the middle circle exhibits the limits of orthodontic treatment combined with growth modification; and the outer circle illustrates the limits with orthodontics and surgical procedures (Vanarsdall Jr & Blasi Jr, 2017).	56
3.1. A, lateral view of the 3D model of the maxillary arch with 1, buccal molars region; 2, buccal premolars region and 3, buccal incisors region. B, occlusal view of the maxillary arch with 4, palatal incisors region; 5, palatal premolars region and 6, palatal molars region.	68
3.2. 3D model of the maxilla, occlusal views of all the different setups. A, Setup 1: RPE + no cut (control); B, Setup 2: RPE + SARPE cut; C, Setup3: RPE + SARPE cut + 0.016*0.022 SS AW; D, Setup 4: RPE + SARPE cut + 0.019*0.025 SS AW and E, Setup 5: MARPE + SARPE cut.	69
3.3. Different views of the sagittal palatal osteotomy captured from ScanIP software. A, axial view; B, coronal view; C, sagittal view of the osteotomy starting anteriorly directly distal to the nasopalatine foramen and D, sagittal view with different masks.	71
3.4. A, brackets and wires imported as STL files; B, fixed appliances were adjusted in size and position using the position and orientation tool and C, fixed appliances were accurately positioned and well centered on all the teeth after the wire was divided between the central incisors into right and left segments.	72
3.5. Occlusal view of the 3D model of the maxilla with the four rectangular areas (delineated with white arches) representing the mini-implants which were created in the palatal region to simulate the MARPE.	73
3.6. A, occlusal view of the meshed model and B, lateral view of the meshed model.	74

3.7. Boundary conditions: models constrained from translation and rotation at areas of attachments of the maxilla to adjacent bones: zygomatic, palatal and sphenoid. A, superior view; B, posterior view, and C, lateral view.	75
3.8. A, Crowns of the first premolar and molar selected. B, Occlusal view of the maxillary arch with the selected regions of the RPE boundary conditions.	76
3.9. A, nodes selected of the first premolar and first molar; B, the direction of the force through the palatal surfaces of the crowns of the teeth; C, occlusal view of the maxilla with the opposite forces in the transverse direction on the anchor teeth of the RPE; D, nodes selected at the rectangular areas simulating the mini-screws of the MARPE, and E, opposite direction of forces simulating the expansion using MARPE.	77
3.10. Selection of element sets. A, PDL of the first premolar and B, PDL of the first molar.	78
3.11. Lateral view of the right side of the model with selected nodes in the 3 regions to measure the amount of expansion.	79
4.1. Von mises stress distribution on the PDL of the teeth in setup 1, buccally, occlusally and palatally respectively. The stresses were at the first premolars and first molars (5.05 MPa and 4.85, respectively) higher on the buccal side than on the palatal side. On the buccal surface, the stresses were concentrated on the middle and cervical thirds of the PDL surface, while on the palatal side the stresses were distributed all over the PDL surface.	82
4.2. Von mises stress distribution on the PDL of the teeth in setup 2, buccally, occlusally and palatally respectively. The stresses were at the first premolars and first molars (4.99 MPa and 4.82 MPa, respectively) with similar pattern of distribution to setup 1.	83
4.3. Von mises stress distribution on the PDL of the teeth in setup 3, buccally, occlusally and palatally respectively. The stresses were distributed on all the teeth and were highest at the first premolars and first molars (4.87 MPa and 4.70 MPa, respectively), with similar pattern of distribution to setups 1 and 2, but of less intensity.	83
4.4. Von mises stress distribution on the PDL of the teeth in setup 4, buccally, occlusally and palatally respectively. The stresses were distributed on all the teeth and were highest at the first premolars and first molars (4.89 MPa and 4.71 MPa, respectively), with similar pattern of distribution to setups 1 and 2, but of less intensity.	84
4.5. Von mises stress distribution on the PDL of the teeth in setup 5. No stress was observed on the teeth.	85
4.6. Expansion in setup 1.	86
4.7. Expansion in setup 2.	87
4.8. Expansion in setup 3.	87
4.9. Expansion in setup 4.	88
4.10. Expansion in setup 5.	88
4.11. A bar graph representing the expansion at the molars (M), premolars (PM) and incisors (IN) in all setups.	89
4.12. A graph representing the effect of expansion at the premolars (PM) region on the stress at the first premolars (PM1) across the different setups.	93
4.13. A graph representing the effect of expansion at the molars (M) region on the stress at the first molars (M1) across the different setups.	93
4.14. A bar graph showing the mean expansion at the premolars (PM) with respect to the mean stresses at the first premolars (PM1) across the different setups.	94
4.15. A bar graph showing the mean expansion at the molars (M) with respect to the mean stresses at the first molars (M1) across the different setups.	94

TABLES

Table

3.1. The different included setups.	70
3.2. Material properties of anatomical components used in orthodontic FEA study (Field et al., 2009; Kojima et al., 2012; Lim et al., 2003).....	75
4.1. Descriptive statistics for the stress on the first premolars and first molars.	81
4.2. Descriptive statistics for the stresses on all teeth for setups 3 and 4.	82
4.3. Descriptive statistics for the expansion at the molars (M), premolars (PM) and incisors (IN).	86
4.4. Descriptive statistics of the cortical bone thickness in different regions.	89
4.5. Pairwise comparison (Wilcoxon test) of the stresses of the first premolars.....	90
4.6. Pairwise comparison (Wilcoxon test) of the expansion	90
4.7. Results of the Friedman test between the different setups 1,2,3,4 and 5.....	91
4.8. Results of the paired t-test to compare the differences between stresses on the first premolars (PM1) and molars (M1) and between cortical bone thicknesses at the molar, premolar, and incisor regions.	91
4.9. Results of the paired t-test to compare the different variables between setups 3 and 4.	92
4.10. Correlation of the stress, expansion, and cortical bone thickness for setup 1.	97
4.11. Correlation of the stress, expansion, and cortical bone thickness for setup 2.	98
4.12. Correlation of the stress, expansion, and cortical bone thickness for setup 3.	101
4.13. Correlation of the stress, expansion, and cortical bone thickness for setup 4.	102
4.14. Correlation of the expansion and the cortical bone thickness for setup 5.	103

CHAPTER 1

INTRODUCTION

1.1 Definition

Maxillary transverse deficiency (MTD) is a dentoskeletal problem found in all types of malocclusions. It is encountered in children, adolescents and adults and it is frequently seen in non-syndromic and syndromic patients including cleft patients (M. Koudstaal, Wolvius, Schulten, Hop, & Van der Wal, 2009). It is of primary importance to have an appropriate transverse dimension of the maxillary arch in order to ensure a stable occlusion and to significantly enhance facial proportions and esthetics.

Clinically, MTD manifests usually as a complete crossbite (unilateral or bilateral), high-vaulted and V-shaped palate, anterior teeth crowding and visible dark buccal corridors when smiling (Zawiślak, Gerber, Nowak, & Kubiak, 2020).

The presence of discrepancies in the transverse dimension frequently complicates patient treatment. Diagnosis of such discrepancies may be difficult for orthodontists trained to evaluate malocclusions and other dentofacial deformities based on clinical manifestations in the static state. Such an approach may have an impact on the treatment plan by camouflaging skeletal deformities solely through orthodontic tooth movement, preventing the practitioner from establishing treatment objectives required to achieve the desired stable and functional occlusion. To properly diagnose transverse deficiency or excess, the orthodontist must be able to visualize the ultimate sagittal and vertical repositioning of skeletal components available through orthopedic or surgical interventions. The establishment and sequencing of treatment objectives

have a significant impact on diagnosis and planning for the transverse dimension as for the other dimensions. (Jacobs, Bell, Williams, & Kennedy III, 1980).

1.2 Prevalence

MTD is estimated to affect 8 to 18% of patients undergoing orthodontic treatment in the deciduous and mixed dentitions. According to research, there is a higher prevalence of unilateral crossbite combined with a lateral shift of the mandible. The prevalence of MTD in the adult population or in skeletally mature subjects; however, cannot be determined from the literature. (Marshall, Southard, & Southard, 2005; Sousa et al., 2014).

A survey data done in the US revealed that around 9.4% of the population have a posterior crossbite, which is most frequently caused by a narrow maxilla, but Proffit et al have reported that 30% of adults seeking consultation for treatment of dentofacial deformity have a component of MTD (L'tanya, White Jr, Proffit, & Turvey, 1997).

CHAPTER 2

LITERATURE REVIEW

2.1 Development of the Human Mid-palatal Suture

Three palatal processes form, separating the nasal cavity from the mouth. The primary palate (median palatine process) and secondary palate are involved in these processes (two lateral palatine processes). In week 5, the primary palate develops from the fusion of the two medial nasal prominences. When the dorsum of the tongue withdraws and is no longer pressed against the nasal septum, the secondary palate develops (week 7). During the seventh week of palatogenesis, the lateral palatine processes elongate and move to a horizontal position superior to the tongue. They also fuse to the primary palate and nasal septum, forming a horizontal shelf. Fusion takes place between weeks 7 and 12 (Figure 2.1).

The premaxilla is formed by membranous bone in the primary palate, while bone from the maxilla and palatine bone extends into the lateral palatine processes to form the hard palate. The soft palate and uvula are not ossified and extend beyond the nasal septum. The mid-palatal suture is made up of three sections. These include the interpremaxillary, maxillary, and interpalatine parts (Revelo & Fishman, 1994).

Latham discovered a well-established interpremaxillary suture in the 47-day-old embryo (primary palate). The first signs of secondary palate sutural formation, in which the maxillary and palatine parts of the mid-palatal suture form, appear around the 10th week of life. By the twelfth week of life, a distinct intermaxillary suture has developed (Latham, 1971).

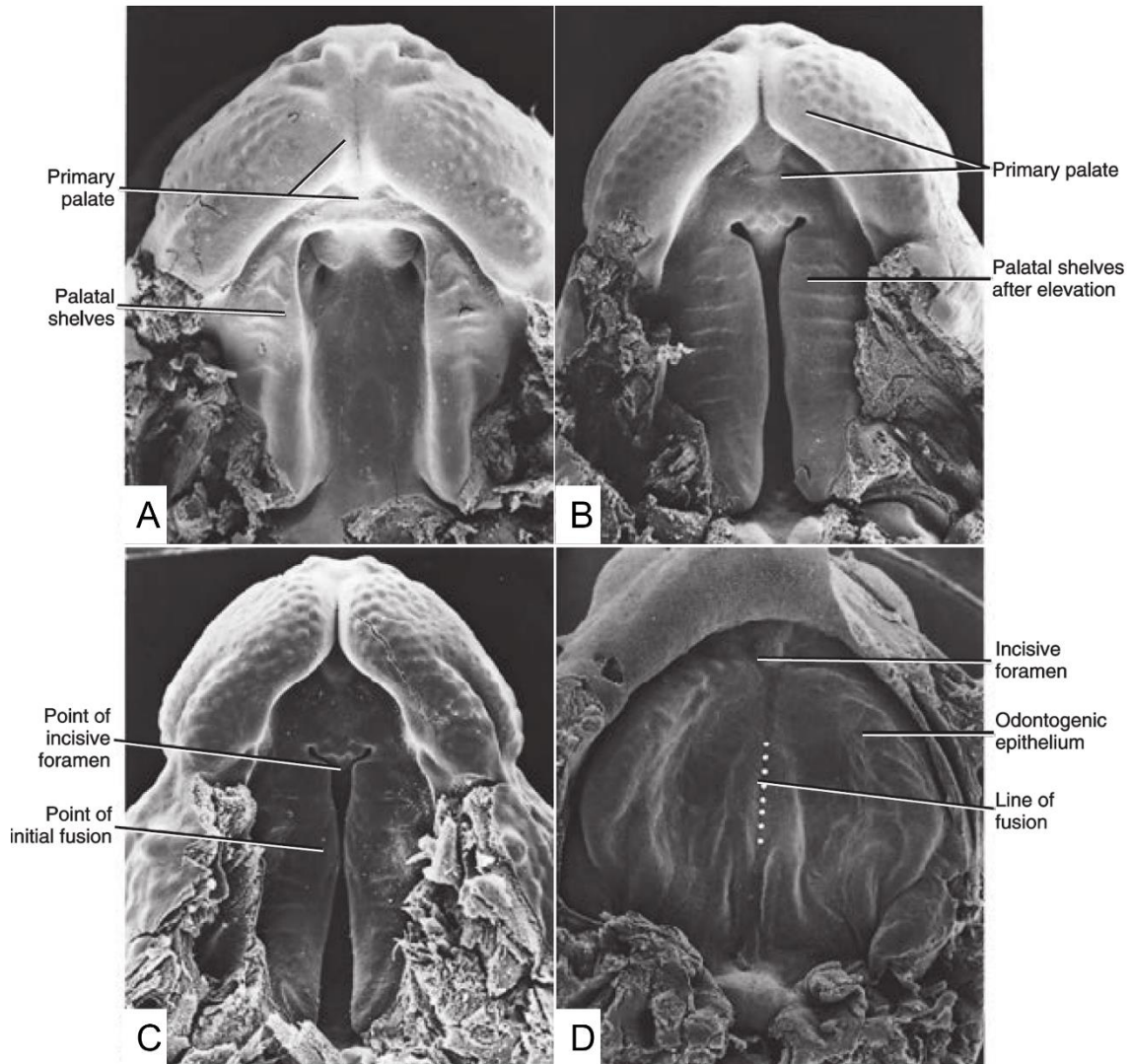


Figure 2.1: Scanning electron micrographs of mouse embryos (which are very similar to human embryos early in embryogenesis), showing the stages in facial development. A, Before the elevation of the palatal shelves. B, Shelves during elevation. C, Initial fusion of the shelves at a point about one third of the way back along their length. D, Secondary palate immediately after fusion (Proffit, Fields, Larson, & Sarver, 2018).

2.2 Transverse Maxillary Skeletal Growth

The sutural and periosteal components of maxillary growth are distinct.

Frontomaxillary, lacrymomaxillary, nasomaxillary, ethmoidomaxillary, zygomaticomaxillary, intermaxillary (midpalatal), and vomeromaxillary sutures are involved in maxillary growth. Bjork and Skieller studied the maxillary transverse

growth of 9 boys who had implant pins inserted intra-orally at various locations. From the age of four to adulthood, annual posteroanterior (PA) and lateral cephalograms were performed. They discovered that sutural growth accounts for the majority of transverse skeletal growth in the maxillary molar region, with periosteal growth accounting for a small amount (bone remodeling). Furthermore, sutural growth was found to be greater in the molar region than in the incisor region. As a result, the two halves of the maxilla rotated. (Björk & Skieller, 1977).

Ricketts et al. reported transverse growth changes on PA cephalograms from ages 9 to 16, for both genders (Figure 2.2). The distance between the left and right Jugale (J-J) increased from 62 mm to 66.2 mm, indicating an increase in maxillary skeletal width (0.6 mm per year). The J point was found at the jugal process, which is the intersection of the outline of the maxillary tuberosity and the zygomatic buttress (Ricketts, Roth, Chaconas, Schulhof, & Engel, 1982). In a later study, Ricketts and Grummons reported in males, from age 3 to 21, an increase in J-J distance from 55mm to 73 mm or 1 mm per year (Ricketts & Grummons, 2003).

Cortella et al. found that males had larger maxillary transverse dimensions than females in a longitudinal study of PA cephalograms of subjects aged 5 to 18. Furthermore, females' maxillary transverse growth (J-J) stopped around the age of 14, whereas males' continued until around the age of 18 (Cortella, Shofer, & Ghafari, 1997).

Wagner and Chung discovered a connection between transverse growth and vertical facial type. Dolichofacial (high mandibular plane angle) subjects had narrower maxillary (J-J) widths than brachyfacial (low mandibular plane angle) subjects at age 6. This pattern continued until the age of 18 (Wagner & Chung, 2005).

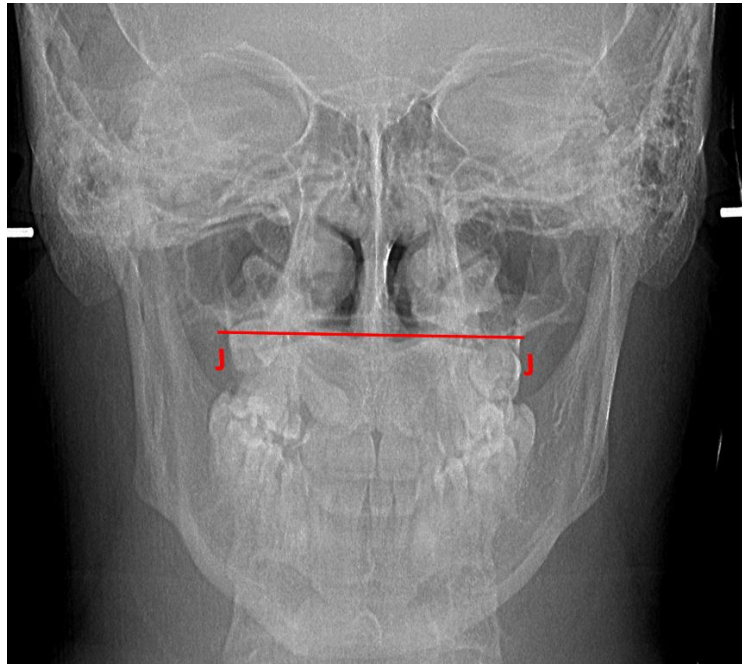


Figure 2.2: Postero-anterior cephalogram showing the location of left Jugale and right Jugale and the corresponding distance between them (J-J).

2.3 Transverse Growth of Maxillary Arches

Moyers et al. reported the arch width development of the maxilla and mandible on canines, premolars, and molars from age 6 to 18 in males and females in their longitudinal study. They discovered that for girls, the mandibular intermolar width at the first molars was established at age 12 and did not change after that; for boys, the increase was only 1mm to age 18. For girls, the maxillary intermolar width was established at age 12; for boys, it increased by 1.4mm from 12 to 18. The intercanine width for maxillary and mandibular arches was determined at the age of 12 for both genders. (Moyers, 1976).

Another longitudinal growth study on transpalatal width was conducted using measurements from the gingival margin of the first molar's lingual groove to the contralateral side. McNamara and Brudon found that the transpalatal width increased by

only 2.6mm between the ages of 7 and 15. There was no change in transpalatal width after the age of 12 (McNamara, Brudon, & Kokich, 2001).

2.4 Etiology

Understanding the etiology of malocclusion is critical for the success of orthodontic treatment, because eliminating the cause is required before correcting the problem (Sousa et al., 2014).

Genetics, environmental factors, and habits are all possible causes. Posterior crossbite is frequently caused by transverse maxillary skeletal deficiency, which can be congenital, developmental, traumatic, or iatrogenic such as cleft palate repair. Asymmetric growth of the maxilla or mandible, discrepant widths of the basilar maxilla and mandible, premature loss or prolonged retention of primary teeth, crowding, abnormalities in eruption sequence, impaired nasal breathing during critical growth periods, tooth anatomy aberrations, and improper temporomandibular joint function are other causes.

Oral digit habits have also been implicated as an etiologic factor. However, at least one study found no difference in the prevalence of sucking habits when examining patients with or without spontaneous correction of a posterior crossbite (Marshall et al., 2005).

Several other etiologies have been mentioned in the literature such as:

- Obstructive sleep apnea
- Muscular (Duchene muscular dystrophy)
- Non-syndromic palatal synostosis

- Syndromes (Klippel-Feil syndrome, cleft lip and palate, Marfan syndrome, craniosynostosis, congenital nasal pyriform aperture stenosis, osteopatia striata, Treacher Collins) (Suri & Taneja, 2008)

2.5 Methods of Assessment

The evaluation of facial growth and the development of dental occlusion is part of the process of diagnosing orthodontic abnormalities that, if prevented or treated, would provide patients with measurable benefits. Orthodontists have recognized that maxillary transverse deficiencies contribute significantly to many malocclusions (Sawchuk, Currie, Vich, Palomo, & Flores-Mir, 2016). Accurate diagnosis of maxillary transverse deficiencies is critical for long-term periodontal stability, as an undiagnosed discrepancy may result in adverse periodontal effects and gingival recession (Vanarsdall Jr, 1999). There is a scarcity of strong evidence and high-quality diagnostic studies assessing the sensitivity and specificity of such diagnostic tools. This could be due in part to a lack of scientific literature supporting the identification of a true gold standard diagnostic tool for evaluating skeletal transverse deficiencies (Sawchuk et al., 2016).

The determination of MTD is the first step in the case selection process. MTD diagnosis is difficult, unlike discrepancies in the vertical and anteroposterior dimensions. There is a much literature on the various methods used to diagnose this condition. For an accurate assessment, clinical evaluation, model analysis, occlusograms, and radiographic measurements have been recommended (Suri & Taneja, 2008).

2.5.1 Clinical evaluation

The assessment of facial symmetry and occlusal harmony at the chairside is critical. Facial and intraoral photography should be used to supplement the chairside examination but should not be used to replace findings obtained directly from the patient (Figure 2.3) (Marshall et al., 2005).

Clinical evaluations consider the shape of the palatal vault, the width of the buccal corridors when smiling, the occlusion, and the primary breathing pattern (nasal or oral). MTD is often characterized by abnormally wide buccal corridors, paranasal hollowing, or small alar bases. The thickness of the soft tissues must be measured. Anteroposterior and vertical maxillary hypoplasias are much easier to diagnose clinically due to visible soft tissue alterations. When anteroposterior and vertical maxillary dysplasias are present, the diagnosis of transverse skeletal discrepancy cannot be made solely on clinical evaluation because they can clinically conceal transverse deficit.(Sawchuk et al., 2016). Unilateral or bilateral crossbite, severe crowding, a V-shaped or an hourglass shaped occlusion, and a high palatal vault are additional visual parameters that can help the practitioner make the first determination of MTD in a patient. Another factor to consider is a mandibular shift during closure. This is frequently caused by a chin deviation with a unilateral crossbite. It may be necessary to use a muscle deprogramming device, such as a bite plate, for a few days to determine the nature of a shift. Adults with established muscular kinesthetic memory and proprioceptive influences require these devices more frequently. A deprogramming device of this type allows the muscles to move the mandible in coordinated function that is unaffected by deflective tooth contacts.(Dawson, 1995).



Figure 2.3: Extra-oral (A,C) and intra-oral (B,D) photographs of a patient with MTD. Based on clinical evaluation: A, Dark buccal corridors upon smiling. B, Bilateral posterior crossbite. C, Paranasal hollowing. D, High and V-shaped palatal vault.

2.5.2 *Dental Model analysis*

Study models should be used to thoroughly assess the arch form and the shape and make specific measurements to evaluate for MTD. Several indexes have been proposed by various authors to measure lateral discrepancies. The most common include the indices of Pont, Linder-Harth, and Korkhaus (Rakosi, Jonas, & Graber, 1993). These indices provide a starting point for diagnosing MTD, although they are population-specific and not entirely trustworthy. It can be inaccurate to estimate the size of a posterior transverse discrepancy by comparing a patient's maxillary and mandibular intermolar width to published "norms" unless dental compensations have first been

eliminated or at least visualized as having been eliminated. Other techniques can be utilized to assess arch form and tooth inclinations as a result of the widespread usage of digital models in everyday clinical practice. It is possible to distinguish between dental and apical base skeletal MTD with more accuracy by analyzing the buccolingual inclination of posterior teeth. For improved visibility, the digital models can be examined in the desired cross-sections. These digital models can also produce occlusogram images, which show how the maxillary and mandibular arches are coordinated (Suri & Taneja, 2008).

Counting the number of posterior teeth in crossbite may help distinguish between skeletal and dental differences; if there are two or more posterior teeth in crossbite, the discrepancy is skeletal. Although easy to implement, this rule could be deceptive. As previously indicated, even in the absence of posterior teeth in crossbite, substantial skeletal transverse discrepancies might be concealed by posterior dental compensations (Figure 2.4). The transverse discrepancy is likely dental in origin and can be corrected with dental movement alone if the physician can picture eliminating transverse compensations (uprighting the molars) on the casts and the posterior transverse interarch relationship improves. Therefore, if the posterior transverse interarch relationship worsens after visually deleting these compensations from the casts, the discrepancy is probably of skeletal origin (Marshall et al., 2005).

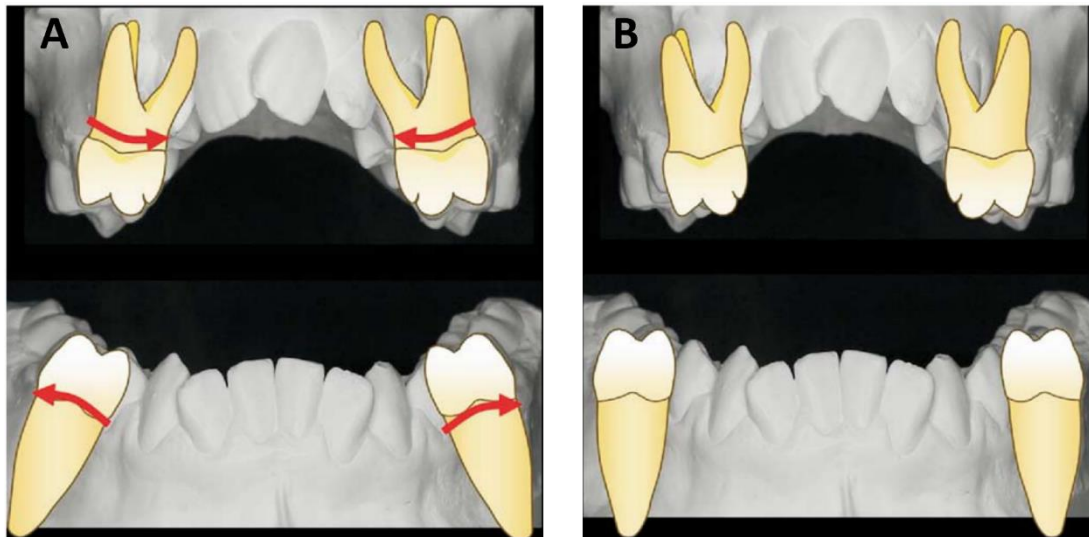


Figure 2.4: Determination of skeletal crossbite following removal of dental compensations based on dental casts. A, If transverse dental compensations, usually labial maxillary crown torque and lingual mandibular torque, are visualized as being removed, B, the transverse interarch relationship usually worsens when the discrepancy is of skeletal origin (Marshall et al., 2005).

Another factor that must be considered is whether the MTD is relative or absolute. This is required for determining sagittal deviations (especially Class III malocclusion). An effort is made to articulate and align the models in Angle Class I molar and canine relationship in order to assess arch coordination. According to relative MTD, the apparent deficit is caused by a sagittal plane misalignment of either the maxilla or both jaws. Absolute MTD implies a real horizontal width deficit. They are frequently associated with open-bite anomalies or Class II malocclusions in the skeleton. The patient's jaw may be held in a position during a simulated Class I relationship that makes palatal constriction obvious and visible. (Jacobs et al., 1980).

2.5.3 Occlusal radiographs/occlusograms

Lehman et al recommended a palatal or an occlusal radiograph as an essential tool to evaluate the ossification of the mid-palatal suture (Lehman Jr, Haas, & Haas,

1984). This, however, is unreliable because of the superimposition of other bony structures on the mid-palatal suture and the lack of adequate visualization of the posterior part of the intermaxillary suture. This is relevant because histologic studies have shown that obliteration of the suture is more common in the posterior region of the intermaxillary suture (W. H. Bell & Epker, 1976).

2.5.4 *Posteroanterior cephalograms*

Betts et al proposed that posteroanterior cephalograms are the most accessible and reliable method of identifying and evaluating transverse skeletal discrepancies between the maxilla and the mandible (Betts, Vanarsdall, Barber, Higgins-Barber, & Fonseca, 1995). Using cephalometric landmarks as described by Ricketts, they presented 2 methods for quantification of the MTD: maxillomandibular width differential and maxillomandibular transverse differential index (Figure 2.5) (Ricketts, 1981).

These methods have been criticized because the transverse discrepancy between the maxilla and the mandible is measured on bony landmarks that are greatly separated from the dentition and the apical bases. In addition, there was no consensus on what the norms of transverse skeletal widths (Jugale-Jugale, Antigonian-Antigonian / J-J, AG-AG) are for males and females determined from PA cephalogram with several studies showing different values. Nevertheless, the difficulties for landmark identification of J and AG on a PA cephalogram posed other problems. Therefore, this analysis was not sensitive enough to detect the transverse problems (Chung, 2019; Suri & Taneja, 2008).

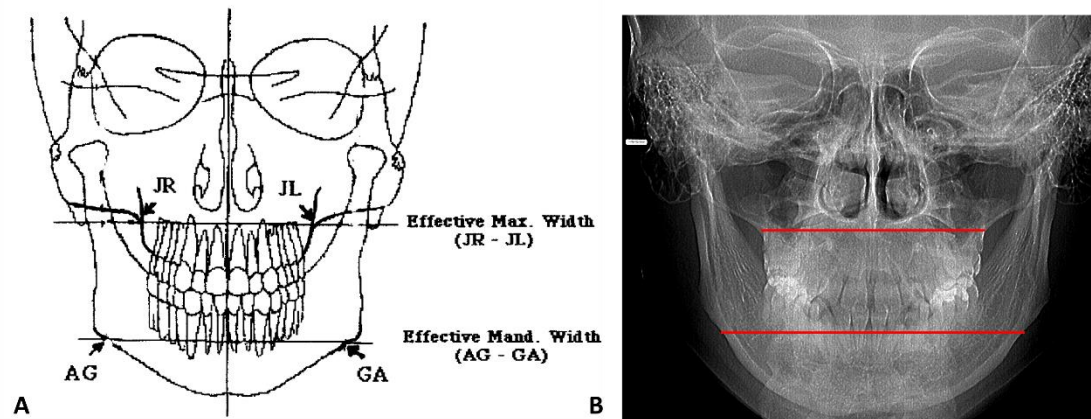


Figure 2.5: A, Schematic drawing and B, Postero-anterior cephalogram of the landmarks used to measure the effective maxillary and mandibular widths (Vanarsdall Jr, 1999).

2.5.5 CBCT evaluation

The majority of studies examining the transverse skeletal effects of maxillary expansion used traditional cephalometric analysis with posteroanterior radiographs, occlusal views, or dental casts. The inherent limitations of all planar two-dimensional (2D) projections, such as magnification, distortion, and difficulties in landmark identification and superimposition of anatomical structures, yield images with low accuracy and reliability, which explains why these methods have been criticized. The advent of 3-dimensional imaging techniques are the most recent tool for diagnosis that have enabled an accurate visualization of the craniofacial region. It allows for evaluation of the spatial relationships of various areas of the jaws (Macchi, Carrafiello, Cacciafesta, & Norcini, 2006).

Because of its diagnostic advantages over traditional 2-dimensional imaging for orthodontic treatment planning, the use of cone-beam computed tomography (CBCT) in clinical practice has increased over the last decade. Its high potential for evaluating maxillary structures has been confirmed, owing to its benefits such as high resolution

and accuracy (only about 2% magnification), precision, non-invasiveness, lower effective radiation dose, and shorter acquisition times (60 s) (Camps-Perepérez, Guijarro-Martínez, Peiró-Guijarro, & Hernández-Alfaro, 2017).

CBCT can produce scans that allow the clinician to perform a 3-dimensional evaluation of the apical bases, including horizontal sections at various levels. These images can assist the clinician in performing an accurate and detailed analysis of the nature and location of the discrepancy, including asymmetries. Therefore, the transverse dimension of dentofacial structures can be visualized and measured without being obstructed by other structures (Figure 2.6). As a result, the widths of the maxillary and mandibular basal bones, as well as their relationship, the buccolingual inclination of each whole tooth, and their root positions in the alveolar bone, can be visualized and analyzed, allowing for an accurate diagnosis. In addition, CBCT may allow the development of a qualitative or quantitative assessment of mid-palatal suture maturation to assist with the decision about whether conventional or surgically assisted maxillary expansion is more appropriate (Chung, 2019; Grünheid, Larson, & Larson, 2017; Suri & Taneja, 2008).

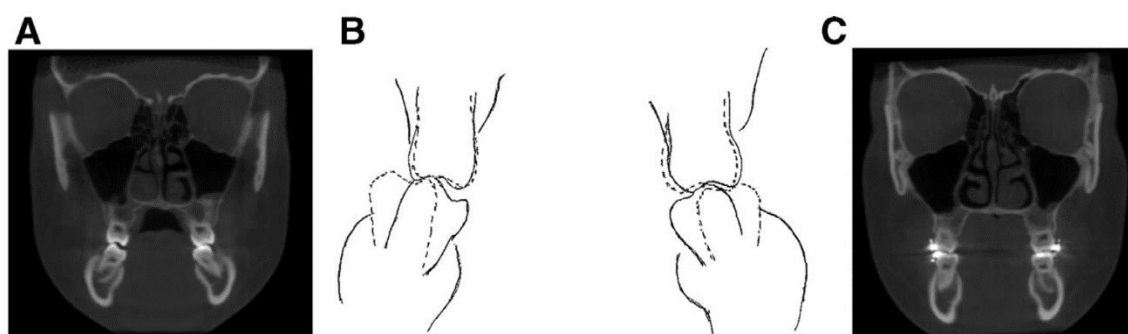


Figure 2.6: CBCT images of a 12 years 9 months girl. A, Pre-treatment radiograph showing transverse skeletal deficiency and significant dental compensations. B, In diagnosis and treatment planning, when maxillary and mandibular molars were decompensated, the molars resulted in posterior crossbite. C, Post-expansion radiograph showing corrected molar relationship. Patient was expanded with a TADs supported RPE. (Courtesy of Dr. Norman Boucher) (Chung, 2019).

2.6 Management of MTD

The treatment of choice is determined by a variety of clinical factors, including the extent of correction required, whether skeletal or dentoalveolar correction is indicated, and the perceived efficacy of expansion based on treatment timing. Failure to correctly identify key clinical signs and provide individual assessments to determine a patient's best expansion treatment option can result in iatrogenic side effects and comorbidities (Isfeld, Lagravere, Leon-Salazar, & Flores-Mir, 2017).

2.6.1 Age: a critical factor

The optimal time for treatment of a maxillary transverse deficiency and the appropriate expansion method has been questioned. Many methods have been used to evaluate the relationships between palatal suture expansion and various indicators. Notably, these indicators include chronological age, skeletal age (assessed by skeletal maturity indicators on hand-wrist radiographs or cervical vertebral maturation indicators on lateral cephalograms), suture morphology, midpalatal suture maturation, and midpalatal suture density ratio (Jia, Zhuang, Zhang, Bian, & Li, 2022).

The literature, however, does not specify unequivocally the age limit, up to which orthodontic maxillary expansion is effective and free of complications. Most authors point towards 14–18 years of age as the upper limit of any orthodontic midpalatal interventions (Zawiślak et al., 2020).

The morphology of the midpalatal suture changes during growth. According to this change, the postnatal development could be divided into three stages (Figure 2.7). During the first stage, covering the infantile period, the suture was very broad and Y

shaped, with the vomerine bone placed in a V-shaped groove between the two halves of the maxilla. During the second stage, which corresponds to the juvenile period, the suture was found to be more wavy. In the third stage, the adolescent period, the suture was characterized by a more tortuous course with increasing interdigitation (Melsen, 1975).

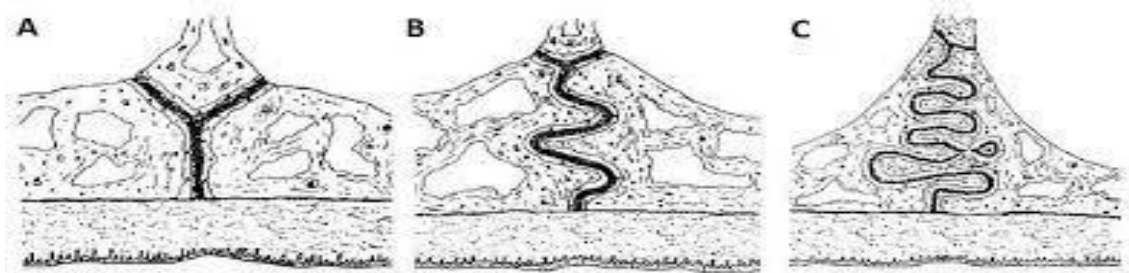


Figure 2.7: Schematic drawing of the mid-palatal suture based on the degree of maturation. A, In the first stage the suture is short, broad, and Y shaped; B, the course is more sinuous; and C, the course is so heavy that a separation of the two halves of the maxilla would not be possible without fracturing the interdigitated processes (Melsen, 1975).

A novel classification method for individual assessment to define the radiographic stages of midpalatal suture maturation using CBCT images (Figure 2.8). Five stages of maturation of the midpalatal suture were identified and defined: stage A, straight high-density sutural line, with no or little interdigitation; stage B, scalloped appearance of the high-density sutural line; stage C, 2 parallel, scalloped, high-density lines that were close to each other, separated in some areas by small low-density spaces; stage D, fusion completed in the palatine bone, with no evidence of a suture; and stage E, fusion anteriorly in the maxilla. As for the results, Stages A and B typically were observed up to 13 years of age; whereas, stage C was noted primarily from 11 to 17 years but occasionally in younger and older age groups. Fusion of the palatine (stage D) and maxillary (stage E) regions of the midpalatal suture was completed after 11 years

only in girls. From 14 to 17 years, boys showed fusion only in the palatine bone (stage D) (Angelieri et al., 2013).

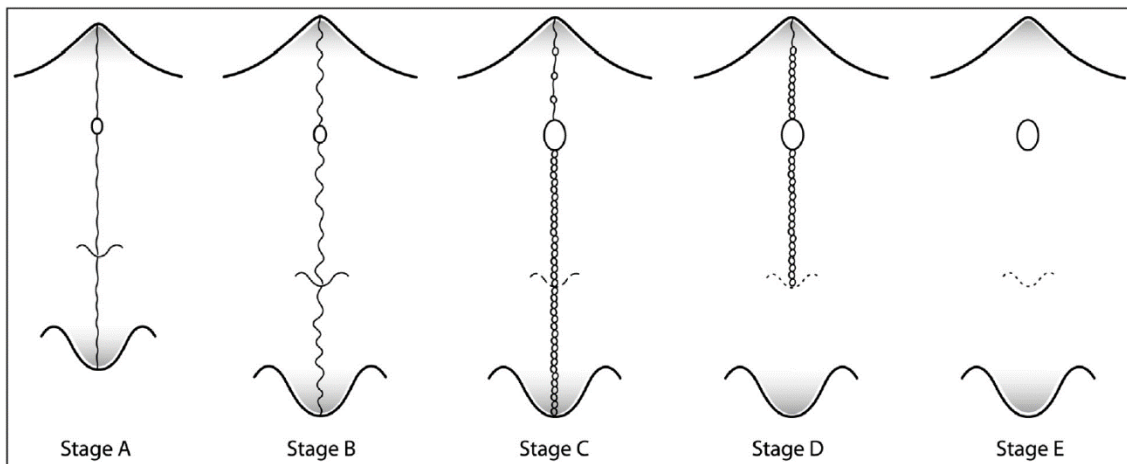


Figure 2.8: Schematic drawing of the maturation stages observed in the mid-palatal suture (Angelieri et al., 2013).

Clinicians frequently report difficulty producing palatal separation after the pubertal growth period, despite favorable orthopedic responses prior to and during pubertal growth. As a result, a direct relationship between increased skeletal expansion resistance and increasing patient age has been quantified and linked to the formation of mechanical interlockings at maxillary articulations as early as 12 to 13 years of age (R. A. Bell, 1982).

2.6.2 Palatal Expansion in the Primary and Early Mixed Dentition

Palatal expansion is relatively easy to obtain in younger children because less force is required to open the suture. All types of expansion appliances cause skeletal and dental changes in the early mixed dentition.

There are three options for palatal expansion in preadolescent children: (1) a split removable plate with a jackscrew or heavy midline spring, (2) a lingual arch,

often of the W-arch or quad-helix design, or (3) a fixed palatal expander with a jackscrew that can be attached to bands or incorporated into a bonded appliance. Removable plates and lingual arches produce slow expansion. The fixed expander can be activated for either rapid (0.5 mm or more per day -14 turns/week), semi-rapid (0.25 mm/day -7 turns/week), or slow (1 mm/week -4 turns/week) expansion.

When working with a removable appliance, the rate of expansion must be quite slow, and the force used during the process must be low, because faster expansion produces higher forces, which cause problems with appliance retention (Figure 2.9). With these appliances, compliance in activation and wear time is always an issue. Successful expansion with a removable appliance can be time-consuming and expensive.



Figure 2.9: Intraoral photograph of the maxillary arch in occlusal view with a removable expander appliance.

In young patients, lingual arches of the W-arch and quad-helix designs have been shown to open the mid-palatal suture (Figure 2.10). These devices typically deliver a few hundred grams of force and expand slowly. They are relatively clean and effective, producing a mix of skeletal and dental change that is roughly one-third skeletal and two-thirds dental.



Figure 2.10: Intra-oral photograph of the maxillary arch in occlusal view with a cemented quad-helix appliance used for expansion in a patient in the early mixed dentition.

Fixed jackscrew appliances attached to bands or bonded splints can also be used to treat maxillary constriction in the early stages, but they must be used with caution. Permanent molars and primary second molars are relatively easy to band. Using a bonded appliance in the mixed dentition is simple but removing it can be difficult if conventional bonding techniques are used. This device can deliver a wide range of forces. A fixed jackscrew appliance has two major disadvantages in young children when compared to an expansion lingual arch. First, it is larger and more difficult to install and remove. The patient will inevitably have difficulty cleaning it, resulting in soft tissue irritation, and either the patient or a parent will need to activate the appliance. Second, an appliance of this type can be activated quickly, which is a disadvantage rather than an advantage in young children. Rapid expansion should not be attempted in a young child. With rapid expansion, there is a risk of distortion of facial structures, and there is no evidence that rapid movement and high forces produce better or more stable expansion.

In young children with primary and early mixed dentitions, slow expansion with an active lingual arch is the preferred approach to maxillary constriction. If used

carefully and slowly, a fixed jackscrew appliance is an acceptable alternative (Geran, McNamara Jr, Baccetti, Franchi, & Shapiro, 2006; Proffit et al., 2018).

2.6.3 Palatal Expansion in the Late Mixed Dentition

With increasing age, the mid-palatal suture becomes more and more tightly interdigitated; however, in most individuals, it remains possible to obtain significant increments in maxillary width up to the end of the adolescent growth spurt (age 15 to 18). Even in the late mixed dentition, sutural expansion often requires placing a relatively heavy force directed across the suture to move the halves of the maxilla apart.

In adolescents, expansion across the suture can be done in three ways: rapid expansion with a jackscrew device attached to the maxillary posterior teeth, typically at the rate of 0.5 to 1 mm/day; (2) slow expansion with the same device at the rate of approximately 1mm per week; (3) expansion with a device attached to bone screws or implants (Proffit et al., 2018).

2.6.4 Rate of Expansion

2.6.4.1 Rapid Palatal Expansion

One of the primary goals of growth modification is to maximize skeletal changes while minimizing dental changes caused by treatment. The goal of maxillary expansion is to widen the maxilla rather than simply expand the dental arch by repositioning the teeth relative to the bone. To help achieve this goal, rapid expansion of the mid-palatal suture was initially recommended. The theory was that by applying

rapid force to the posterior teeth, there would be insufficient time for tooth movement, the force would be transferred to the suture, and the suture would open while the teeth moved only slightly relative to their supporting bone.

Emerson Angell described rapid maxillary expansion in 1860, and Haas popularized it later. RPE design can be divided into two major categories: i) appliances that are tooth-borne (Figure 2.11, B), and ii) appliances that are tooth-tissue-borne (Figure 2.11, A). The tooth-borne appliances, such as the Hyrax appliance, are made of metal and have an expander that is attached to the teeth. The hyrax appliance is available in two or four band configurations. In a 2-banded appliance, only one tooth on each side of the maxilla is banded (usually the first molars), whereas a 4-banded appliance includes two premolars along with the molars. Because tooth-borne appliances do not cover the palatal tissue, they are easier to clean and more hygienic, making them less irritating to the palatal mucosa. Dr. Andrew Haas created the tooth-tissue borne expander, which covers the palatal tissue with acrylic while connecting to the molars and premolars bilaterally. The large acrylic framework, on the other hand, makes cleaning extremely difficult. The hypothesis and the proposed rationale for the palatal coverage was that when the expansion screw is activated, the expansion force is distributed on the palatal tissues which allows the adaptation and the remodeling of the palate. Thus, Dr. Haas proposed that this led to more skeletal or orthopedic expansion than tooth-borne expanders. The bonded appliance has become increasingly popular because it can be easily cemented during the mixed dentition stage, when retention from other appliances can be poor. The buccal capping is thought to limit extrusion of the molars during treatment and therefore improve overbite control (Gill, Naini, McNally, & Jones, 2004; Thakkar, 2021).

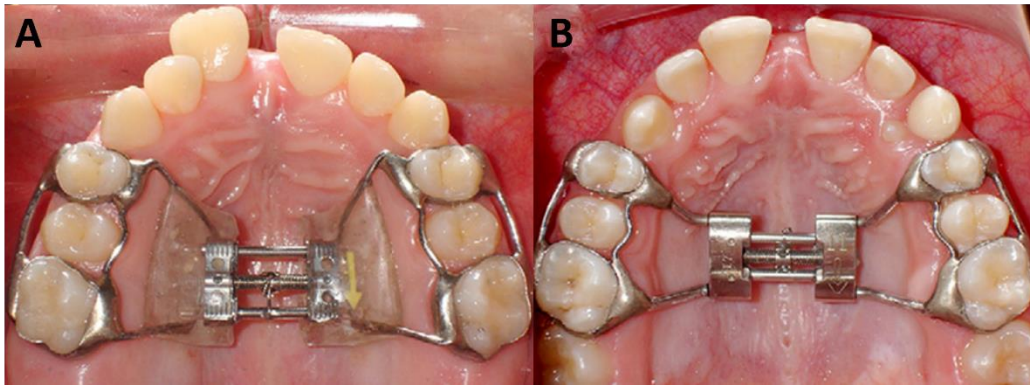


Figure 2.11: Intra-oral photographs of the maxillary arch. A, Haas-type expander and B, hyrax-type expander at the end of the active phase of RPE (Weissheimer et al., 2011).

A centimeter or more of expansion is obtained in 2 to 3 weeks with RPE at a rate of 0.5 to 1 mm/day, with most of the movement being separation of the two halves of the maxilla. The rapid palatal expansion is accomplished by turning the expansion screw in both designs. Typically, one turn of the expansion screw results in 0.25 mm of screw opening. Different screws, however, are available with activations per turn ranging from 0.1 mm to 0.3 mm. The usual protocol for the activation of the expansion screws used for rapid palatal expansion is two turns per day (or one turn in the morning, one turn in the evening) which amounts to approximately 0.5mm of opening of the screw (M. Koudstaal et al., 2009). There is a diastema created between the central incisors. The space created at the mid-palatal suture is initially filled by tissue fluids and hemorrhage, and the expansion is highly unstable at this point. The expansion device must be stabilized so that it cannot screw itself back shut and must be left in place for three to four months. By then, new bone had filled in the suture space, and the skeletal expansion was stable. During this time, the midline diastema decreases and may disappear (Proffit et al., 2018).

If the changes were represented graphically, the plot for rapid expansion would look like figure 2.12, A. It is worth noting that when the expansion was completed, 8

mm of skeletal expansion and only 2 mm of tooth movement would have resulted in 10 mm of total expansion. The same 10 mm of dental expansion would still be present at 4 months, but there would be only 5 mm of skeletal expansion, with tooth movement accounting for the remaining 5 mm of total expansion. As a result, rapid jack-screw activation is ineffective for minimizing tooth movement (Huynh et al., 2009).

2.6.4.2 Slow Palatal Expansion

The mid-palatal suture tissues can adapt at a maximum rate of approximately 0.5 mm per week. If a jackscrew device attached to the teeth is activated every other day at the rate of one-quarter turn of the screw (0.25 mm), the ratio of dental to skeletal expansion is approximately 1 to 1, tissue damage and hemorrhage at the suture are minimized, and a large midline diastema never appears. Ten mm of expansion over a 10-week period would consist of 5 mm of dental and 5 mm of skeletal expansion at a rate of 1 mm per week (Figure 2.12, B). When active expansion is completed, the situation is roughly analogous to RPE 2 to 3 months later, when bone fill-in has occurred. Thus, the overall result of rapid versus slow expansion is similar, but slower expansion produces a more physiological response (Huynh et al., 2009).

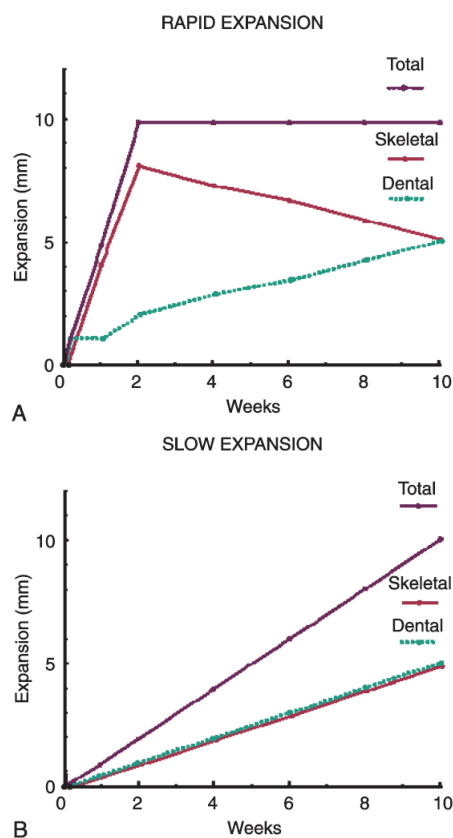


Figure 2.12: Diagrammatic representation of the typical skeletal and dental response to rapid (A) versus slow (B) palatal expansion (Proffit et al., 2018).

2.6.5 *Mini-implant Assisted Rapid Palatal Expansion*

In late adolescents and adults, more force is required to open the mid-palatal suture due to its increased degree of interdigitation. Treatment with a conventional RPE could lead to unwanted dental side effects. Therefore, clinicians have begun to explore alternative approaches to correct the transverse problem. In post-pubertal patients, a rigid element that transfers the expansion force directly to the basal bone may allow for a disjunction. To accomplish this therapeutic goal, orthodontic micro-implants have been included as an auxiliary anchorage to which a jackscrew can be attached in the palatal vault to achieve expansion. During expansion on skeletally mature patients, the mechanism applies a mechanical force to the circummaxillary sutures. This type of

design is generally called mini-implant assisted rapid palatal expansion (MARPE).

MARPE has received widespread attention in recent years and several researchers have studied the efficacy of MARPE (Chuang et al., 2021; Kapetanović, Theodorou, Bergé, Schols, & Xi, 2021).

In comparison to conventional RPE, most clinicians agree that MARPE has increased the rate of success in separating the mid-palatal suture in young adults. According to published research reports, MARPE had a success rate of approximately 84% to 87% (Kapetanović et al., 2021). A recent prospective study looked at the outcomes of maxillary transverse discrepancy treated with MARPE at various ages. Before and after expansion, CBCT scans and dental casts were taken, and the data was compared across four age groups. They discovered that the success rates of mid-palatal suture separation for early adolescents, late adolescents, young adults, and old adults were 100%, 100%, 88.2%, and 85.7%, respectively. Furthermore, MARPE could expand the mid-palatal suture more easily in patients aged less than 20 years than in patients over 20 years of age (Jia et al., 2022).

Through mini-screws placed near the target, the mid-palatal suture, MARPE can deliver expansion force directly to the palatal bone. When compared to conventional RPE, the close force application points are thought to be the reason for more effective skeletal changes and applicability to older patients (Baik, Kang, & Choi, 2020).

Several predictors of mid-palatal suture separation with MARPE have also been proposed. While age, palate length, and mid-palatal suture maturation stage were found to be negatively correlated with suture separation, vertical and sagittal skeletal pattern, mid-palatal suture density ratio, and gender were found to be unrelated (Shin et al., 2019).

There are several recommended MARPE designs, which can be classified as bone-anchored or tooth-bone-anchored (hybrid) appliances. The hybrid type uses both tooth and skeletal anchorage (Figure 2.13, B), whereas the bone-borne type only uses skeletal anchorage (Figure 2.13, A). Some designs include two mini-implants, while others recommend four to six screws. Because of the high degree of suture consolidation in adults undergoing MARPE, mini-implants that support the expander may experience a large magnitude of force (Chuang et al., 2021; Oliveira et al., 2021). The MARPE and activation protocol were designed differently in each study. The length, diameter, position, and number of mini-screws used all varied greatly. These differences are thought to be the primary cause of disparities in results among studies investigating MARPE effects (Baik et al., 2020).

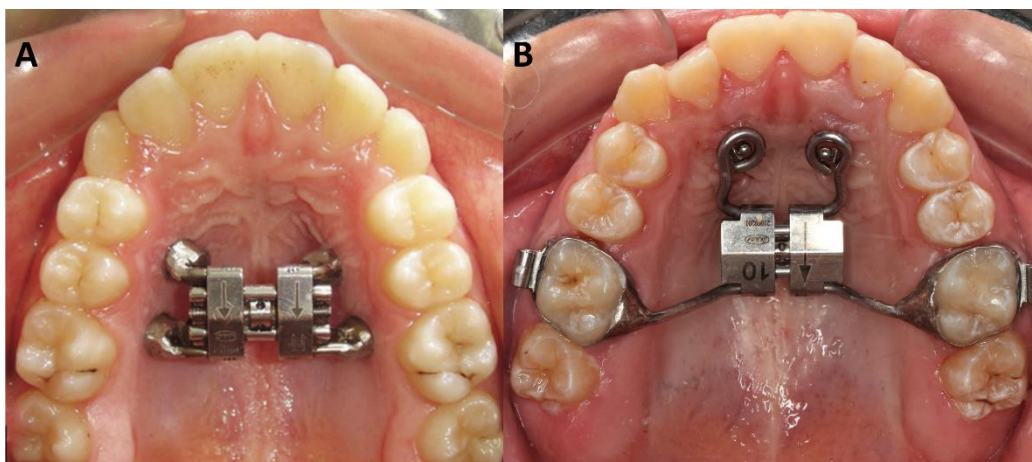


Figure 2.13: Intra-oral photographs of the maxillary arch. A, Bone-borne MARPE supported by 4 mini-screws (Celenk-Koca et al., 2018) and B, tooth-bone-borne or hybrid MARPE supported by 2 anterior mini-screw.

MARPE treatment was associated with a few adverse events. In some cases, the micro-implants in the post-MARPE CBCT were inclined at an angle. There are three possible causes: either the mini-screws were implanted flawlessly from the start, the relative position of the mini-screws in maxillary bone changed due to the low density of maxillary bone, or the resistance from circummaxillary sutures of adult patients may be

too high to be overcome by mini-screws, resulting in mini-screw inclination. Furthermore, some patients would report mild to moderate pain following maxillary expansion. To avoid these side effects, it is recommended that the palatal vault region be cleaned with water as often as possible; that strict sterilization be performed prior to the placement of mini-implants; and that mini-implants be placed parallel. If the appliance was wrapped in soft tissue or the mini-implants became loose due to infection, the expander should be removed immediately and hydrogen peroxide and saline must be applied. However, if the patients complained of moderate to severe pain, the jack-screw should be stopped or the rate of expansion should be reduced (Zong, Tang, Hua, He, & Ngan, 2019).

2.6.6 Surgically Assisted Rapid Palatal Expansion

As previously mentioned, osseous interdigitation increases after skeletal maturity due to fusion of the mid-palatal suture. Attempting to expand the maxilla orthopedically may cause pain at this stage, and removing the expander will result in a relapse of the transverse discrepancy. Dento-alveolar tipping, rather than skeletal expansion, would cause the expansion. When posterior teeth are pushed against the vestibular wall, these forces can cause periodontal problems (Dergin, Aktop, Varol, Ugurlu, & Garip, 2015).

Because of the increased complications associated with attempts to orthopedically alter the transverse dimension of the maxilla as one gets older, surgical procedures to correct transverse discrepancies have been recommended. Traditionally, these procedures have been divided into two categories: segmenting the maxilla during

a LeFort osteotomy to reposition the individual segments in a widened transverse dimension, and surgically assisted rapid palatal expansion (SARPE). The criteria for choosing either of these to correct the MTD are not well defined. The procedure of choice is frequently determined by the surgeon's preference (M. Koudstaal et al., 2009).

Steinhauser described segmental osteotomy in 1972 as a 2-piece Le Fort I osteotomy technique that combined a classical Le Fort I osteotomy with a surgical splitting of the palate over the midline (Figure 2.14). When a single surgical procedure to correct all maxillo-mandibular discrepancies is planned, segmental osteotomy is the preferred choice for MTD correction. When MTD is corrected with segmental osteotomy, vertical and sagittal repositioning of the maxilla and mandible can be done concurrently. After that, the maxillary halves are separated and retained in their new position. The maxillary halves are then separated and retained in the new position. The relative inelasticity of the palatal mucoperiosteum limits the degree of expansion that may be achieved. Orthodontic treatment prior to surgery involves moving the roots of the maxillary central incisors apart to improve surgical access to the osteotomy site. Correction of MTD, on the other hand, is done as a first step with SARPE, and a separate second surgery is required for discrepancies of the maxilla and mandible in the other planes of space. Besides that, SARPE is the preferred technique for patients with isolated transverse deficiency who do not have coexisting sagittal and vertical maxillary discrepancies (Barrabé et al., 2018; Gill et al., 2004; Suri & Taneja, 2008).

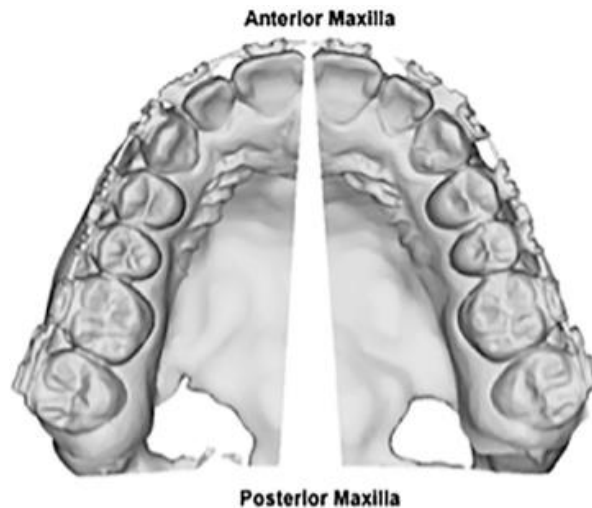


Figure 2.14: Schematic representation of a 2-piece Le Fort 1 osteotomy with the maxillary segments in a widened transverse dimension (O. H. Junior et al., 2017).

Nevertheless, SARPE is a combination of orthodontics and surgical procedures to free the sites of resistance. It has proven to be a stable and dependable method for correcting transverse maxillomandibular deficiencies in patients who are not growing. However, there have been very few published cases to date. The reason for this could be a reluctance on the part of orthodontists and surgeons to convince patients to undergo a relatively traumatic procedure just to achieve transverse correction, especially if additional orthognathic procedures were to follow. Unfortunately, because it is an invasive surgical procedure with risks and high costs for the patient, this treatment is frequently rejected. Furthermore, general anesthesia with hospitalization has traditionally been recommended for these procedures (de Oliveira et al., 2021).

2.6.6.1 SARPE Indications

There are several indications for SARPE on a skeletally mature patient with a constricted maxillary arch reported in the literature such as:

1. Correction of the posterior crossbite, increase in the arch perimeter when no additional surgical jaw movements are planned.
2. Widening of the maxillary arch as a preliminary procedure, even if further orthognathic surgery is planned. This is to avoid increased risks, inaccuracy, and instability associated with segmental maxillary osteotomy.
3. Increase space for a crowded maxillary dentition when extractions are not indicated.
4. Reduction of wide black buccal corridors when smiling.
5. Overcoming the resistance of the sutures when orthodontic maxillary expansion has failed (Suri & Taneja, 2008).

2.6.6.2 SARPE Conventional Approaches

First, planning extension and placement of osteotomies is a patient-tailored procedure that is dependent on each patient's skeletal and dental characteristics as well as stated objectives (Hernández-Alfaro & Valls-Ontañón, 2021).

SARPE techniques have been developed since the early twentieth century. The primary considerations have conflicting interests. One side is a more invasive technique with maximum mobility of the maxillary halves for correction over greater distances with less force but more potential complications. The other option is less invasive, with fewer complications, but with higher relapse, periodontal problems, and unexpected fractures. However, there is disagreement about which specific bony structures should be surgically weakened in order to achieve a smooth course of transverse expansion with ideal movement of the maxillary segments as the palatal suture opens (M. J. Koudstaal et al., 2005).

Commonly, general anesthesia is required for more extensive surgical procedures that may result in excessive bleeding of the nasal mucosa, maxillary sinus, sphenopalatine, or descendent palatine arteries. SARPE has proven to be feasible with local anesthesia and minimal morbidity for simplified techniques that use restricted osteotomies only in areas of greater resistance. This procedure can be performed as an outpatient procedure, resulting in less surgical time and lower costs (De Freitas, Gonçalves, Moniz, & Maciel, 2008).

Several technical approaches have been explained since the first description by Brown (Brown, 1938), who used a medial palatal osteotomy, the hypothesis being that this area was the most resistant to maxillary expansion. Since then, several authors have proposed different areas of resistance and advocated several combined osteotomies to mobilize them. The areas of resistance have been classified as anterior support (piriform aperture pillars), lateral support (zygomatic buttresses), posterior support (pterygoid junctions), and medial support (mid-palatal suture). There is no agreement in the literature on the extent of the necessary osteotomies for SARPE. Various surgical procedures such as exclusive osteotomy in the mid-palatal suture, bilateral osteotomy from the piriform rim to the pterygoid plate without palatal surgery, subtotal Le Fort I osteotomy combined with median palatine suture osteotomy, total bilateral maxillary osteotomy from the piriform rim to the pterygomaxillary fissure along with mid-palatal split and release of nasal septum and pterygoid plates, and three-piece SARPE with complete mobilization have been reported in the literature (Figure 2.15) (Suri & Taneja, 2008; Zandi, Miresmaeili, Heidari, & Lamei, 2016).

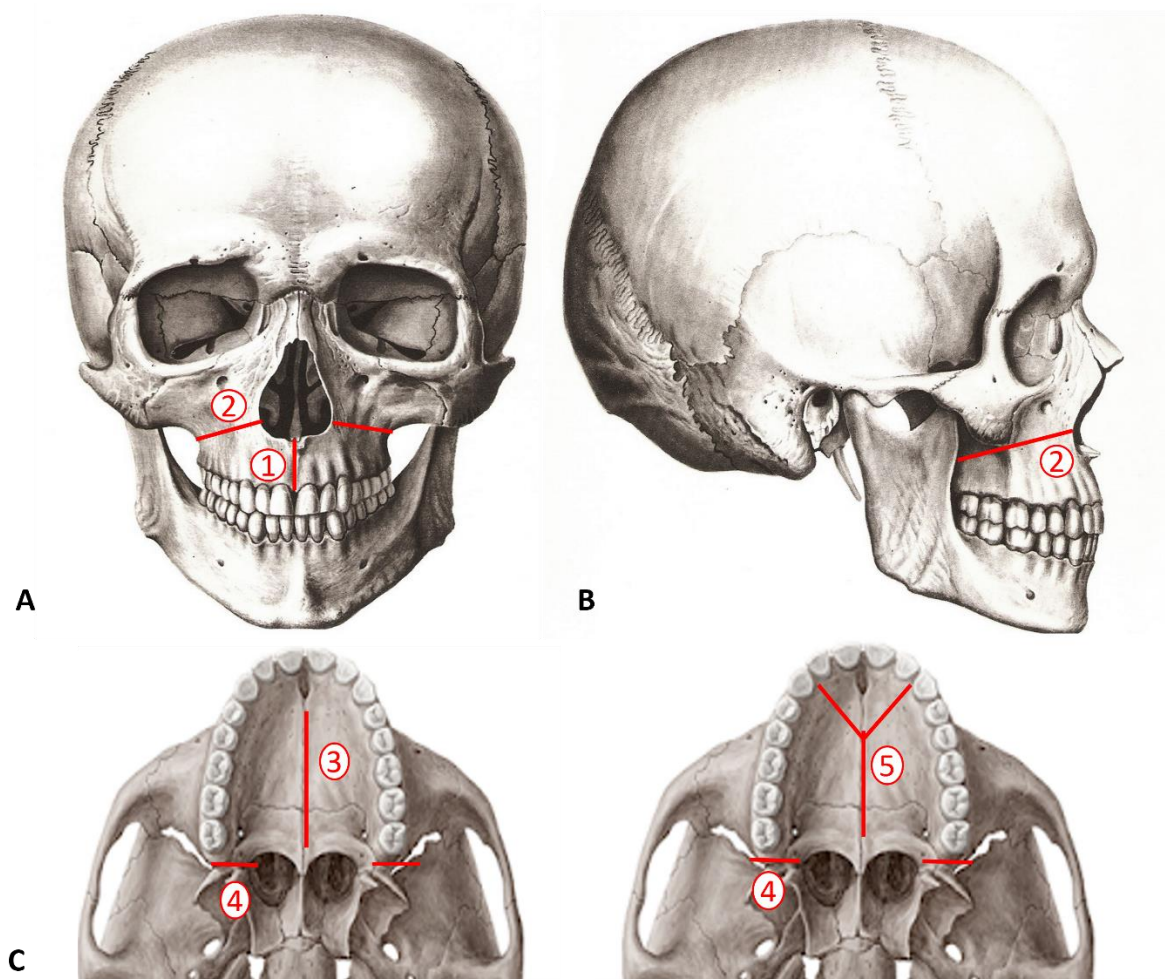


Figure 2.15: Different human skull views: A, frontal view; B, lateral view and C, occlusal views. 1, anterior mid-cut; 2, bilateral cuts from the piriform rim to the pterygoid plate; 3, mid-palatal cut; 4, pterygomaxillary disjunction, and 5, 3-piece segmental osteotomies (Adapted from (Sinelnikov, Sinelnikov, & Sinelnikov, 1996)).

When osteotomy lines similar to a Le Fort I osteotomy were analyzed, the stress distributions in the maxillofacial skeleton and skull base were found to be the lowest (Habersack, Becker, Ristow, & Paulus, 2014).

A study also compared the differences between two surgical techniques, the 2-piece and 3-piece SARPE. The expansion of the posterior part of the maxilla did not differ significantly between the two treatment groups after 6 weeks, but the increase in intercanine distance was significantly greater in the 2-piece SARPE group. After 12 months, both groups had some relapse, mostly dental and, to a lesser extent, skeletal.

The advantages of the 3-piece SARPE over the 2-piece SARPE in this regard include less esthetic impairments, such as smaller and less conspicuous gaps between the lateral incisors and canines, and lower risks of damaging the roots of the central incisors, broadening the columella, and nasal septum deviation (Habersack et al., 2014).

Furthermore, the pterygomaxillary disjunction (PTMD) is a contentious step in SARPE. In 2016, a meta-analysis comparing SARPE procedures with and without PTMD was published. As a result, no statistically significant difference existed between the two techniques, and both were effective in achieving dental and skeletal expansion (Sangsari et al., 2016). Furthermore, pterygoid plate disjunction lengthens the operation, general anesthesia is usually required, and trauma to the palatine artery or cranial nerve are known complications (Sygouros, Motro, Ugurlu, & Acar, 2014). As a result, the authors recommend SARPE without PTMD for the correction of transverse maxillary deficiency. This surgical technique not only improves surgical outcomes but also reduces surgery time and the risk of perioperative complications and morbidities (S. C. Möhlhenrich et al., 2020; Zandi et al., 2016). Therefore, avoiding PTMD makes the surgical procedure less traumatic, more streamlined, and feasible under local anesthesia in an office setting (O. L. H. Junior et al., 2022).

There is a controversy in the literature regarding the SARPE expansion patterns. Some authors claimed that the expansion patterns differed according to the expander appliance used in conjunction with the surgery, while others stated that the expansion pattern varied relative to the associated surgical procedures done. Kunz et al declared that the hyrax appliance should be expected to result in a parallel pattern of expansion with the transverse increase at its largest between the premolars. But the transpalatal distractor should be selected whenever a more V-shaped pattern of transverse expansion

with a more anterior maximum increase is required. Thus, they concluded that specific patterns of distraction can be selectively achieved by taking advantage of specific appliances and various options of positioning. (Kunz, Linz, Baunach, Böhm, & Meyer-Marcotty, 2016). Yet, Verstraaten et al found that without PTMD, and with the distractor placed at the level of the second premolar, the transverse opening between the maxillary halves was V-shaped with more expansion anteriorly than posteriorly. While, with PTMD and the distractor placed at the level of the first molar, the expansion was more parallel. In addition, they said that with the PTMD, the center of resistance of the maxilla would be in the posterior region (Verstraaten et al., 2010). Furthermore, a more study aimed to determine whether the distractor position has a supportive or even greater effect on the transverse expansion pattern than PTMD during SARPE. As a result, they noticed that PTMD appears to play a more important role in achieving a uniform and parallel transverse expansion of the maxilla than the position of the distractor, provided it is placed at the same level on both sides of the palate. However, a posterior distractor seems to intensify the effects of PTMD (S. Möhlhenrich et al., 2021).

2.6.6.3 SARPE Minimally Invasive Approaches

A minimally invasive surgical approach (i.e., small incision and limited periosteal reflection) has the benefits of diminishing surgical exposure and tissue dissection, and thereby improves recovery and shortens the rehabilitation period. The development of special intraoperative instruments and equipment has enabled surgeons to perform various procedures in a more gentle and precise manner, with minimal invasiveness. The endoscope and piezoelectric osteotome are two remarkable tools used

in various surgical specialties and have proven to be important tools in minimally invasive surgeries (AlAsseri & Swennen, 2018).

The concept of a minimal approach in orthognathic surgery is not new in the literature. In 1997, Morselli described in his opinion a less traumatic procedure for maxillary osteotomy in SARPE by performing the osteotomies entirely without a mucosal incision or mucoperiosteal reflection under general anesthesia, with the use of a 2-mm osteotome for midline and horizontal and pterygopalatine suture osteotomies (Figure 2.16). However, this surgery is considered as a blind surgery, since all the cuts were done without the exposure of the underlying bone which is usually performed in traditional techniques (Morselli, 1997).

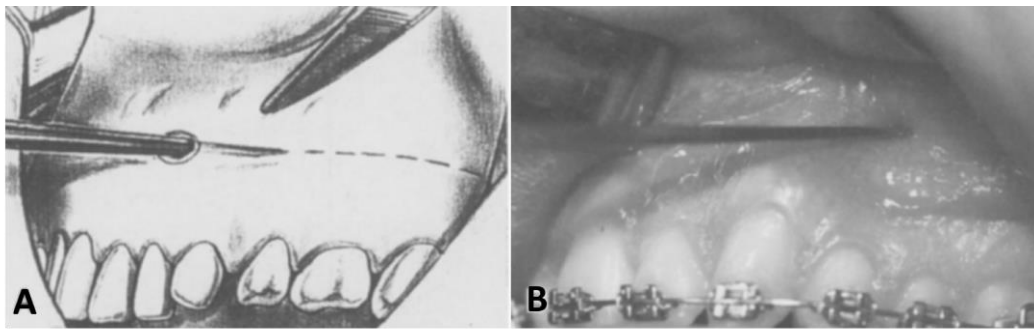


Figure 2.16: Insertion of a 2 mm osteotome to perform the horizontal osteotomy line in the maxillary lateral wall; this technique eliminates the need to make a mucoperiosteal flap for exposing the underlying bone, unlike what is usually done in the traditional open technique. A, Sketch and B, Intraoperative view (Morselli, 1997).

In 2010, Hernandez-Alfaro et al described a new approach for SARPE also considered minimally invasive. Local anesthetic in addition to intravenous sedation was administered in all patients. A through-and-through vestibular incision 10mm over the keratinized mucosa limit was performed and the incision ran horizontally to reach the level of the laterals (Figure 2.17). Osteotomies of lateral walls and pterygoid disjunction were performed in all cases with total liberation of the anterior, lateral, posterior, and medial buttresses as traditionally executed in a maxillary Le Fort 1 surgery. Yet, this

procedure is technically sensitive and depends largely on the surgeon's experience and skill, since all osteotomies are done with a limited access (Hernandez-Alfaro, Bueno, Diaz, & Pagés, 2010).



Figure 2.17: Surgical field when the osteotomies have been completed (Hernandez-Alfaro et al., 2010).

In 2017, Luxi et al applied a mid-palatal cortex osteotomy assisted RPE for the correction of MTD in 14 young adults. The cut was performed under local anesthesia along the mid-palatal suture from the incisive canal to the transverse palatine suture. A ball drill was used to remove bone with an incision depth half the thickness of the palatal bone (Luxi, Xiaoja, Juan, Pengruofeng, & Jun, 2017).



Figure 2.18: Intra-oral photographs of the maxillary arch. A, corticotomy in the palate; B, a periodontal dressing was used to promote wound healing; C, Hyrax rapid maxillary expansion device was placed 1 week after surgery (Luxi et al., 2017).

2.6.7 Other Adjunctive Treatment Approach to Facilitate Expansion

A case report involved an adult patient treated with a method called corticopuncture facilitated MARPE where eight total perforations 2mm apart were performed along the mid-palatal suture under local anesthesia (Figure 2.18). This method was done in order to reduce the resistance and optimize the mid-palatal suture opening (Suzuki, Braga, Fujii, Moon, & Suzuki, 2018).

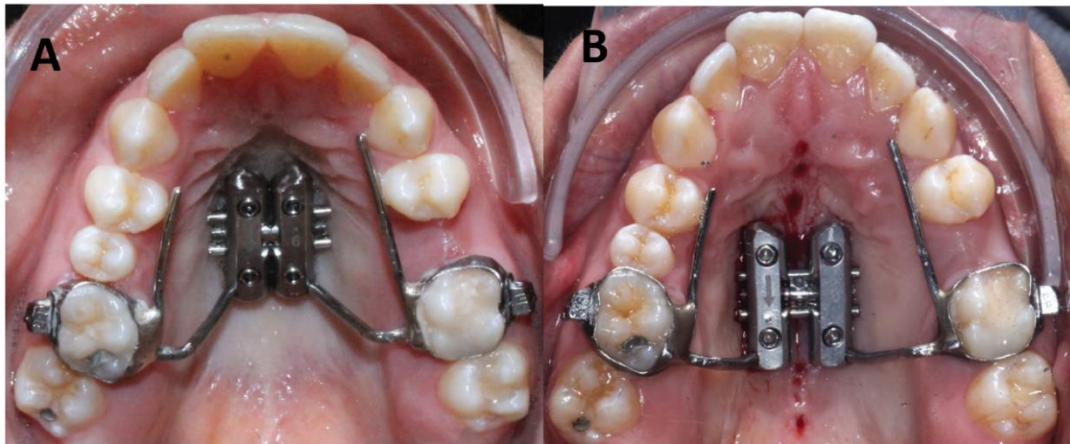


Figure 2.19: Intra-oral photographs of the maxillary arch with the MARPE in place and minimally invasive surgical procedure to reduce suture resistance: A, day of installation; B, after corticopuncture procedure (Suzuki et al., 2018).

2.6.8 Structural Effects of Expansion

A meta-analysis published in 2020 studied the short-term effects of RPE with the accuracy and 3D imaging provided by computed tomography. The transverse increase in the nasal cavity was lower than that at the basal bone level, which was also lower than the increase at the alveolar bone level. This data confirmed the presence of a positive expansion gradient in the maxilla from the cranial to the caudal region (Giudice, Spinuzza, Rustico, Messina, & Nucera, 2020).

- **On the Maxilla**

Generally, the maxilla proceeds in forward and downward direction due to expansion (Haas, 1961).

On the Mid-palatal Suture: according to a systematic review published by Lui et al, the mid-palatal suture opening during RPE orthodontic treatment accounted for 12 to 52.5 percent of total screw expansion. After RPE, the suture appeared to be reorganized, and the expansion was stable after the appliance was retained for 3 to 12 months (Liu, Xu, & Zou, 2015).

Another study using the RPE found that skeletal expansion amounts were greater in the anterior compared to the posterior (Figure 2.19). The pattern of expansion was triangular, with a wider base at the anterior portion of the maxilla. The resistance of the sphenoid bone's medial and lateral pterygoid plates to maxillary tip movement during the RPE could explain the greater expansion in the anterior region. Another possibility is maxillary expansion biomechanics: the direction of the expansion force produced by the expanders would be anterior to the center of resistance of each maxillary half (Weissheimer et al., 2011).

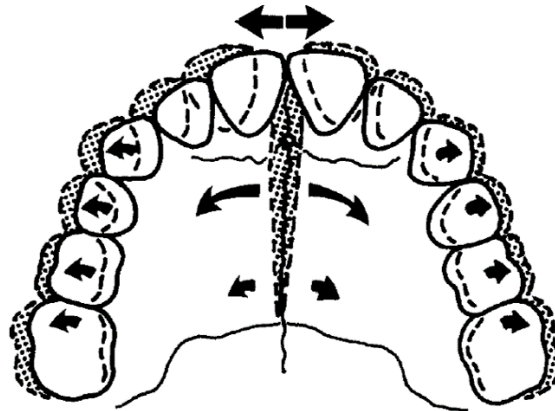


Figure 2.20: Occlusal view of maxillary expansion illustrating mid-palatal suture opening with greatest separation occurring anteriorly, lateral rotation of palatal halves, bony remodeling of maxillary elements, and lateral/ rotational movement of the maxillary teeth (Weissheimer et al., 2011).

When the expansion obtained with an expander anchored to the teeth or two mini-screws were added, a pyramidal maxillary expansion pattern was noticed.

However, a parallel expansion pattern was observed with expanders on 4 mini-screws (Park et al., 2017).

On the Palatal Vault: a horizontal outward displacement of the maxillary halves resulted in a lowered palatine process (Haas, 1961).

- **On the Circummaxillary Sutures**

Cranial sutures respond to external orthopedic forces differently depending on their anatomic location and degree of interdigitation. Sutures articulating directly to the maxilla (zygomaticomaxillary and frontomaxillary) had a higher average amount of suture opening, whereas sutures articulating further away from the maxilla had a lower degree of disarticulation (Bazargani, Feldmann, & Bondemark, 2013; Ghoneima et al., 2011).

Another study used finite element analysis to examine the stress distribution along the craniofacial sutures with RPE, revealing that the medial aspect of the frontomaxillary suture, the superior portion of the nasomaxillary suture, and the lateral aspect of the frontonasal suture experienced the highest stresses (Gautam, Valiathan, & Adhikari, 2007).

- **On the Mandible**

The mandible rotates downward and backward as the maxilla expands. There is some disagreement about the magnitude and permanence of the change. The opening of the mandibular plane during RPE is most likely explained by occlusion disruption caused by maxillary posterior teeth extrusion and tipping, as well as alveolar bending; thus, premature dental contacts may cause mandibular rotation (Figure 2.20) (Bishara & Staley, 1987; Patil, Lakhe, & Niranjane, 2023). This is supported by the fact that bonded appliances cause less downward and backward movement of the mandible, most likely due to the absence of occlusal interference, even though these movements are not eliminated. The evidence supporting this outcome, however, is still insufficient to justify the use of bonded appliances in patients with vertical growth patterns (R Bucci et al., 2016).

Nonetheless, the vertical measurements in the MARPE group showed no discernible change, whereas the conventional RPE groups showed a significant increase. The conventional RPE group was found to have more clockwise rotation of the mandible, and a bone-borne expander could be an acceptable alternative to avoid this effect (Chuang et al., 2021).



Figure 2.21: Intra-oral photographs. A, frontal view prior expansion; B, frontal view after expansion and C, lateral view after expansion. Note the bite opening because of the premature dental contact at the first molar due to extrusion and buccal tipping.

- **On the Temporomandibular Joint (TMJ)**

A systematic review published in 2020 based on CT scans and magnetic resonance imaging (MRI) demonstrated that the use of RPE in growing patients can modify the condyle-fossa relationship in the short term, without changing the position or shape of the articular disc, but can maintain or improve the intercondylar symmetry relationship (Torres et al., 2020).

Furthermore, a study using bone scintigraphy demonstrated a condylar reaction to RPE. While splitting the mid-palatal suture, they discovered a statistically significant increase in metabolic activity. The increased metabolic activity showed a decreasing trend at the end of the active expansion. Furthermore, mandibular condyles adapt to

transversal and rotational residual loads and tend to return to normal shortly after the mid-palatal suture is opened (Gok et al., 2021).

Another retrospective study investigated the effects of SARPE on the TMJ and discovered that SARPE has no negative impact on TMJ function or condylar integrity, and thus the decision for or against this approach can be made without making TMJ consequences a major issue for the decision (Kustermans, Van de Castele, Asscherickx, Van Hemelen, & Nadjmi, 2022).

2.6.9 Functional Effects of Expansion

- **Nasal Breathing**

Maxillary expansion is an effective procedure to correct dental and skeletal transversal discrepancies; consequently, this therapy showed promising positive results on the airway dimension, both in the short-term and in the long-term. Significant increase in nasal cavity width and volume is reported with both bi- and three-dimensional radiographic methods and the reduction in nasal resistance is observed with functional examinations. However, due to the low quality of systemic reviews supporting these results, this treatment cannot be indicated only for upper airways enhancement purposes but must be supported by an orthodontic indication. Therefore, whenever a constricted maxilla is present, orthodontists should be familiar with the potential improvement provided by the maxillary expansion, but still this treatment cannot be solely indicated for breathing improvement purposes, as the clinical relevance of the results is not yet well established (Rosaria Bucci et al., 2019; Niu, Di Carlo, Cornelis, & Cattaneo, 2020).

Furthermore, a study evaluated the long-term effects on airway in patients MARPE, RPE, and controls with CBCT analysis. Accordingly, they found a significant increase in total airway volume, total airway area, and minimal cross-sectional area with MARPE and RPE immediately after expansion, but at post-treatment, the changes in the MARPE and RPE groups were similar to the change in the control group. However, MARPE led to a significant long-term increase in nasopharyngeal volume. The amount of expansion did not correlate with the increase in pharyngeal airway volume (Mehta et al., 2021).

In summary, airway studies demonstrated that MARPE could help in respiratory function by enlarging volume and decreasing the total resistance in the upper airway. Nevertheless, the follow-up period was short in most of the studies. Further investigations assessing the long-term effects may still be needed (Chuang et al., 2021).

- **On Speech**

There is little evidence in the literature about the effect of maxillary expansion on speech. A study of patients with deep palatal vaults found that those with narrow arches may have speech problems (Patil et al., 2023). Furthermore, some patients may experience difficulty speaking immediately following the cementation of the expander appliance, which will resolve with adaptation.

- **On Hearing**

A systematic review and meta-analysis discovered that maxillary expansion improved conductive hearing loss in children. However, without an additional orthodontic indication, such as maxillary constriction, results on children with conductive hearing loss cannot be concluded. It demonstrated that existing prospective

studies had qualitative weaknesses, making it difficult to obtain conclusive evidence about the role of maxillary expansion in conductive hearing loss (Calvo-Henriquez et al., 2022).

2.6.10 Envelope of Discrepancy: Limits for Dental Expansion

There are clear boundaries to dental expansion. There will be negative consequences if these boundaries are not followed. Defining the envelope of discrepancy and the limits of these boundaries is critical and should be done for each individual patient. Figure 2.21 illustrates and simplifies the limitations of the three major treatment modalities for skeletal discrepancies. The inner envelope depicts the limits of camouflage with orthodontic treatment alone; the middle envelope depicts the limits of orthodontic treatment combined with orthopedics and growth modification; and the outer circle depicts the limits of orthodontic and orthognathic surgical procedures. The numbers on the diagram are only guidelines and may under- or overestimate the potentials for any given patient; however, they help put the three major treatment options into context. When these limits are exceeded, teeth are put in danger of being traumatized and possibly lost.

In children, orthopedic transverse correction utilizing growth is the preferred approach to any skeletal discrepancy when growth potential exists. With orthopedics, the envelope of discrepancy is greatly expanded, which may allow the clinician to provide a non-extraction treatment if the transverse skeletal discrepancy is corrected. Moving only the teeth to conceal the transverse skeletal deficiency may result in periodontal problems and occlusal instability. Camouflage consideration necessitates a thorough examination of the patient's ultimate periodontal status, occlusal function and

stability, and facial esthetics. If clinical and radiographic analysis show that the mature patient has less significant transverse maxillary deficiency, sufficient buccal maxillary bone may remain to allow dental tipping and camouflage of the transverse skeletal dimension. (Vanarsdall Jr & Blasi Jr, 2017).

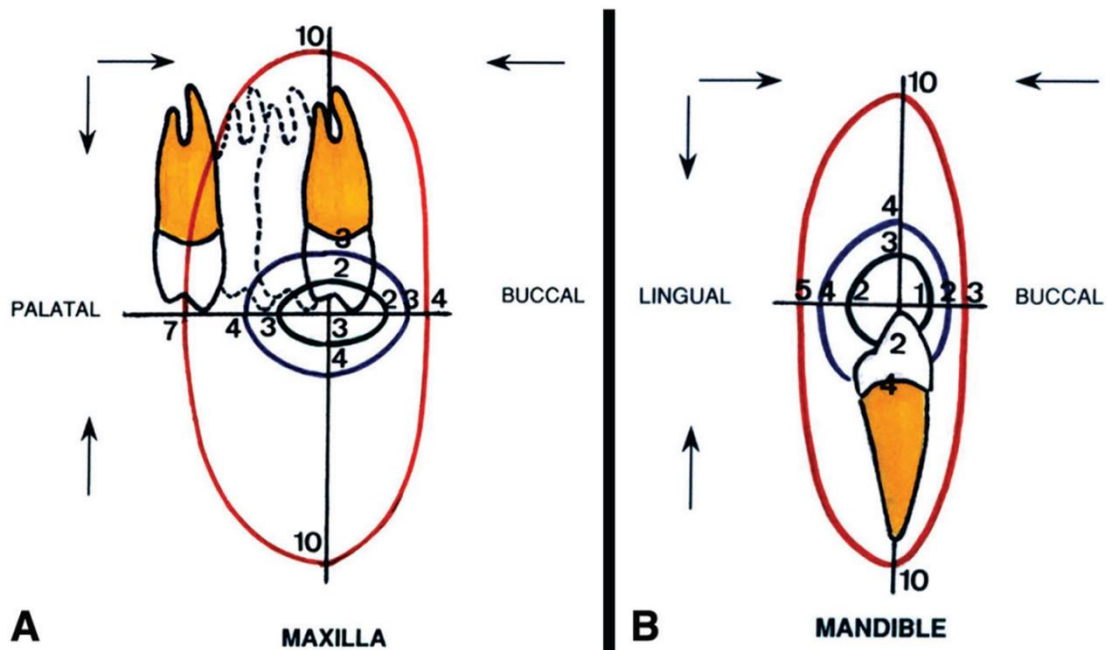


Figure 2.22: Envelopes of discrepancy for the transverse dimension of the maxilla (A) and mandible (B). The inner circle establishes the limits of orthodontic treatment alone; the middle circle exhibits the limits of orthodontic treatment combined with growth modification; and the outer circle illustrates the limits with orthodontics and surgical procedures (Vanarsdall Jr & Blasi Jr, 2017).

2.6.11 Adverse Effects of Expansion

2.6.11.1 Dental Effects

The buccal tipping of the maxillary molars is one of the dental effects of maxillary arch expansion. Rapid palatal expansion has been linked to dental complications such as buccal dehiscence, fenestration, and root resorption. As a result, there has been a growing interest in using different designs of expansion appliances to achieve more skeletal effects and less dental effects (Thakkar, 2021).

Chuang et al discovered a large amount of buccal tipping of the upper first molars after expansion in the bonded and banded RPE groups (11.75° and 10.25° , respectively), but only a small amount of palatal tipping (3.5°) in the bone-borne group. The authors concluded that the palatal tipping of the molars was caused by the bone-borne appliance's lack of tooth support. Because the amount of palatal tipping was small, an overcorrection of the maxilla was unnecessary as the molars translated more bodily. It was concluded that the change of tooth axis was negligible, and a bone-borne expander could produce less alveolar bending, less dental tipping and less vertical alveolar bone loss than a conventional RPE after expansion (Chuang et al., 2021).

Tooth-related complications are common in SARPE procedures. Because they anchor the expansion device in tooth-borne expanders, the affected teeth are usually molars and premolars. Periodontal issues such as gingival pockets and buccal bone loss, which can lead to tooth loss, have frequently been discussed. Complications at the central incisors have also been observed as a result of the median osteotomy. There have been reports of incisor discoloration, periodontal pockets, mobility, and even incisor loss. The loss of a central incisor as a result of SARPE procedures is considered a major complication due to its esthetic significance. Tooth loss will necessitate additional surgical procedures, such as the placement of dental implants and alveolar reconstruction with bone grafts (Carvalho et al., 2020).

However, the use of skeletal anchorage may reduce the side effects of tooth-borne expansion appliances such as dental tipping and alveolar bending. The bone resistance of maxillary expansion was lower in children and adolescents with less mature pterygomaxillary and zygomaxillary sutures. Adult patients' bone resistance was

significantly higher, and a significant portion of orthopedic force would be exerted on anchored teeth, resulting in both dental tipping and alveolar bending (Zong et al., 2019)

Within the limitations of the study by Naoum et al, it can be concluded that both SARPE and orthopedic maxillary expansion reduce but do not eliminate pulpal blood flow to maxillary anterior teeth and thus do not cause pulp vitality loss. Surgery for SARPE has no effect on pulpal blood flow to maxillary anterior teeth; however, the process of maxillary expansion has an effect on pulpal blood flow. Caution must be taken when using carbon dioxide (CO₂) and electric pulp (EPT) tests alone to assess pulp status after SARPE because the capacity for CO₂ or EPT to provide negative sensibility responses despite the presence of pulpal blood flow was observed (Naoum, Goonewardene, Abbott, Karunanayake, & Budgeon, 2019).

2.6.11.2 Periodontal Effects

It is critical for a clinician to recognize the periodontally susceptible patient. When examining a patient clinically, it is essential to assess the gingival tissues and gingival biotype in order to provide the best treatment. A patient with a thin biotype should be carefully evaluated. The biotype of both soft and hard tissue is essential to the treatment's success. Orthodontic movement of teeth within the alveolar housing should be done with caution. Despite the fact that gingival recession has a multifactorial etiology, failure to make an accurate diagnosis may result in orthodontics being a contributing etiologic factor to periodontal breakdown and gingival recession (Vanarsdall Jr & Blasi Jr, 2017).

The literature has shown that bone dehiscence can occur in the alveolar bone when teeth are tipped buccally, but orthodontic movement does not always result in

connective tissue loss. Gingival recession is known to be caused by teeth that are positioned or moved buccally, bone dehiscence, and the presence of thin and brittle keratinized mucosa. Gingival recession, on the other hand, is only triggered by mechanical trauma from brushing or inflammation caused by the presence of plaque. Therefore, the quality of the keratinized mucosa and, in particular, tooth brushing should be closely monitored in patients undergoing SARPE (Siqueira, Cardoso, Capelozza Filho, Goldenberg, & Fernandes, 2015).

Furthermore, the type of anchorage used by the expander device appears to influence the periodontal effects in MARPE or SARME. Although evidence is limited, it appears that the bicortical anchorage (cortical of the palatal bone and nasal floor) transmits the forces generated by expander device activation directly to the bone, minimizing alveolar inclination. A MARPE bone-borne or MARPE tooth-bone-borne with bicortical anchorage must be used to reduce dental inclination. Excessive dental inclination due to stress mechanisms on the teeth could be avoided if forces were applied directly to the bone using bicortical anchorage. (Vidalón et al., 2021).

2.7 Finite Element Analysis (FEA)

2.7.1 *Principles and Applications of FEA*

Finite element analysis (FEA), a computer simulation technique, was introduced in the 1950s using the mathematical matrix analysis of structures to finite continuum bodies. Over the past 30 years, FEA has become widely used to predict the biomechanical performance of various medical devices and biological tissues due to the

ease of assessing irregular-shaped objects composed of several different materials with mixed boundary conditions. Unlike other methods (e.g., dynamometer, strain gauge), which are limited to points on the surface of evaluated structures, the finite element method (FEM) can quantify stresses and displacement throughout the anatomy of a three-dimensional configuration (Ko, Rocha, & Larson, 2012).

2.7.2 FEA in Orthodontics

In orthodontics, different questions are difficult to be answered because of the biomechanical complexity of the stomatognathic system and the ethical issue of simulating invasive procedures on human patients. In these cases, the computational techniques such as the Finite Element Analysis can come to the rescue. The FEA is an engineering resource applied to calculate the stress and deformation of complex structures, and has been widely used in orthodontic research. With the advantage of being a non-invasive and accurate method that provides quantitative and detailed data on the physiological reactions possible to occur in tissues, applying the FEA can anticipate the visualization of these tissue responses through the observation of areas of stress created from applied orthodontic mechanics (Knop, Gandini Jr, Shintcovsk, & Gandini, 2015).

There are three fundamental steps to proceed with finite element analysis: Pre-processing, processing and post-processing. The pre-processing consists of the creation of the geometric model and its finished conversion element, representation of the data of the properties of the materials, definition of the boundary conditions and configuration of the loading. With post-processing the results are interpreted and conclusions are

drawn based on the calculated stresses, movements and strains induced on the models as a result of the applied forces (Singh, Kambalyal, Jain, & Khandelwal, 2016).

2.7.3 FEA and Maxillary Expansion

FEA is a useful method to analyze effects of palatal expansion. A number of articles have employed FEA to ideally compare every kind of orthodontic expansion device in terms of results obtained and stress involved (Bignotti, Gracco, Bruno, & De Stefani, 2019). Some studies have compared two expanders to each other in terms of resulted stresses and amount of displacement achieved. Other studies have incorporated various SARPE cuts into their models and compared the different outcomes.

A FEA study compared the effects of activation between two expanders and found that a single activation of the bone-borne expander resulted in similar mid-palatal suture aperture of three tooth-borne expander activations (Trojan, González-Torres, Melo, & de Las Casas, 2017). As well, a different study showed that screw position affects the stress and displacement pattern within the nasomaxillary complex and maxillary dental arch. Closer teeth feel more stress and undergo more displacement than the farther ones. Moreover, skeletal effects of the bone-borne expander were greater than that of the tooth-borne expander in all different positions (Tehranchi, Ameli, Najirad, & Mirhashemi, 2013).

Another study aimed to evaluate and compare the stress distribution and displacements along the craniofacial sutures in between RPE and implant-supported RPE (I-RPE). They found that the stresses generated in the case of plain RPE were considerably less than that of the implant-supported RPE for all the sutures. In addition,

they concluded that plain RPE produced increased amount of dentoalveolar tipping, whereas the I-RPE produced less dento-alveolar tipping as the RPE was directly anchored to the palate (Jain, Shyagali, Kambalyal, Rajpara, & Doshi, 2017).

Furthermore, a study used FEA to check the stress distribution with the use of RPE on the craniofacial complex. Displacements were noted more in the structures located anteriorly and along the midline, while the posterior and lateral structures demonstrated minimal displacement but high stresses (Baldawa & Bhad, 2011). Similarly, a study evaluated the stress and displacement patterns on the craniofacial skeleton and concluded that mid-palatal suture shows a maximum von Mises stress followed by pterygomaxillary, nasomaxillary, and frontomaxillary sutures in the descending order of frequency (Priyadarshini et al., 2017).

Moreover, a study aimed to analyze the displacement pattern and stress distribution during SARPE Le Fort 1 osteotomy with bilateral pterygomaxillary disjunction and midpalatal split osteotomy with three different types of RPE devices by constructing a finite element model. As a result, the tooth-borne appliance had more rotational tendencies and the bone-borne and the hybrid appliances exhibited similar stress patterns for the dissipation of the forces produced by the expanders (Singaraju et al., 2015).

In a study published in 2021, six facial skeleton models were created, five with various variants of osteotomy and one without osteotomy and two different types of expanders were used for each model. They concluded that higher levels of stresses and covered areas of the facial skeleton were found for the bone-borne appliance, especially in the model without an osteotomy and in models without an incision in the palatal suture. Also, only in the case of a complete separation of the maxilla at all its junctions,

as well as an osteotomy of the palatal suture, the type of expander (tooth-borne vs. bone-borne) had no significant effect on the distribution of the reduced stresses in the facial skeleton (Nowak, Olejnik, Gerber, Frątczak, & Zawisłak, 2021).

Lee et al analyzed stress distribution and displacement of the craniofacial structures resulting from bone-borne RPE with and without surgical assistance using FEA. Five models were created: a tooth-borne hyrax expander (type A); a bone-borne expander (type B); and 3 bone-borne surgically assisted modalities: separation of the midpalatal suture (type C), added separation of the pterygomaxillary sutures (type D), and added LeFort I corticotomy (type E). The surgical types C, D, and E demonstrated more transverse movement than did the nonsurgical types A and B. The 3 surgical models showed similar amounts of stress and displacement along the teeth, midpalatal sutures, and craniofacial sutures (S. C. Lee et al., 2014).

Additionally, Dalband et al created five models with various surgical procedures: G1: control; G2: Le Fort I osteotomy; G3: Le Fort I osteotomy and para-median osteotomy; G4: Le Fort I osteotomy and bilateral pterygomaxillary separation; and G5: Le Fort I osteotomy and para-median osteotomy and bilateral pterygomaxillary separation. Maxillary displacement showed a gradual increase from G1 to G5 in all three planes of space. The Surgical relief and bone-borne devices significantly reduced stress on anchored teeth (Dalband, Kashani, & Hashemzahi, 2015). Likewise, Mohlenrich et al concluded that increased weakening of the bony pillars of the maxillofacial complex, such as with an additional lateral osteotomy in combination with pterygomaxillary separation, will lead to less stress distribution across the maxillofacial complex as well as at the midpalatal suture and will allow a more uniform transverse expansion of the maxilla (S. Möhlhenrich et al., 2017).

A different study evaluated the distribution of stresses that affect the expander's anchor teeth when the osteotomy is varied. Five virtual models were built and SARPE was simulated. Results showed that the subtotal Le Fort I osteotomy without a step in the zygomaticomaxillary buttress, combined with intermaxillary suture osteotomy and pterygomaxillary disjunction may be the osteotomy of choice to reduce tensions on anchor teeth, which tend to move mesiobuccally (premolar) and distobuccally (molar) (De Assis et al., 2013).

2.8 Significance

This study is adding the missing piece to the knowledge of palatal expansion in orthodontics portrayed by the finite element method. FEA enables the closest reproduction of the various anatomical components (teeth, bone, periodontal ligament) involved in the biologic response to forces created by palatal expansion and accordingly simulating the real clinical condition. The available studies in the literature were all based only on one CT or CBCT scan corresponding to just one individual. Thus, this limits their findings and further widens the gap between finite element method and the clinical reality. In contrast, our study accounts for the individual variations by including actual measurements from an array of patients, and therefore, narrows the gap between the virtual finite element models and the actual clinical situations. This is accomplished through the inclusion of different cortical bone thicknesses of real patients. While previous studies evaluated the stress resulting from different expansion modalities, they did not factor in the effect of cortical bone thickness on the stresses. We aim to

determine how cortical bone thickness affect the amount of stress on the teeth during expansion.

In addition, our research evaluated the efficacy and the dental side effects of a modified minimally invasive SARPE osteotomy that has been proven to be effective in expansion in skeletally mature patients (S. C. Lee et al., 2014; Luxi et al., 2017). Most of the present studies derived useful conclusions about the stress and displacement distribution on the craniofacial complex excluding the teeth. It is well known that expansion is accompanied by several adverse effects. Very few studies reported the side effects of palatal expansion on the teeth. FEA represents a perfect tool to assess the stresses on the dentition and circummaxillary structures. The dental side effects are not assessed accurately in the available studies in the literature. Our study evaluated the amount of stress on the anchor teeth and on the adjacent teeth while comparing various expansion setups. We have also introduced brackets and two different wire sizes in two of our models and studied their effect on the teeth and expansion.

Another important aspect in SARPE is the type of force-generating device used for expanding the maxilla. To evaluate the most efficient method of treatment in SARPE therapy, five variant scenarios and two types of expanders were modeled.

2.9 Specific Objectives

1. Evaluate stress on the teeth and define the setup with the least stresses.
2. Assess the relationship between bone thickness and the amount of stress generated on the teeth during expansion.

3. Assess the relationship between bone thickness and the amount of skeletal expansion in the different models.
4. Determine the tooth-borne setup with the least side effects relative to the bone-borne setup.
5. Evaluate the effects of adding brackets with different wire sizes on the amount of stress on the teeth and the amount of expansion at the level of the bone.
6. Evaluate the relationship of stress and the amount of expansion.
7. Investigate a potential pattern between amount of stress and expansion with respect to the bone thickness variations between the models.
8. Define the setup with the maximum amount of expansion.

CHAPTER 3

MATERIALS AND METHODS

3.1 Materials

The 3D models of the maxillary arch previously created by Ammoury et al (Ammoury, 2017) were adapted in our study. These models were initially generated from a pre-treatment cranial CT scan of an adult patient seeking radiologic assessment (at the Department of Radiology at the American University of Beirut Medical Center). The scan disclosed a well-aligned complete dentition, parallel roots, and a Class I occlusion with the midlines on, suggesting a normal occlusion and possibly a previous orthodontic treatment.

The different anatomical variations related to the bone morphology which represent 13 different individuals were incorporated into 13 models. These models differ in the cortical bone thickness at several maxillary regions which are the incisors, premolars and molars and each divided into buccal and palatal sections respectively (Figure 3.1).

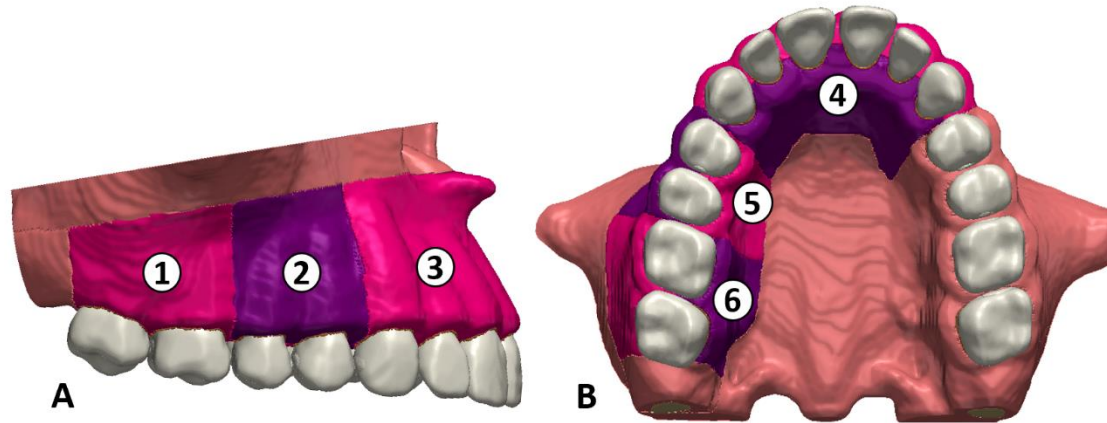


Figure 3.1: A, lateral view of the 3D model of the maxillary arch with 1, buccal molars region; 2, buccal premolars region and 3, buccal incisors region. B, occlusal view of the maxillary arch with 4, palatal incisors region; 5, palatal premolars region and 6, palatal molars region.

3.2 Methods

3.2.1 Expansion Setups

Our study comprises 5 different setups which correspond to distinct clinical situations. The first setup is considered our control model where only a tooth-borne expander was added with no cuts included (Figure 3.2, A). The second setup incorporates the sagittal palatal osteotomy and a tooth-borne expander (Figure 3.2, B). The third setup includes the sagittal palatal osteotomy, a tooth-borne expander, and 0.016*0.022 inch stainless steel (SS) arch wire (AW) engaged into fixed brackets on the teeth (Figure 3.2, C). The fourth setup consists of the sagittal palatal osteotomy, a tooth-borne expander, and 0.019*0.025 inch SS AW engaged into fixed brackets on the teeth (Figure 3.2, D). The fifth setup includes the same osteotomy and a bone-borne expander (Figure 3.2, E).

The abovementioned setups were applied to the 13 models obtained from Ammouy et al yielding to 65 models in total which were included in our study.

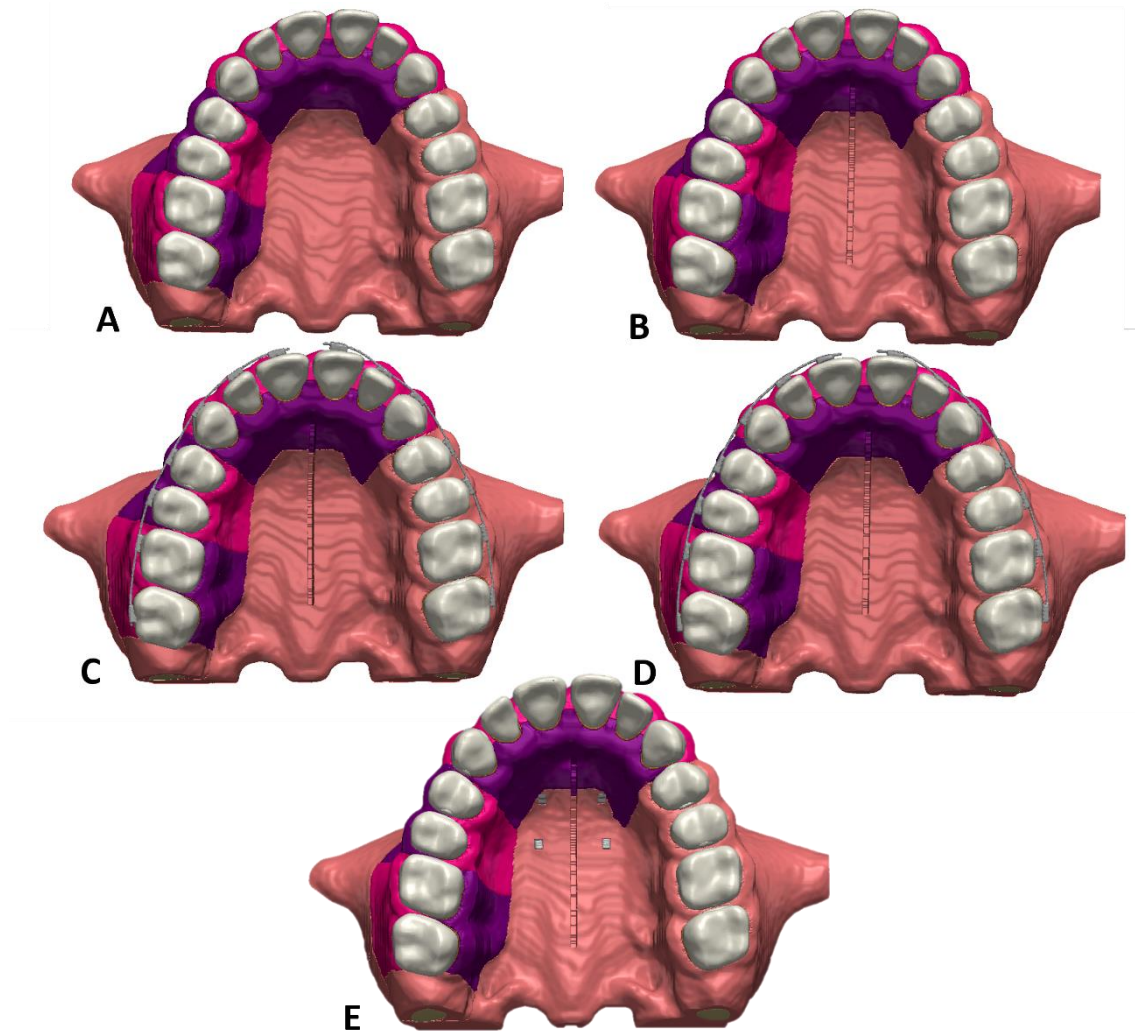


Figure 3.2: 3D model of the maxilla, occlusal views of all the different setups. A, Setup 1: RPE + no cut (control); B, Setup 2: RPE + SARPE cut; C, Setup3: RPE + SARPE cut + 0.016*0.022 SS AW; D, Setup 4: RPE + SARPE cut + 0.019*0.025 SS AW and E, Setup 5: MARPE + SARPE cut.

Table 3.1: The different included setups.

Setup 1	Tooth-borne expander without sagittal palatal osteotomy (control)
Setup 2	Sagittal palatal osteotomy + Tooth-borne expander
Setup 3	Sagittal palatal osteotomy + Tooth-borne expander + Fixed appliance with 0.016*0.022 inch SS AW
Setup 4	Sagittal palatal osteotomy + Tooth-borne expander + Fixed appliance with 0.019*0.025 inch SS AW
Setup 5	Sagittal palatal osteotomy + Bone-borne expander

The sagittal palatal osteotomy is considered a minimally invasive SARPE cut also known as the mid-palatal cut. This cut is done on the mid-palatal suture and extends anteriorly distal to the incisive foramen across the palate reaching posteriorly the distal limit of the first molar (Luxi et al., 2017).

All models were modified in ScanIP™ S-2021.06 Build 1266 software (Simpleware, Synopsys, Mountain View, CA, USA). The pre-existing screw was eliminated on all models and the different bone types were accordingly filled in its place. In addition, the bracket that was placed at the level of the right canine was also removed. The sagittal palatal osteotomy was made through the *paint tool* using the square shape after creating a separate mask for it (Figure 3.3). The same cut was then imported into all the models as a mask for better replicability and then it was subtracted using the *boolean tool* from all the models at the level of the maxillary palatal bone. This osteotomy is of 1 mm in width relative to the blade's thickness and 4mm in depth while taking into consideration the average palatal bone thickness. According to a study done Kang et al, the greatest palatal bone thickness anteriorly was 6.5 ± 1.5 mm.

Therefore, a depth of 4mm will include the whole palatal cortical bone thickness and part of the trabecular bone while steering away from the nasal cortical floor (Kang, Lee, Ahn, Heo, & Kim, 2007).

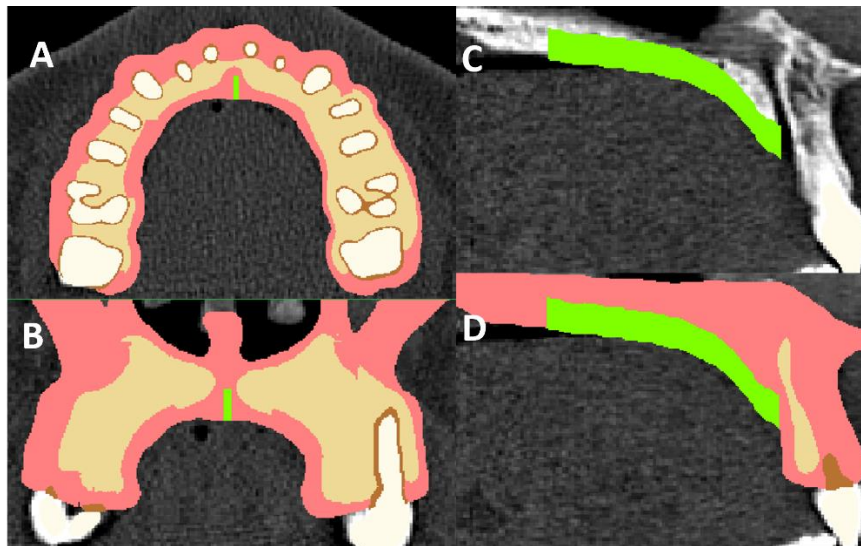


Figure 3.3: Different views of the sagittal palatal osteotomy captured from ScanIP software. A, axial view; B, coronal view; C, sagittal view of the osteotomy starting anteriorly directly distal to the nasopalatine foramen and D, sagittal view with different masks.

Moreover, the 3D maxillary model was imported into Solidworks Premium 2015 (Dassault Systèmes, Solidworks Corps, Providence, RI), a 3D modeling computer-aided design software. The brackets and wires were designed using the software's 3D modeling tools according to the actual dimensions of the maxillary teeth in the imported model of the upper jaw. The brackets were fabricated with the corresponding dimensions of 2 mm in length, 3 mm in width and 1.5 mm in thickness. The wire sizes were 0.016*0.022 inch and 0.019*0.025 inch which are equal to 0.406*0.5588 mm and 0.4826*0.635 mm respectively. Brackets and wires were then imported into the ScanIP software as STL files (Figure 3.4, A). Each wire was first imported as a separate surface and modified its size and position to have it centered on the teeth on the models through the *position and orientation tool* (Figure 3.4, B). Then, the wire was divided between

the central incisors into a right and left one with its corresponding brackets. After, each side of the wire surfaces were converted into masks through the *mask to surface tool* (Figure 3.4, C).

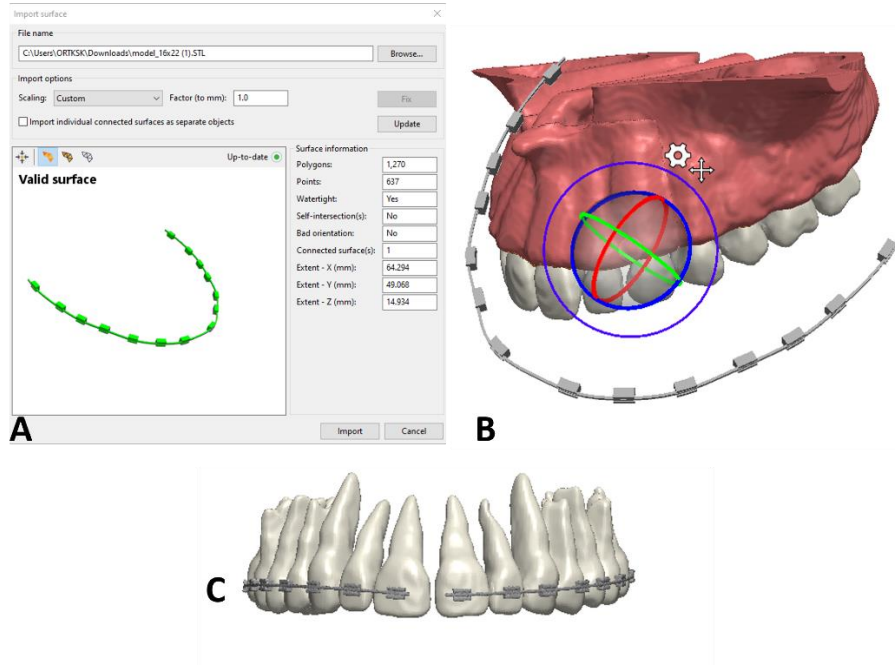


Figure 3.4: A, brackets and wires imported as STL files; B, fixed appliances were adjusted in size and position using the *position and orientation tool* and C, fixed appliances were accurately positioned and well centered on all the teeth after the wire was divided between the central incisors into right and left segments.

For the fifth setup, since we were not interested in the stresses on the mini-implants and for the sake of simplifying the simulation, the mini-implants were simulated as four rectangular areas of 2 mm in length, 1mm in width and 1 mm in height attached to the palatal cortical bone adjacent to the mid-palatal suture to which the expansion displacement was applied (Figure 3.5).

Two areas were placed anteriorly facing the canines and two others were inserted posteriorly facing the second premolars. These were made through the *paint tool* and were designated a separate mask. This mask was also then imported into all the

corresponding models. These areas would simulate the presence of a MARPE with four mini-implants.

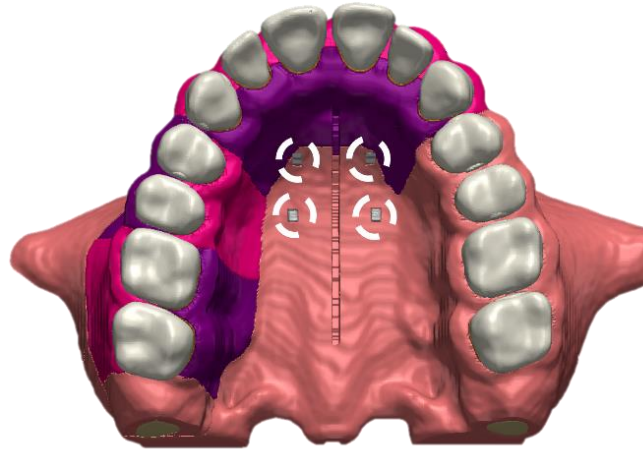


Figure 3.5: Occlusal view of the 3D model of the maxilla with the four rectangular areas (delineated with white arches) representing the mini-implants which were created in the palatal region to simulate the MARPE.

3.2.2 *Meshing*

All the 3D models underwent the process of meshing, which is the discretization of models into elements, in preparation for the finite element analysis (Figure 3.6). The size of the mesh was set at 0.604 mm (corresponding to coarseness level of -36) following a convergence testing to determine the largest element size at which the results of the solution are similar as previously tested by Ammoury et al (2017). Models were then exported from ScanIP as “*inp.*” file format. A total number of 65 models were exported.

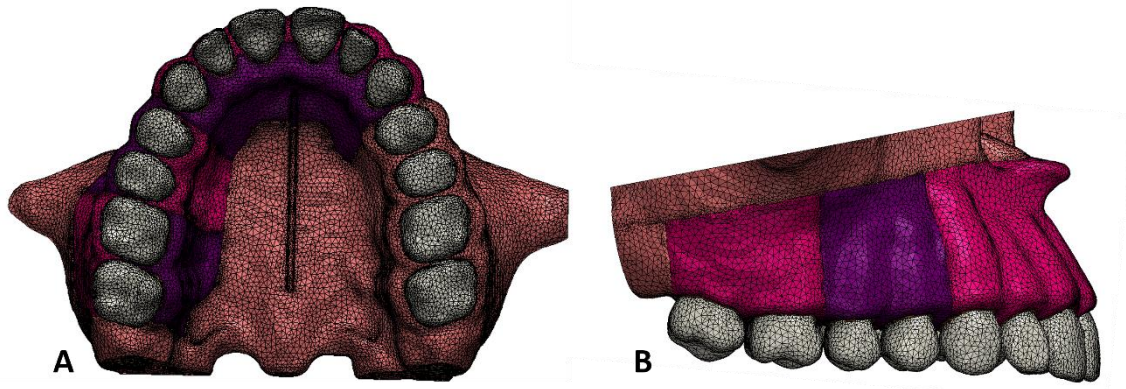


Figure 3.6: A, occlusal view of the meshed model and B, lateral view of the meshed model.

3.2.3 *Finite Element Analysis*

The meshed models in the input file format were imported into Abaqus 6.14 (Dassault Systèmes®, Vélizy-Villacoublay, France), a different engineering software. The entire process from beginning to end is detailed in the following section:

3.2.4 *Materials properties*

FEA results are only as good as the initial data used to set the parameters of tissue response (Middleton, Jones, & Wilson, 1996). Assumptions on the various skeletal elements are made based on scientific computations commonly used in FEA applications in orthodontics. The material properties (Young's Modulus of Elasticity and Poisson's ratios) of cortical and trabecular bones, teeth, brackets, wires and mini-screws were defined from data available in the literature (Table 3.3). The material property of the PDL was assigned based on the work of Kojima et al (Kojima, Kawamura, & Fukui, 2012). All materials used were homogeneous, isotropic, and linearly elastic (Field et al., 2009; Lim, Kim, Kim, Son, & Byun, 2003).

Table 3.2: Material properties of anatomical components used in orthodontic FEA study (Field et al., 2009; Kojima et al., 2012; Lim et al., 2003).

Material	Young's Modulus (N/mm ² = MPa)	Poisson's Ratio
Stainless Steel	200,000	0.3
Tooth	20,000	0.2
Cortical Bone	13,700	0.33
Trabecular Bone	1,500	0.33
PDL	0.68	0.45

3.2.5 Boundary Conditions

The following boundary conditions were applied in all parts of the study: models were fully constrained in translation and rotation at 2 surfaces of the maxilla superiorly and posteriorly, representing the attachments of the maxilla to its neighboring structures, the zygomatic, palatal, and sphenoid bones (Figure 3.7).

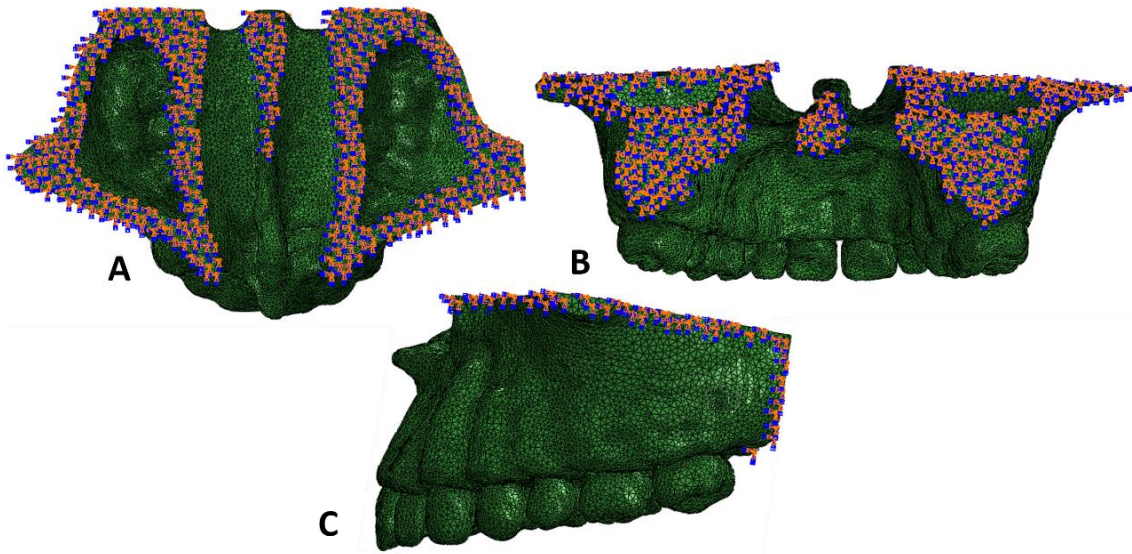


Figure 3.7: Boundary conditions: models constrained from translation and rotation at areas of attachments of the maxilla to adjacent bones: zygomatic, palatal and sphenoid. A, superior view; B, posterior view, and C, lateral view.

3.2.6 Application of expansion

Several different sets were created in this software. The first set was created by selecting only the crowns of the first premolars and first molars for the models with an RPE (Figure 3.8). After, this set was allowed only to move in the x-axis while having the y and z-axes designated as 0. This would simulate the presence of the bands of the RPE on those teeth that would limit the movement only to the transverse direction and eliminate their movement in the anteroposterior direction simulating the effect of a cemented palatal expander.

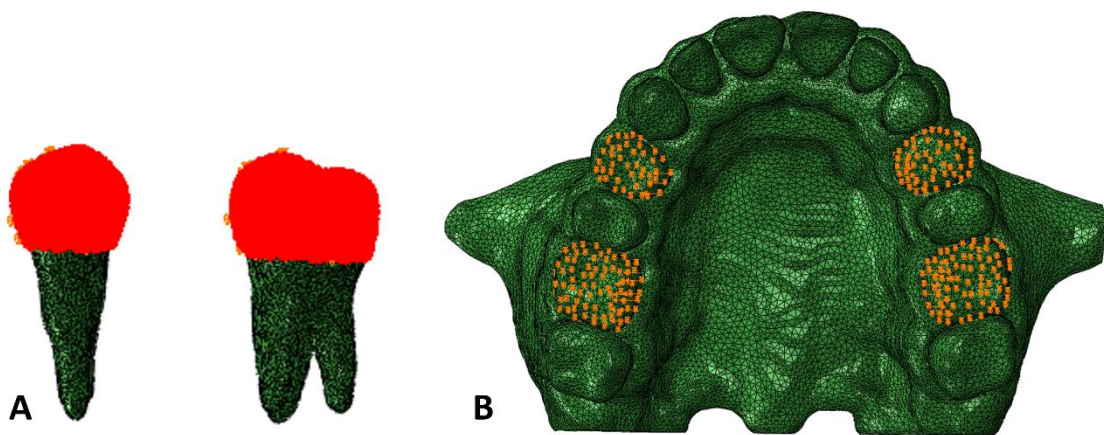


Figure 3.8: A, Crowns of the first premolar and molar selected. B, Occlusal view of the maxillary arch with the selected regions of the RPE boundary conditions.

Furthermore, other sets were created for the application of the load of expansion. Nodes were selected at the palatal surface of the crowns of the first premolars and first molars for the models with an RPE. The displacement forces of 4 mm were then added. These forces were applied only on the x-axis which is relative to the transverse dimension. They were assigned on the right and left sides as -4 mm and 4 mm respectively. Hence, an overall of 8 mm of expansion was applied to the maxillary

arches. Similarly, nodes were selected at the level of mini-implant heads/attachment regions previously added in the MARPE models which represent the mini-implants and the same amount of expansion was applied in all setups. In general, similar numbers of nodes were selected on all models.

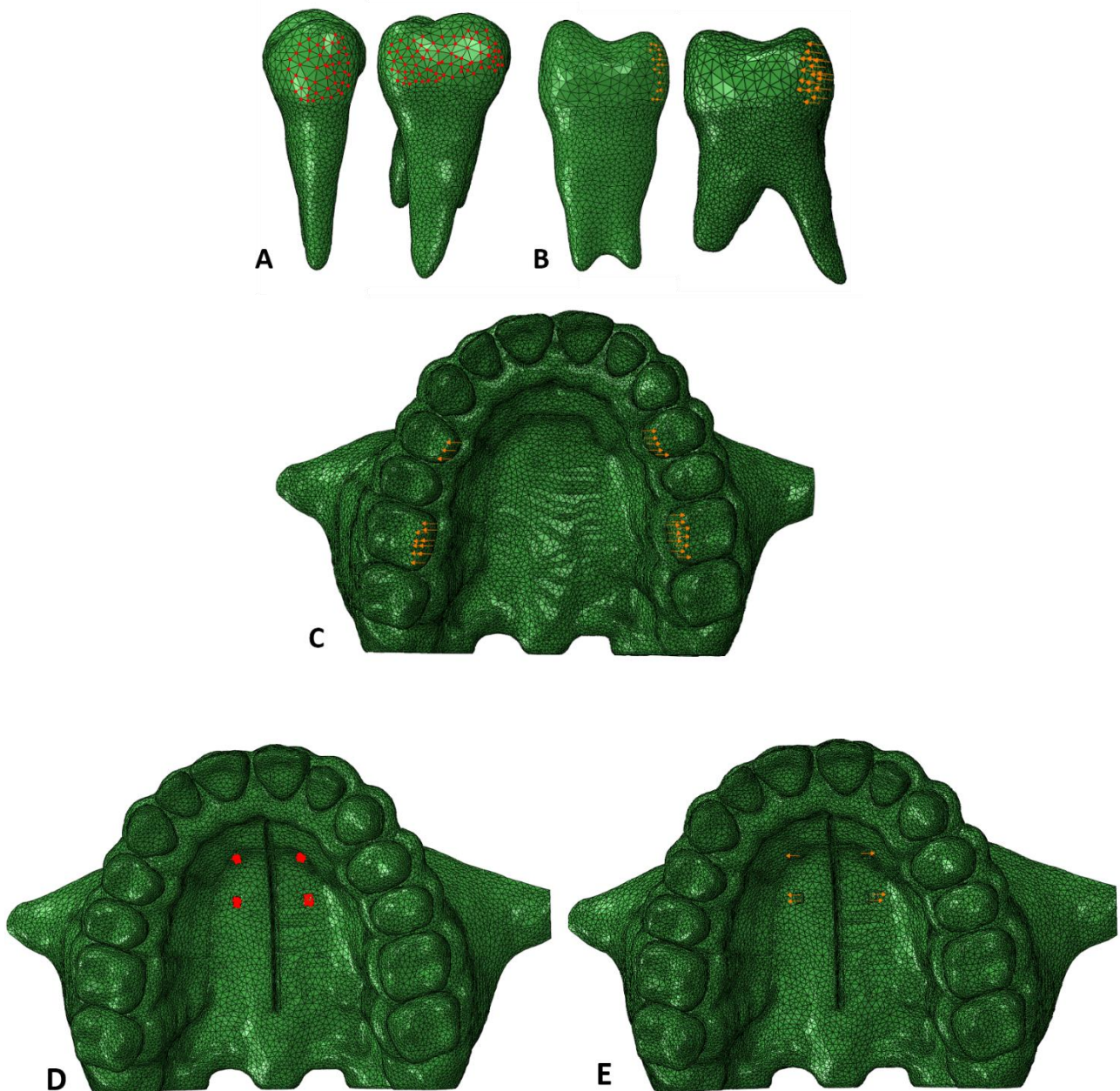


Figure 3.9: A, nodes selected of the first premolar and first molar; B, the direction of the force through the palatal surfaces of the crowns of the teeth; C, occlusal view of the maxilla with the opposite forces in the transverse direction on the anchor teeth of the

RPE; D, nodes selected at the rectangular areas simulating the mini-screws of the MARPE, and E, opposite direction of forces simulating the expansion using MARPE.

3.2.7 Data collection and Export

Since the maxilla is a mirror image, all data were collected on the right side where the individual variations were applied. The stresses at the level of the teeth were measured. For the models with no wires added, the stresses were evaluated on the first premolars and first molars which are the anchor teeth of the RPE. Whereas all the teeth were considered for the models with included wires. Sets containing randomly selected elements uniformly dispersed along the whole surfaces of the periodontal ligaments of the involved teeth were created (Figure 3.10). On the uniradicular and biradicular teeth, around 200 elements were chosen; however, on the multiradicular teeth approximately 400 elements were selected to be able to cover the whole surfaces. The average stress of these sets were calculated to obtain the resultant stress on each tooth (Zeno, 2017).

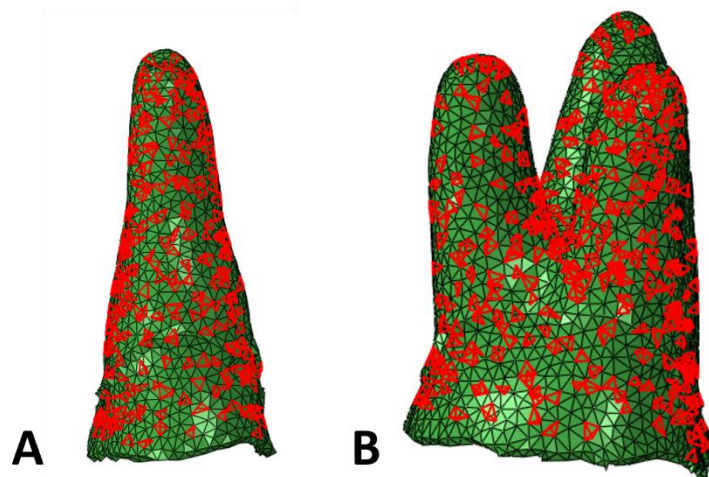


Figure 3.10: Selection of element sets. A, PDL of the first premolar and B, PDL of the first molar.

Moreover, to measure the amount of skeletal expansion on all the models, around 10 nodes were selected at several regions (Figure 3.11). The areas were

designated at the maximum convexity of the cervical region of the alveolar bone. Three regions were considered which are at the level of the central incisor, first premolar and first molar which correspond to the anterior, middle, and posterior expansion respectively.

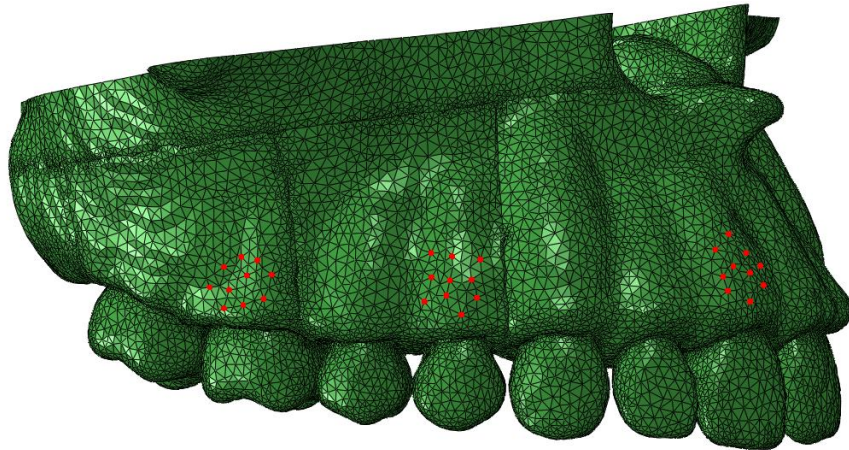


Figure 3.11: Lateral view of the right side of the model with selected nodes in the 3 regions to measure the amount of expansion.

After running the finite element analysis, the stress and displacement results were exported as “*DAT.*” files into Excel (Microsoft Excel, Office16, United States of America) where the averages were calculated. Finally, the averages were put in the final data sheets. As usual, FEA results were evaluated using color mapped representations and arrows. However, to assess individual variations, statistical analysis was applied on the numerical data.

3.3 Statistical Analysis

Descriptive statistics (means and standard deviations) were generated for the stresses on the first premolars and first molars, as well as the expansion at the molars, premolars and incisors regions for the 5 setups. The Shapiro-Wilk normality test was used to determine if the outcome variables have a normal distribution. The Friedman test for non-parametric data was employed to compare the means of the stress and expansion variables among the different setups, followed by pairwise comparisons using the Wilcoxon test. A Bonferroni adjusted p-value was used to evaluate the significance of the pairwise comparisons tests.

The paired samples t-test was conducted to compare the means of the cortical bone thicknesses between the buccal and palatal areas, as well as the stresses between the first premolars and first molars among all the setups. The paired samples t-test was also used to compare the means of the stress values depicted on each tooth within the arch between setups 3 and 4.

Associations between parameters were evaluated through the Spearman product moment, specifically the stresses teeth, the expansion between the different regions and bone thickness within and across all setups.

All statistical analyses were performed using SPSS statistical software and the level of significance was set at 0.05.

CHAPTER 4

RESULTS

4.1 Descriptive Data

4.1.1 Stress on the teeth

The stress was observed in setups 1 and 2 (expansion without added arch wires) only on the anchor teeth of the RPE namely, the first premolars and first molars (Table 4.1, Figures 4.1, 4.2). However, in setups 3 and 4 (expansion with added arch wires), stress was observed on all the teeth (Table 4.2, Figures 4.3, 4.4). The individual and mean stresses of all the setups on the first premolar (4.95 ± 0.33 MPa) higher than on the first molar (4.77 ± 0.36 MPa). The highest stresses on the premolars and molars were in setup 1 (5.05 MPa and 4.85 MPa, respectively). Setups 3 and 4 had the lowest amount of stress on both teeth.

Table 4.1: Descriptive statistics for the stress on the first premolars and first molars.

Stress	Setup number	Number of models	Mean	SD	CI for mean		Range
					lower bound	upper bound	
at PM1	1	13	5.05	0.34	4.84	5.25	4.06-5.36
	2	13	4.99	0.31	4.81	5.18	4.14-5.23
	3	13	4.87	0.33	4.67	5.07	3.94-5.2
	4	13	4.89	0.35	4.68	5.10	3.81-5.22
	<i>Total</i>	52	4.95	0.33	4.86	5.04	3.81-5.36
at M1	1	13	4.85	0.37	4.62	5.07	4.13-5.23
	2	13	4.82	0.37	4.59	5.04	4.05-5.08
	3	13	4.70	0.33	4.50	4.90	4.03-5.05
	4	13	4.71	0.37	4.48	4.93	4.04-5.18
	<i>Total</i>	52	4.77	0.36	4.67	4.87	4.03-5.23

Stress in MPa; **SD**: Standard deviation; **CI**: Confidence interval; **PM1**: first premolar; **M1**: first molar.

Table 4.2: Descriptive statistics for the stresses on all teeth for setups 3 and 4.

Stress	Setup number	Mean	SD
at IN1	3	0.43	0.05
	4	0.48	0.05
at IN2	3	0.43	0.04
	4	0.49	0.04
at C	3	0.70	0.08
	4	0.72	0.05
at PM1	3	4.87	0.33
	4	4.89	0.35
at PM2	3	0.75	0.12
	4	0.75	0.12
at M1	3	4.70	0.33
	4	4.71	0.37
at M2	3	0.50	1.07
	4	0.17	0.06

Stress in MPa; **SD:** Standard deviation; **IN1:** central incisor; **IN2:** lateral incisor; **C:** canine; **PM1:** first premolar; **PM2:** second premolar; **M1:** first molar; **M2:** second molar.

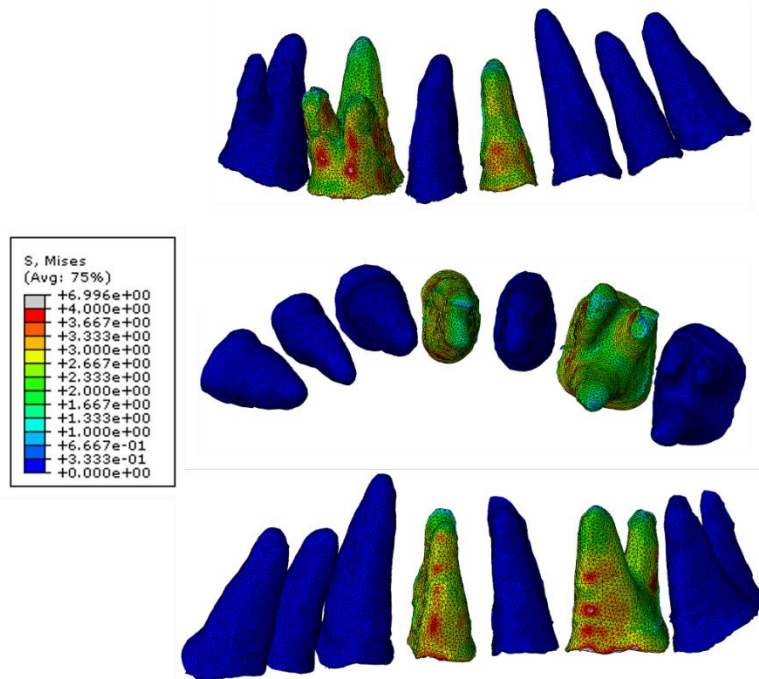


Figure 4.1: Von mises stress distribution on the PDL of the teeth in setup 1, buccally, occlusally and palatally respectively. The stresses were at the first premolars and first molars (5.05 MPa and 4.85, respectively) higher on the buccal side than on the palatal side. On the buccal surface, the stresses were concentrated on the middle and cervical thirds of the PDL surface, while on the palatal side the stresses were distributed all over the PDL surface.

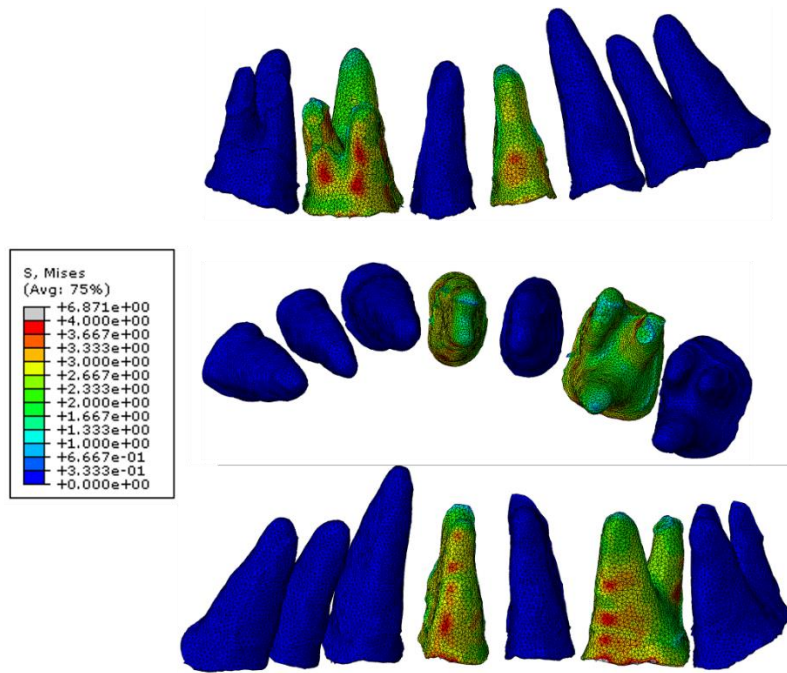


Figure 4.2: Von mises stress distribution on the PDL of the teeth in setup 2, buccally, occlusally and palatally respectively. The stresses were at the first premolars and first molars (4.99 MPa and 4.82 MPa, respectively) with similar pattern of distribution to setup 1.

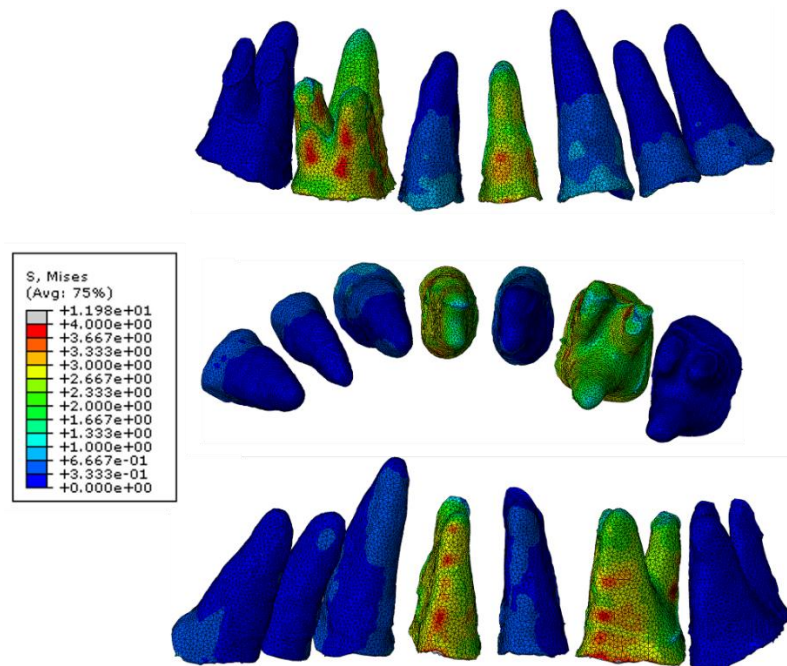


Figure 4.3: Von mises stress distribution on the PDL of the teeth in setup 3, buccally, occlusally and palatally respectively. The stresses were distributed on all the teeth and were highest at the first premolars and first molars (4.87 MPa and 4.70 MPa, respectively), with similar pattern of distribution to setups 1 and 2, but of less intensity.

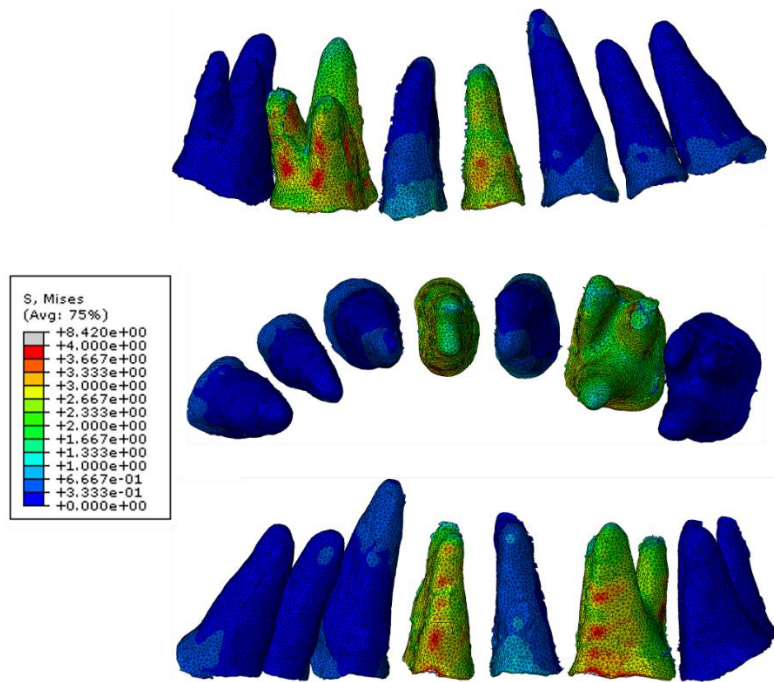


Figure 4.4: Von mises stress distribution on the PDL of the teeth in setup 4, buccally, occlusally and palatally respectively. The stresses were distributed on all the teeth and were highest at the first premolars and first molars (4.89 MPa and 4.71 MPa, respectively), with similar pattern of distribution to setups 1 and 2, but of less intensity.

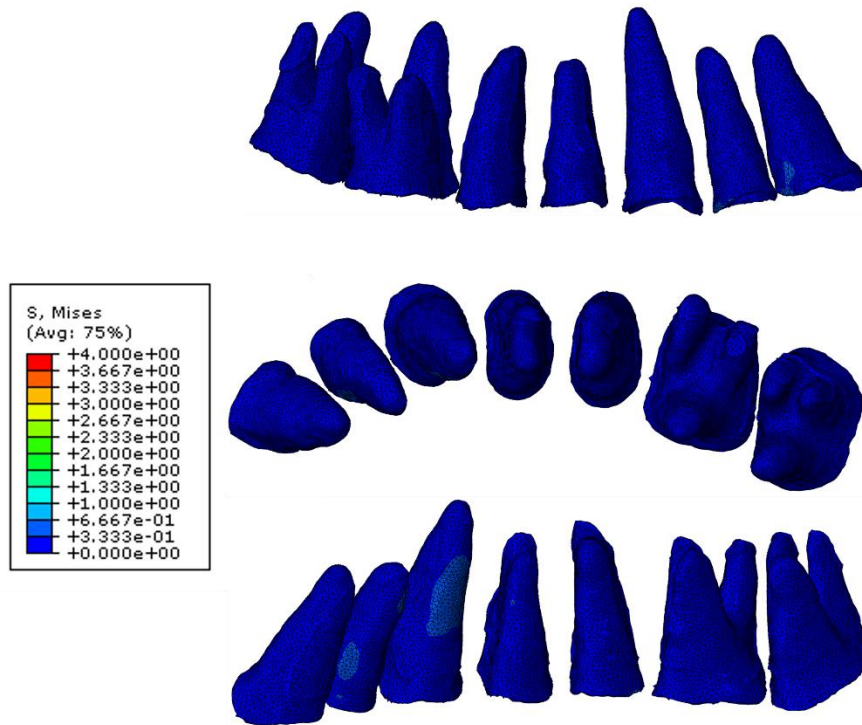


Figure 4.5: Von mises stress distribution on the PDL of the teeth in setup 5. No stress was observed on the teeth.

4.1.2 Expansion within the different setups

The mean expansion was higher at the posterior teeth, (0.76 ± 0.76 mm at the molars and 0.58 ± 0.42 mm at the premolars) than at the incisors (0.36 ± 0.35 mm) (Table 4.3). Setups 1, 2, 3, and 4 had the highest amount of expansion at the molars (Figures 4.6 – 4.9); however, in setup 5 the highest amount of expansion was at the incisors (Figure 4.10). Moreover, more expansion occurred posteriorly with setups 1, 2, 3, and 4 that decreased gradually towards the incisors. An opposite trend was observed in setup 5, the expansion averaging 1.01 ± 0.19 mm anteriorly and decreasing at the posterior teeth (0.89 ± 0.13 mm at the premolars, 0.54 ± 0.09 mm at the molars) (Figure 4.11).

Table 4.3: Descriptive statistics for the expansion at the molars (M), premolars (PM) and incisors (IN).

Expansion	Setup number	Number of models	Mean	SD	CI for mean		Range
					lower bound	upper bound	
at M	1	13	0.70	0.73	0.26	1.14	0.15-2.25
	2	13	0.83	0.91	0.28	1.38	0.26-2.65
	3	13	0.87	0.86	0.35	1.39	0.34-2.7
	4	13	0.88	0.92	0.32	1.43	0.28-2.81
	5	13	0.54	0.09	0.49	0.60	0.41-0.73
	<i>Total</i>	65	0.76	0.76	0.58	0.95	0.15-2.81
at PM	1	13	0.36	0.27	0.20	0.52	0.14-1.14
	2	13	0.50	0.42	0.25	0.76	0.21-1.66
	3	13	0.56	0.48	0.27	0.86	0.27-1.98
	4	13	0.56	0.52	0.25	0.88	0.24-2.11
	5	13	0.89	0.13	0.81	0.97	0.67-1.16
	<i>Total</i>	65	0.58	0.42	0.47	0.68	0.14-2.11
at IN	1	13	0.16	0.10	0.10	0.22	0.06-0.44
	2	13	0.18	0.11	0.11	0.24	0.09-0.48
	3	13	0.22	0.11	0.15	0.28	0.12-0.5
	4	13	0.22	0.12	0.15	0.29	0.12-0.53
	5	13	1.01	0.19	0.90	1.13	0.8-1.32
	<i>Total</i>	65	0.36	0.35	0.27	0.45	0.06-1.32

Expansion in mm; **SD:** Standard deviation; **CI:** Confidence interval.

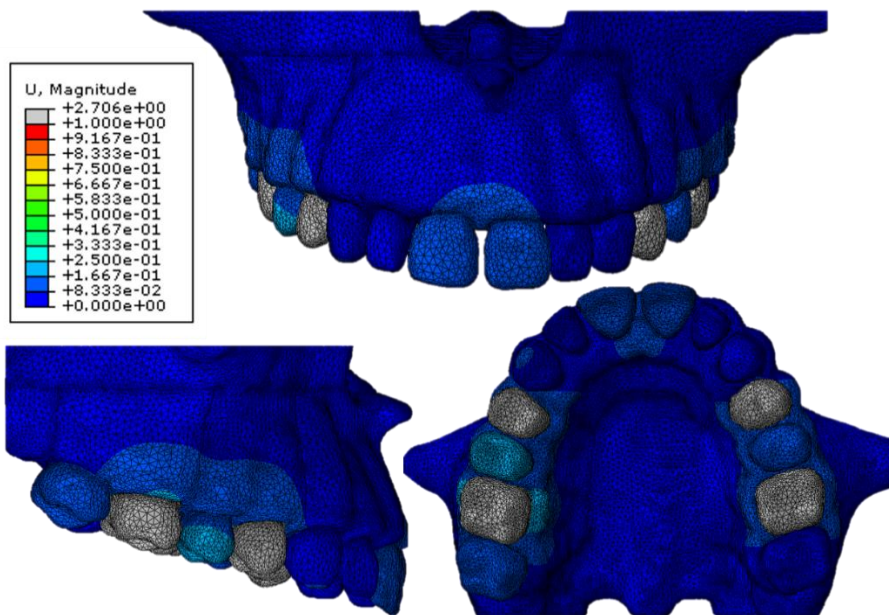


Figure 4.6: Expansion in setup 1.

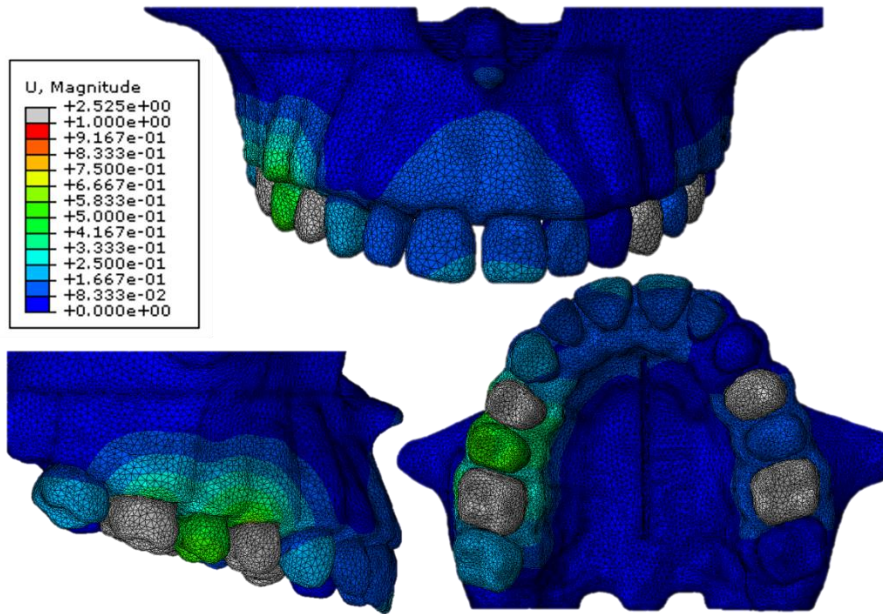


Figure 4.7: Expansion in setup 2.

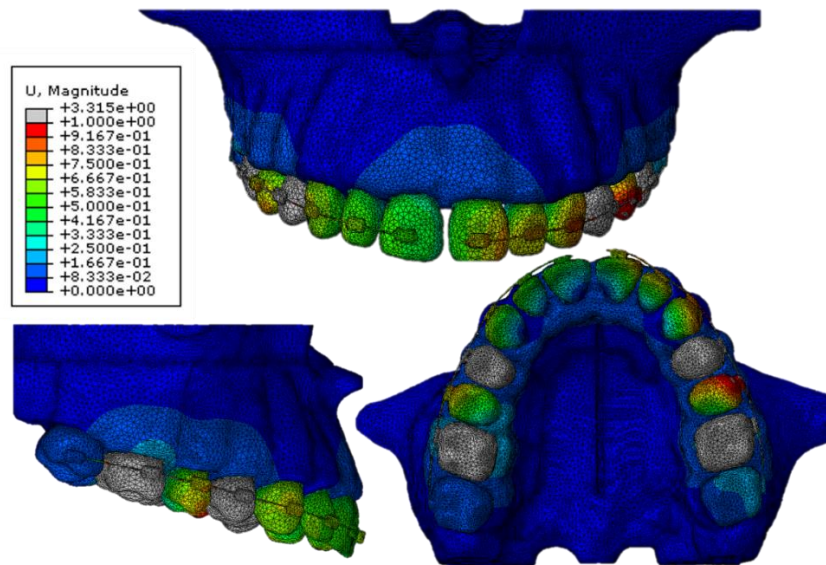


Figure 4.8: Expansion in setup 3.

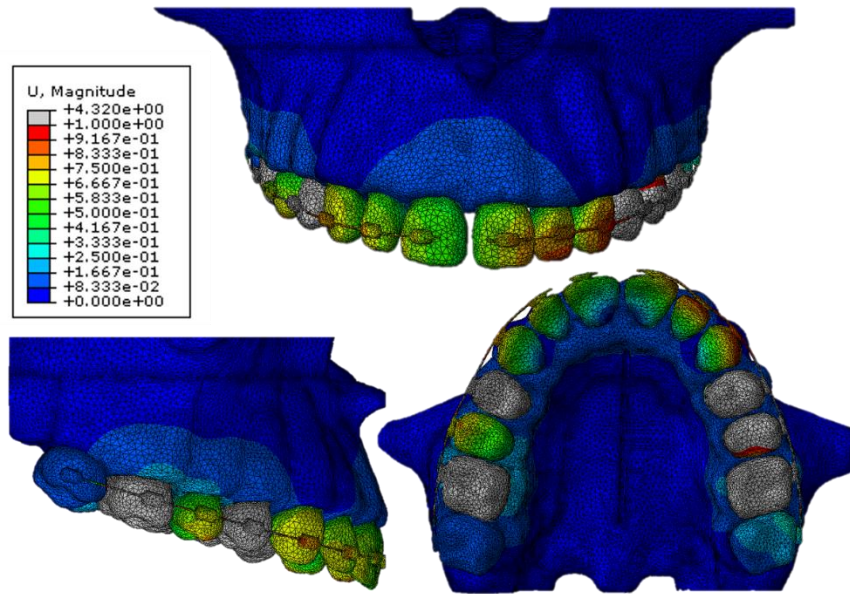


Figure 4.9: Expansion in setup 4.

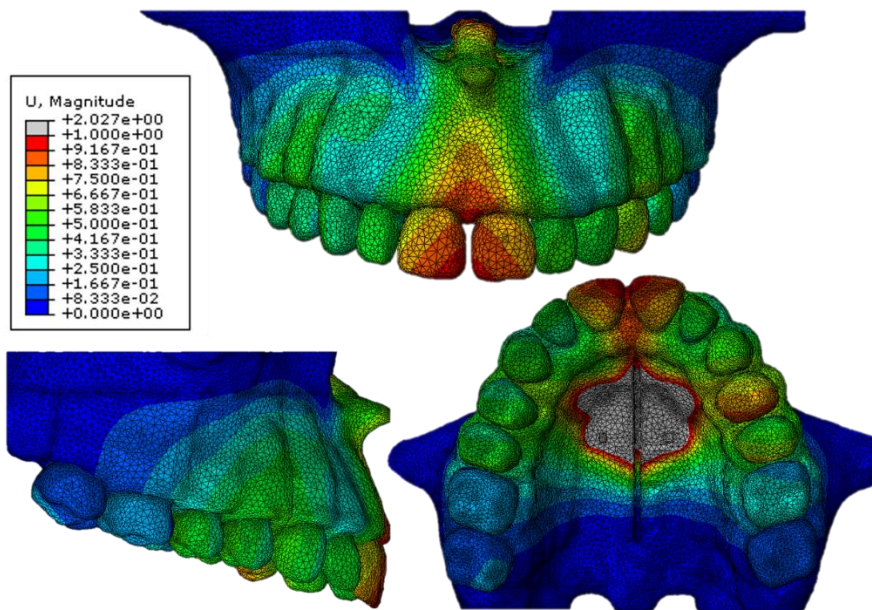


Figure 4.10: Expansion in setup 5.

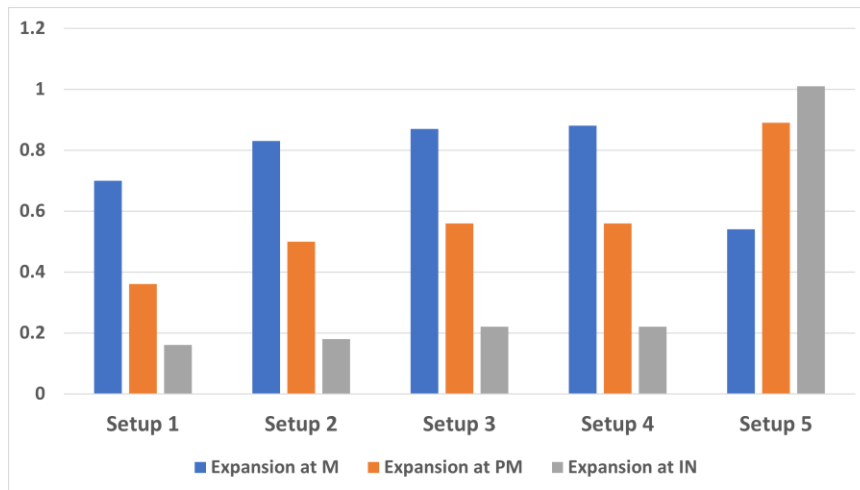


Figure 4.11: A bar graph representing the expansion at the molars (M), premolars (PM) and incisors (IN) in all setups.

4.1.3 Cortical bone thickness in different regions

All buccal and palatal thicknesses differed from each other except at the premolars; the mean thicknesses of both regions were approximately equal (Table 4.4). The highest thickness mean value was at the buccal level of the incisors (2.46 ± 1.68 mm). The lowest mean thickness was at the palatal side of these teeth (1.74 ± 0.58 mm).

Table 4.4: Descriptive statistics of the cortical bone thickness in different regions.

	Number of Models	Mean	SD
BThickM	13	2.07	0.93
PThickM	13	1.97	0.95
BthickPM	13	2.41	1.46
PThickPM	13	2.40	1.14
BThickIN	13	2.46	1.68
PThickIN	13	1.74	0.58

Cortical bone thickness (**Thick**) in mm: **B**: buccal; **P**: palatal; **M**: average first and second molars; **PM**: average first and second premolars; **IN**: incisors. **SD**: Standard deviation.

4.2 Comparison of stresses between setups

The stresses were statistically significantly different on the first premolars between setups 1 and 3. The stresses on the first molars were statistically significant between setups 1 and 3, and 1 and 4 (Table 4.5).

Table 4.5: Pairwise comparison (Wilcoxon test) of the stresses of the first premolars and molars between different setups.

Setup Numbers	Stress at PM1	Stress at M1
Setup 1-2	1	1
Setup 1-3	0.005*	0.005*
Setup 1-4	0.009	0.005*
Setup 2-3	0.023	0.014
Setup 2-4	0.037	0.014
Setup 3-4	1	1

*Significant at $p < 0.008$. **PM1**: first premolar; **M1**: first molar.

4.3 Comparison of expansion between setups

The expansion was statistically significant at the molars and premolars regions with all the setups compared to setup 1 except with setup 5 at the molars region (Table 4.6). At the incisors, all the differences were statistically significant except between setups 3-4.

Table 4.6: Pairwise comparison (Wilcoxon test) of the expansion at the molars (M), premolars (PM), and incisors (IN) between different setups.

Setup numbers	Expansion		
	M	PM	IN
Setup 1-2	0.001*	0.001*	0.001*
Setup 1-3	0.001*	0.002*	0.001*
Setup 1-4	0.001*	0.001*	0.001*
Setup 1-5	0.507	0.002*	0.001*
Setup 2-3	0.023	0.019	0.002*
Setup 2-4	0.016	0.011	0.001*
Setup 2-5	0.507	0.016	0.001*
Setup 3-4	0.552	0.917	0.345
Setup 3-5	0.6	0.023	0.001*
Setup 4-5	0.552	0.023	0.001*

*Significant at $p < 0.005$.

4.4 Comparisons of stress, bone thickness, and expansion across setups

In comparisons across setups through the Friedman test, the stresses on the first premolars and molars, and the regional expansions (posterior, middle, and anterior) were statistically significantly different ($p= 0.001$; Table 4.7).

Table 4.7: Results of the Friedman test between the different setups 1,2,3,4 and 5.

	p-value
Stress at PM1	0.001*
Stress at M1	0.001*
Expansion at M	0.001*
Expansion at PM	0.001*
Expansion at IN	0.001*

*Significant at $p<0.05$. **PM1**: first premolar; **M1**: first molar; **M**: molars; **PM**: premolars; **IN**: incisors.

When comparing the stresses at the first premolars to those at the first molars across all setups, the difference was statistically significant ($p < 0.001$; Table 4.8).

Parallel comparisons between the cortical bone thicknesses at the palatal and buccal regions of the molars, premolars, and incisors did not reveal significant differences.

Table 4.8: Results of the paired t-test to compare the differences between stresses on the first premolars (PM1) and molars (M1) and between cortical bone thicknesses at the molar, premolar, and incisor regions.

Pairs	Mean	SD	P-value
Stress at PM1 – Stress at M1	0.18	0.24	0.001*
BThickM - PThickM	0.09	0.90	0.719
BthickPM - PThickPM	0.01	0.64	0.963
BThickIN - PThickIN	0.71	1.45	0.1

*Significant at $p<0.05$. **PM1**: first premolar; **M1**: first molar. Cortical bone thickness (**Thick**): B: buccal; P: palatal; M: average first and second molars; **PM**: average first and second premolars; IN, incisors.

When setups 3 and 4 were compared, the mean differences between the stresses on the central and lateral incisors were statistically significant ($p=0.013$ and $p=0.009$, respectively- Table 4.9). The stresses measured on the rest of the dentition were not significantly different. The resultant expansion at the molar, premolar and incisor regions also were not significantly different.

Table 4.9: Results of the paired t-test to compare the different variables between setups 3 and 4.

Paired Sample Test (Paired Differences)			
Pairs below correspond to setups 3 and 4	Mean	SD	p-value
Stress at IN1	-0.06	0.07	0.013*
Stress at IN2	-0.05	0.06	0.009*
Stress at C	-0.02	0.11	0.468
Stress at PM1	-0.03	0.12	0.469
Stress at PM2	-0.01	0.097	0.969
Stress at M1	0.00	0.10	0.857
Stress at M2	0.32	1.03	0.277
Expansion at M	-0.01	0.09	0.692
Expansion at PM	0.00	0.07	0.935
Expansion at IN	0.00	0.03	0.546

*Significant at $p < 0.05$. **IN1**: central incisor; **IN2**: lateral incisor; **C**: canine; **PM1**: first premolar; **PM2**: second premolar; **M1**: first molar; **M2**: second molar; **M**: molars; **PM**: premolars; **IN**: incisors.

Setup 1 represented the highest amount of stresses at the premolars and molars with the least amount of expansion within all the models. Setups 3 and 4 showed similar

results with the least amount of stresses and highest amount of expansion (Figs 4.12 – 4.15).

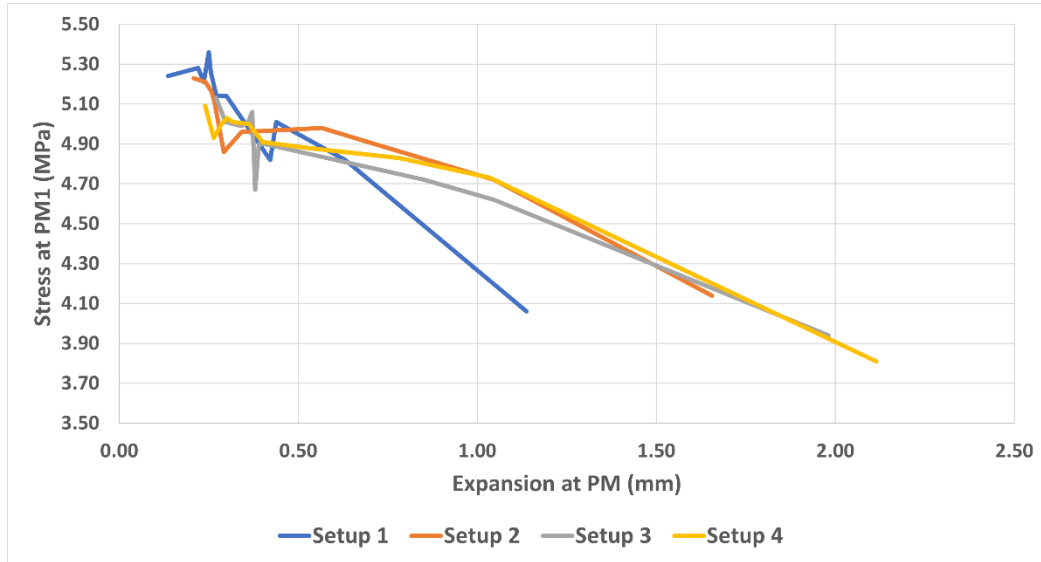


Figure 4.12: A graph representing the effect of expansion at the premolars (PM) region on the stress at the first premolars (PM1) across the different setups.

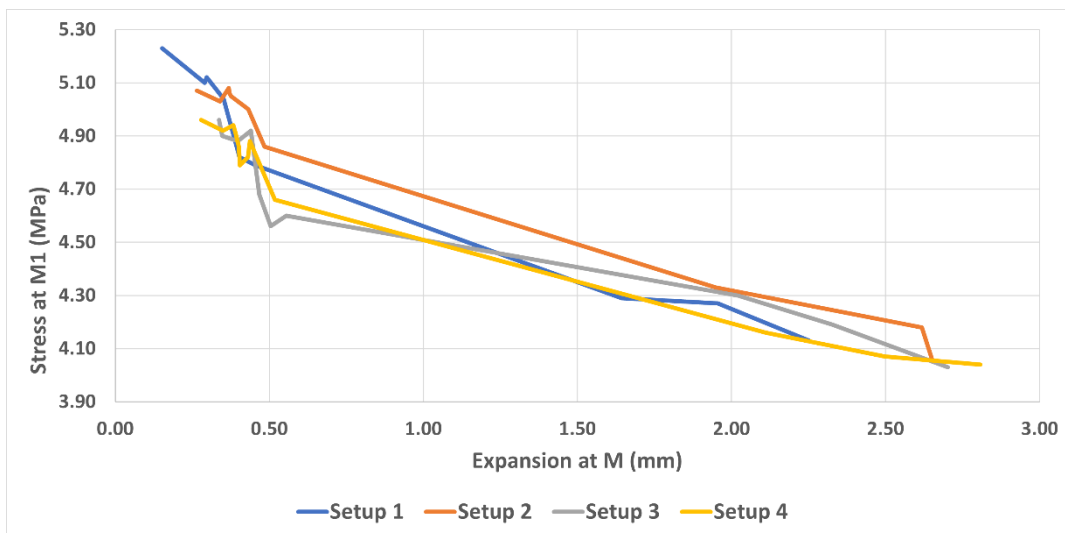


Figure 4.13: A graph representing the effect of expansion at the molars (M) region on the stress at the first molars (M1) across the different setups.

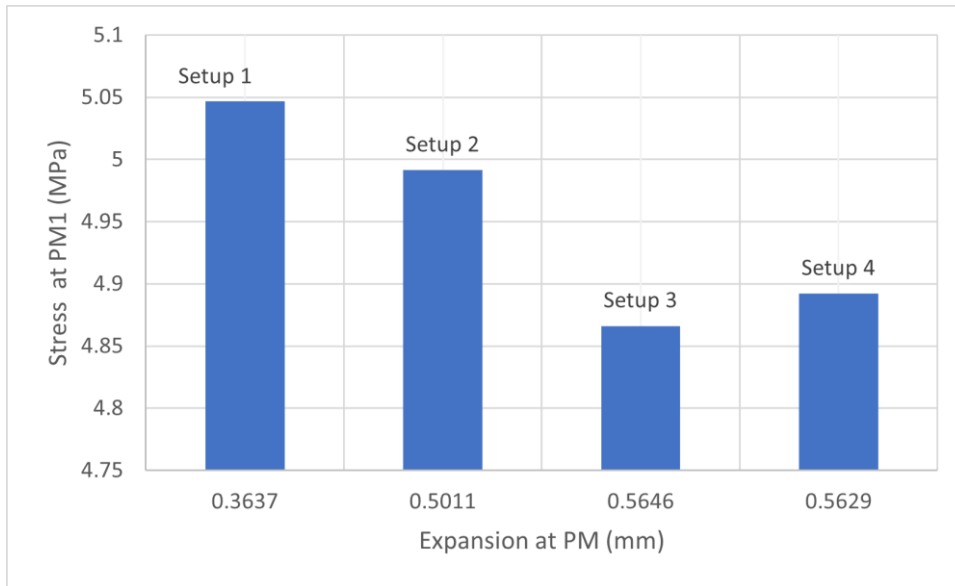


Figure 4.14: A bar graph showing the mean expansion at the premolars (PM) with respect to the mean stresses at the first premolars (PM1) across the different setups.

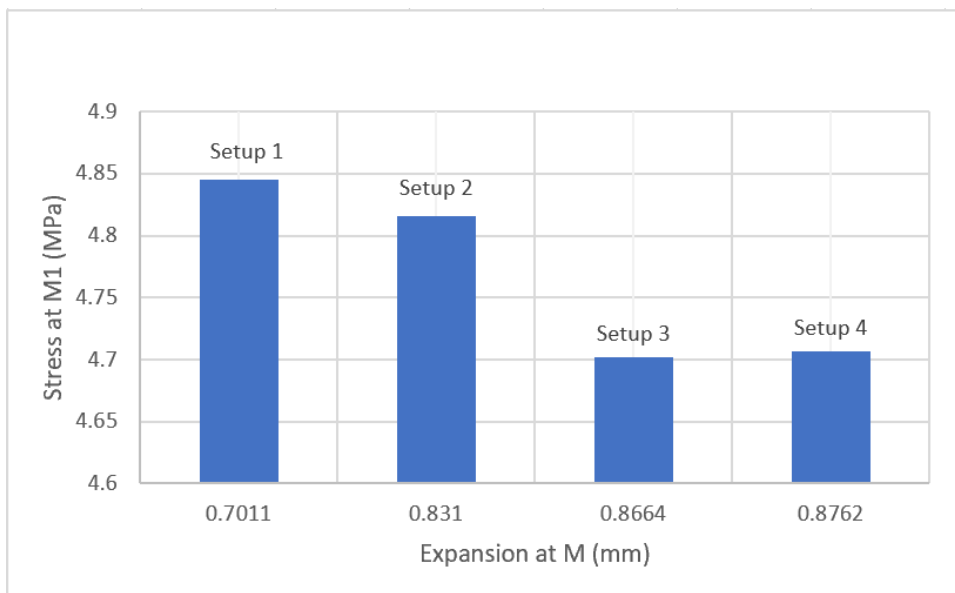


Figure 4.15: A bar graph showing the mean expansion at the molars (M) with respect to the mean stresses at the first molars (M1) across the different setups.

4.5 Correlations between variables within each setup

In setup 1, the stresses at PM1 were positively correlated to those at the M1 (Table 4.10). The stresses at the PM1 and M1 were strongly negatively correlated to the expansion at the molar, premolar and incisor regions. The highest correlation was between the stresses at the PM1 and the expansion at the premolars region ($r = -0.961$) and between the stresses at the M1 and the expansion at the molars region ($r = -0.956$).

The stresses on the first premolars were not correlated to the different cortical bone thicknesses, whereas the stresses at the first molars were positively correlated to the cortical bone thicknesses and significant at the buccal and palatal molars regions and palatal premolars region.

Similar trends were observed in setup 2, but with higher correlation coefficient values for the stresses and the expansion (Table 4.11). In contrast to setup 1, the stresses at PM1 and M1 were positively correlated to the cortical bone thicknesses and showed significant correlations at the buccal and palatal molars regions and palatal incisors region. In addition, the palatal premolar cortical bone thickness was significantly correlated with the stresses at the M1.

The difference between the two setups is that stresses at PM1 and M1 showed significant correlations with the palatal bone thickness at the incisors in setup 2 only.

The expansion regions were positively correlated to each other; the highest between the premolars and incisors ($r = +0.971$ in setup 1 and $r = +0.978$ in setup 2).

In both setups 1 and 2, the cortical bone thicknesses were positively correlated to each other; the highest correlation was between the buccal and palatal bone thicknesses ($r = +0.909$).

The expansion was negatively correlated to the cortical bone thickness in both setups; the highest correlation was between the expansion at the molars with the palatal bone thickness at the premolars ($r = -0.741$ in setup 1 and $r = -0.724$ in setup 2). The correlation coefficient values were lower in setup 2 compared to setup 1 except between the expansion at the three regions with the palatal bone thickness at the incisors which showed higher values in setup 2.

Table 4.10: Correlation of the stress, expansion, and cortical bone thickness for setup 1.

	Stress at PM1	Stress at M1	Expansion at M	Expansion at PM	Expansion at IN	BThickM	BThickPM	BThickIN	PThickM	PThickPM	PThickIN
Stress at PM1	1	0.713**	-0.724**	-0.961**	-0.907**	0.479	0.329	0.392	0.298	0.473	0.445
		0.006	0.005	0.000	0.000	0.097	0.272	0.186	0.322	0.103	0.128
Stress at M1		1	-0.956**	-0.796**	-0.825**	0.701**	0.434	0.371	0.623*	0.658*	0.47
			0.000	0.001	0.001	0.008	0.139	0.212	0.023	0.014	0.105
Expansion at M			1	0.827**	0.874**	-0.681*	-0.589*	-0.399	-0.671*	-0.741**	-0.650*
				0.000	0.000	0.01	0.034	0.177	0.012	0.004	0.016
Expansion at PM				1	0.971**	-0.618*	-0.471	-0.415	-0.513	-0.599*	-0.594*
					0.000	0.025	0.105	0.158	0.073	0.031	0.032
Expansion at IN					1	-0.675*	-0.555*	-0.46	-0.579*	-0.665*	-0.636*
						0.011	0.049	0.113	0.038	0.013	0.02
BThickM						1	0.666*	0.572*	0.538	0.835**	0.466
							0.013	0.041	0.058	0.000	0.109
BThickPM							1	0.528	0.434	0.909**	0.715**
								0.064	0.138	0.000	0.006
BThickIN								1	0.072	0.524	0.542
									0.815	0.066	0.055
PThickM									1	0.557*	0.655*
										0.048	0.015
PThickPM										1	0.672*
											0.012
PThickIN											1

Correlation is significant at the: *0.05 level (2-tailed); **0.01 level (2-tailed). **PM1**: first premolar; **M1**: first molar; **M**: molars; **PM**: premolars; **IN**: incisors. Cortical bone thickness (**Thick**): **B**: buccal; **P**: palatal; **M**: average first and second molars; **PM**: average first and second premolars; **IN**: incisors.

Table 4.11: Correlation of the stress, expansion, and cortical bone thickness for setup 2.

	Stress at PM1	Stress at M1	Expansion at M	Expansion at PM	Expansion at IN	BThickM	BThickPM	BThickIN	PThickM	PThickPM	PThickIN
Stress at PM1	1	0.775**	-0.822**	-0.934**	-0.970**	0.609*	0.423	0.376	0.568*	0.548	0.608*
		0.002	0.001	0.000	0.000	0.027	0.15	0.206	0.043	0.052	0.028
Stress at M1		1	-0.986**	-0.875**	-0.832**	0.650*	0.499	0.341	0.670*	0.690**	0.595*
			0.000	0.000	0.000	0.016	0.083	0.254	0.012	0.009	0.032
Expansion at M			1	0.920**	0.891**	-0.650*	-0.580*	-0.379	-0.663*	-0.724**	-0.655*
				0.000	0.000	0.016	0.038	0.202	0.013	0.005	0.015
Expansion at PM				1	0.978**	-0.608*	-0.494	-0.413	-0.54	-0.624*	-0.615*
					0.000	0.027	0.086	0.161	0.057	0.023	0.025
Expansion at IN					1	-0.637*	-0.547	-0.456	-0.55	-0.650*	-0.646*
						0.019	0.053	0.117	0.051	0.016	0.017
BThickM						1	0.666*	0.572*	0.538	0.835**	0.466
							0.013	0.041	0.058	0.000	0.109
BThickPM							1	0.528	0.434	0.909**	0.715**
								0.064	0.138	0.000	0.006
BThickIN								1	0.072	0.524	0.542
									0.815	0.066	0.055
PThickM									1	0.557*	0.655*
										0.048	0.015
PThickPM										1	0.672*
											0.012
PThickIN											1

Correlation is significant at the: *0.05 level (2-tailed); **0.01 level (2-tailed). **PM1**: first premolar; **M1**: first molar; **M**: molars; **PM**: premolars; **IN**: incisors. Cortical bone thickness (**Thick**): **B**: buccal; **P**: palatal; **M**: average first and second molars; **PM**: average first and second premolars; **IN**: incisors.

In setup 3, stresses among adjacent teeth were strongly correlated: between the central incisor and the lateral incisor and canine ($r = +0.926$ and $r = +0.842$, respectively; Table 4.12); between the lateral incisor and the canine ($r = +0.912$); between PM1 and M1 ($r = +0.831$). In contrast, the stress at PM1 was negatively correlated to the stress at the second molar ($r = -0.868$). However, setup 4 showed lower correlation coefficients among the stresses on the teeth in comparison to setup 3 except between M1 and M2, which showed a strong negative correlation ($r = -0.952$; Table 4.13). In addition, no correlation was observed between the stress at the lateral incisor and canine in setup 4.

The expansion at the three different regions were all positively correlated to each other with slightly lower values in setup 4.

In setups 3 and 4, the stresses at PM1 and M1 correlated negatively with the expansion at the three regions, in contrast to positive correlations at the second molars. All correlations were higher in setup 4 than in setup 3.

Correlations between stresses and cortical bone thickness were mainly positive in setups 3 and 4. In setup 3, the stresses on the central and lateral incisors were correlated to buccal bone thickness at the incisors; the stress on the PM1 was significantly positively correlated to the buccal and palatal bone thicknesses at the molars. Stress on M1 was also correlated to the buccal and palatal bone thicknesses at the molars and the palatal bone thickness at the premolars in both setups. However, no correlations were observed in setup 4 between stresses at the incisors and the premolars with the cortical bone thicknesses.

The expansion in setups 3 and 4 were negatively correlated to the cortical bone thickness. No significant correlations were found between the expansion at the three regions and the buccal bone thickness at the incisors.

Cortical bone thicknesses at the different regions were positively correlated to each other in both setups with similar significance values.

In setup 5, the expansion at the molars was positively correlated to the expansion at the premolars but was negatively correlated to the expansion at the incisors ($r = +0.878$ and $r = -0.582$, respectively; Table 4.14). Moreover, the expansion at the molars, premolars and incisors was not correlated to any of the cortical bone thickness regions.

Table 4.12: Correlation of the stress, expansion, and cortical bone thickness for setup 3.

	Stress at IN1	Stress at IN2	Stress at C	Stress at PM1	Stress at PM2	Stress at M1	Stress at M2	Expansion at M	Expansion at PM	Expansion at IN	BThickM	BThickPM	BThickIN	PThickM	PThickPM	PThickIN
Stress at IN1	1	0.926**	0.842**	0.39	-0.132	0.358	-0.351	-0.388	-0.401	-0.377	0.514	0.384	0.626*	0.09	0.47	0.456
		0.000	0.000	0.188	0.667	0.23	0.24	0.191	0.174	0.205	0.073	0.196	0.022	0.77	0.105	0.118
Stress at IN2		1	0.912**	0.232	-0.272	0.252	-0.217	-0.276	-0.253	-0.217	0.513	0.385	0.563*	-0.032	0.45	0.365
			0.000	0.445	0.369	0.406	0.477	0.361	0.403	0.477	0.073	0.193	0.045	0.918	0.123	0.22
Stress at C			1	0.009	-0.257	0.023	0.023	-0.015	0.023	0.056	0.217	0.122	0.356	-0.141	0.151	0.2
				0.976	0.397	0.941	0.941	0.96	0.942	0.856	0.476	0.692	0.233	0.646	0.622	0.513
Stress at PM1				1	0.393	0.831**	-0.868**	-0.770**	-0.934**	-0.842**	0.560*	0.337	0.164	0.605*	0.529	0.475
					0.184	0.000	0.000	0.002	0.000	0.000	0.047	0.26	0.592	0.028	0.063	0.101
Stress at PM2					1	0.39	-0.233	-0.294	-0.32	-0.455	0.116	0.004	-0.311	0.422	0.003	0.066
						0.188	0.444	0.33	0.287	0.118	0.707	0.989	0.301	0.151	0.993	0.832
Stress at M1						1	-0.513	-0.937**	-0.798**	-0.738**	0.673*	0.467	0.226	0.690**	0.668*	0.526
							0.073	0.000	0.001	0.004	0.012	0.107	0.458	0.009	0.013	0.065
Stress at M2							1	0.559*	0.905**	0.836**	-0.376	-0.33	-0.226	-0.358	-0.394	-0.442
								0.047	0.000	0.000	0.205	0.27	0.458	0.23	0.183	0.13
Expansion at M								1	0.857**	0.831**	-0.621*	-0.555*	-0.365	-0.667*	-0.697**	-0.642*
									0.000	0.000	0.024	0.049	0.22	0.013	0.008	0.018
Expansion at PM									1	0.950**	-0.542	-0.498	-0.315	-0.579*	-0.604*	-0.613*
										0.000	0.056	0.083	0.295	0.038	0.029	0.026
Expansion at IN										1	-0.568*	-0.582*	-0.377	-0.637*	-0.632*	-0.705**
											0.043	0.037	0.205	0.019	0.02	0.007
BThickM											1	0.666*	0.572*	0.538	0.835**	0.466
												0.013	0.041	0.058	0.000	0.109
BThickPM												1	0.528	0.434	0.909**	0.715**
													0.064	0.138	0.000	0.006
BThickIN													1	0.072	0.524	0.542
														0.815	0.066	0.055
PThickM														1	0.557*	0.655*
															0.048	0.015
PThickPM															1	0.672*
																0.012
PThickIN																1

Correlation is significant at the: *0.05 level (2-tailed); **0.01 level (2-tailed). IN1: central incisor; IN2: lateral incisor; C: canine; PM1: first premolar; PM2: second premolar; M1: first molar; M2: second molar; M: molars; PM: premolars; IN: incisors. Cortical bone thickness (Thick): B: buccal; P: palatal; M: average first and second molars; PM: average first and second premolars; IN: incisors.

Table 4.13: Correlation of the stress, expansion, and cortical bone thickness for setup 4.

	Stress at IN1	Stress at IN2	Stress at C	Stress at PM1	Stress at PM2	Stress at M1	Stress at M2	Expansion at M	Expansion at PM	Expansion at IN	BThickM	BThickPM	BThickIN	PThickM	PThickPM	PThickIN
Stress at IN1	1	0.797**	0.666*	0.243	0.321	0.3	-0.237	-0.208	-0.228	-0.263	0.011	-0.11	-0.438	0.449	0.111	0.106
		0.001	0.013	0.423	0.286	0.319	0.435	0.495	0.454	0.385	0.971	0.721	0.135	0.123	0.717	0.731
Stress at IN2		1	0.523	0.462	0.146	0.482	-0.411	-0.35	-0.408	-0.345	0.092	-0.147	-0.384	0.561*	0.097	0.223
			0.067	0.112	0.634	0.095	0.163	0.241	0.166	0.249	0.766	0.631	0.195	0.046	0.753	0.464
Stress at C			1	-0.041	-0.054	0.18	-0.126	-0.187	0.005	-0.006	-0.432	-0.158	-0.482	0.29	-0.117	0.149
				0.895	0.86	0.556	0.682	0.54	0.987	0.985	0.14	0.606	0.095	0.337	0.703	0.627
Stress at PM1				1	0.034	0.737**	-0.855**	-0.719**	-0.956**	-0.846**	0.471	0.283	0.282	0.421	0.454	0.43
					0.913	0.004	0.000	0.006	0.000	0.000	0.105	0.349	0.351	0.152	0.119	0.143
Stress at PM2					1	0.047	-0.091	-0.08	-0.187	-0.374	0.391	0.386	-0.063	0.502	0.303	0.251
						0.878	0.769	0.795	0.541	0.208	0.187	0.193	0.838	0.08	0.314	0.407
Stress at M1						1	-0.952**	-0.957**	-0.808**	-0.740**	0.650*	0.5	0.26	0.677*	0.707**	0.524
							0.000	0.000	0.001	0.004	0.016	0.082	0.391	0.011	0.007	0.066
Stress at M2							1	0.972**	0.933**	0.887**	-0.639*	-0.551	-0.364	-0.628*	-0.706**	-0.622*
								0.000	0.000	0.000	0.019	0.051	0.221	0.021	0.007	0.023
Expansion at M								1	0.835**	0.825**	-0.654*	-0.580*	-0.381	-0.670*	-0.729**	-0.645*
									0.000	0.001	0.015	0.038	0.199	0.012	0.005	0.017
Expansion at PM									1	0.945**	-0.575*	-0.484	-0.356	-0.522	-0.599*	-0.586*
										0.000	0.04	0.094	0.233	0.067	0.031	0.035
Expansion at IN										1	-0.663*	-0.563*	-0.445	-0.579*	-0.661*	-0.663*
											0.014	0.045	0.127	0.038	0.014	0.013
BThickM											1	0.666*	0.572*	0.538	0.835**	0.466
												0.013	0.041	0.058	0.000	0.109
BThickPM												1	0.528	0.434	0.909**	0.715**
													0.064	0.138	0.000	0.006
BThickIN													1	0.072	0.524	0.542
														0.815	0.066	0.055
PThickM														1	0.557*	0.655*
															0.048	0.015
PThickPM															1	0.672*
																0.012
PThickIN																1

Correlation is significant at the: *0.05 level (2-tailed); **0.01 level (2-tailed). IN1: central incisor; IN2: lateral incisor; C: canine; PM1: first premolar; PM2: second premolar; M1: first molar; M2: second molar; M: molars; PM: premolars; IN: incisors. Cortical bone thickness (Thick): B: buccal; P: palatal; M: average first and second molars; PM: average first and second premolars; IN: incisors.

Table 4.14: Correlation of the expansion and the cortical bone thickness for setup 5.

	Expansion at M	Expansion at PM	Expansion at IN	BThickM	BThickPM	BThickIN	PThickM	PThickPM	PThickIN
Expansion at M	1	0.878**	-0.582*	-0.258	0.124	-0.131	-0.328	-0.085	-0.156
		0.000	0.037	0.395	0.687	0.669	0.275	0.781	0.61
Expansion at PM		1	-0.551	-0.413	-0.072	-0.169	-0.275	-0.312	-0.147
			0.051	0.161	0.816	0.582	0.362	0.299	0.632
Expansion at IN			1	0.428	-0.035	0.228	0.142	0.212	-0.206
				0.145	0.909	0.455	0.643	0.486	0.5
BThickM				1	0.666*	0.572*	0.538	0.835**	0.466
					0.013	0.041	0.058	0.000	0.109
BThickPM					1	0.528	0.434	0.909**	0.715**
						0.064	0.138	0.000	0.006
BThickIN						1	0.072	0.524	0.542
							0.815	0.066	0.055
PThickM							1	0.557*	0.655*
								0.048	0.015
PThickPM								1	0.672*
									0.012
PThickIN									1

Correlation is significant at the: *0.05 level (2-tailed); **0.01 level (2-tailed). **M**: molars; **PM**: premolars; **IN**: incisors. Cortical bone thickness (**Thick**): **B**: buccal; **P**: palatal; **M**: average first and second molars; **PM**: average first and second premolars; **IN**: incisors.

CHAPTER 5

DISCUSSION

5.1 Strengths

We established in this study modalities that had not been evaluated or documented previously. The strengths are illustrated in their relevant contexts in the various chapters and are expanded in this comprehensive summary.

5.1.1 Originality of the research

The concepts and designs are unique and have not been considered in previous studies, most of which focused on the dental effects after expansion. The study specifically combined the minimal invasive osteotomy with the fixed appliances and both the tooth-borne and bone-borne expanders across different clinical setups.

5.1.2 Individual variation

The inclusion of individual variation in finite element modeling orthodontic study has been introduced and followed in our departmental research program and has proven to be directly applicable in other investigated orthodontic applications (eg. distalization of maxillary posterior teeth (Ghafari & Ammoury, 2020)). Most FEA studies generated inferences and readings from a single mathematical model, which corresponded to a single set-up or simplified fractioned clinical setup. Individual variations, however, lead to different results for a similar clinical problem in the medical and dental fields, necessitating the study of larger samples to determine not only central tendencies but also potential outliers. FEA applications have emerged

because their intended goals may not be carried out directly on living organs. Accordingly, the best available reconstructions have been simplified with segmented elements of anatomy. To account for individual variation and adequately apply engineering methods, we incorporated cortical bone thickness from studies on real cadavers to simulate differences between real patients. Alternatively, at least as many scanned images of real patients would have to be individually processed through FEA, a task fraught with immeasurable amount of work. The inclusion of a biologic sample with the transferred individual data from the cadavers facilitated the use of statistical analyses that revealed the effect of variances on different outcome measures, leading to formulate conclusions or new hypotheses.

5.1.3 Complete 3D model

Building a complete and accurate FE model requires significant effort and time. In most studies, modelling of the investigated structures was compromised by using simplified models containing only the anchored teeth of the expander (De Assis et al., 2013), not differentiating between the trabecular and cortical bones, or building cortical bone assuming of thicknesses that might not match the reality (Dalband et al., 2015; De Assis et al., 2013; Tehranchi et al., 2013). In contrast, our model was based on a CT scan of a patient and contained all structures except for the enamel, dentin, and pulp, discarded for simplification purposes as they do not impact tooth movement or stress expression.

5.2 Model construction

5.2.1 Anatomical considerations

The 3D model was created from a CT scan of an adult patient and comprised the maxillary and palatal bones with a complete set of teeth along with their corresponding

periodontal ligaments. Structures adjacent to the maxilla were not needed in the model because the main objective was to study the effects of expansion on the maxillary teeth. The included anatomical structures were assigned material properties that were previously validated. The mid-palatal suture was assumed to have the same properties as the surrounding bone and was ascribed the same Poisson ration and elastic modulus, as was applied by other authors (H. Lee, Ting, Nelson, Sun, & Sung, 2009; S. C. Lee et al., 2014; Nowak et al., 2021; Shi, Zhu, & Xie, 2020). This assumption of similar properties presumes that the mid-palatal suture is fused to the bone, presenting an indication for SARPE. Moreover, the mid-palatal suture was considered as linear elastic, homogeneous isotropic material, because the expansion was evaluated at one timepoint. This consideration was reported to yield accurate results (Romanyk et al., 2013).

5.2.2 Variations in loading and expansion

Investigators loaded the teeth anchoring the expander with forces that varied between studies (100 to 500 Newton (N)) as (Dalband et al., 2015; Ludwig et al., 2013; Priyadarshini et al., 2017; Sankar et al., 2021). However, other researchers varied the amount of expansion in mm. Other sources of variation studied the dissipation of forces in either the early or late stages of the expansion, the latter ranging from 0.25 to 10 mm (De Assis et al., 2013; Jain et al., 2017; S. Möhlhenrich et al., 2017; Tehranchi et al., 2013). In our study, the maxilla was expanded 8mm, 4 mm on each side, a setup mirroring the clinical situation whereby a severe to moderate posterior crossbite is corrected. Applying the expansion in mm rather than in N, is a better representation of the clinical setting in the simulation of the palatal expander action, since the jackscrew

opens to a specific range of expansion dictated by the turns done. While applying a force in N has a continuous effect which might exaggerate the results and might not simulate the clinical situation accurately.

5.3 Sagittal Palatal osteotomy

5.3.1 Designs

The sagittal palatal osteotomy incorporated in our experimental setups is a SARPE cut limited to the mid-palatal suture, which offers significant resistance to the expansion. Whereas the palatal osteotomy extended from the incisal foramen to the level of the distal surface of the first molar, other regimens included different definitions of minimally invasive cuts, such as corticopuncture (Suzuki et al., 2018) and palatal osteotomy extending to the incisors (Sant'Ana, Pinzan-Vercelino, Gurgel, & Carvalho, 2016).

The traditional more invasive SARPE cuts require general anesthesia in a hospital setting and commonly include the separation of the mid-palatal suture, separation of the pterygomaxillary sutures, and LeFort I corticotomy. Many patients reject such extensive and costly procedures. In a finite element analysis of three surgical models Lee et al (2014) reported similar amounts of stress and displacement along the teeth, mid-palatal sutures, and craniofacial sutures. They recommended a less invasive mid-palatal suture separation to complement the use of a bone-borne rapid maxillary expander in adults. In another FEA study, Shi et al (2020) found that partial paramedian osteotomy was sufficient to reduce stress during posterior maxillary expansion. Their results were similar for adolescent and adult patients.

Sant'Ana et al compared SARPE with and without a mid-palatal split. They concluded that SARPE involving mid-palatal separation was more effective. Patients treated without the split experience worse postoperative pain and discomfort during expander activation (Sant'Ana et al., 2016) and most had failed surgery. Luxi et al (2017) applied mid-palatal cortex osteotomy assisted RPE to correct MTD in 14 young adults with a mean age of 20.4 ± 3.5 years old. The cut was performed under local anesthesia along the mid-palatal suture from the incisive canal to the transverse palatine suture. They used a ball drill to remove bone with an incision depth half the thickness of the palatal bone (Figure 2.18). They found their micro-invasive method to be effective. Suzuki et al (2018) performed corticopunctures along the palatal suture (Figure 2.19) in an adult female patient after many unsuccessful attempts to activate the MARPE. They concluded that combining MARPE and corticopuncture was a viable non-surgical treatment option to correct MTD. However, this protocol may not be generalized and should be investigated in a larger sample.

5.3.2 Surgical considerations

The shift from the 'wide-open' conventional approach to short incisions and minimal dissection allows the surgeon to perform less extensive procedures, thus reduced morbidity, faster recovery, and lower cost. The sagittal palatal osteotomy simulated in our study would be performed clinically under local anesthesia in a relatively short period. The anesthesia would be injected anteriorly at the incisive foramen and posteriorly at the greater palatine foramen on right and left sides. Expertise in anatomy and piezosurgery would be required. Initially, a CBCT is required for diagnosis and treatment planning, allowing the measurement of the palatal bone height.

After cutting through the palatal mucosa with a blade, the bone is pierced using a piezoelectric bone cutting device, then the cortical bone and part of the trabecular bone should be removed at a depth of around 4 mm in average (Kang et al., 2007). A significant reduction in bleeding and post-operative complications have been shown in patients who underwent surgery with piezoelectric devices, which also offer soft tissue preservation, higher precision and control, and the ability to provide a dry operation field because of the cavitation effect and micromovement (AlAsseri & Swennen, 2018). A periodontal dressing may be applied to prevent infection and promote wound healing.

5.4 Results and clinical implications

The results and interpretations are summarized in this section.

5.4.1 *Sagittal Palatal Osteotomy*

1. The observation of increased stresses on first premolar and first molars when using the RPE corroborates prior evidence (De Assis et al., 2013). The fact that these stresses were not significantly decreased with the sagittal palatal osteotomy (setup 2) but significantly increased the expansion demonstrates that the osteotomy decreased the skeletal bony resistance to expansion. This conclusion is further supported by the finding that higher correlations were observed between the stresses and the expansion in setup 2 compared to setup 1.
2. The addition of the sagittal palatal osteotomy induced greater expansion but higher positive correlations between the stresses on the teeth and the different regions of cortical bone thicknesses. Thus, the osteotomy decreased the skeletal

resistance to expansion but led to stresses at the teeth being more dependent on their dentoalveolar housing.

5.4.2 Greater expansion and stresses

1. The stresses were distributed on all the teeth in setup 3 and setup 4 and were lower (< 0.75 MPa) on the teeth engaged into the arch wires than on the anchoring first premolars and first molars (4.88 MPa and 4.70 MPa, respectively), which exhibited less stress than in setup 1 and more expansion. Of primary importance is cutting the wire between the central incisors into two sectionals to avoid hindering the expansion. The difference in arch wire size did not impact the amount of expansion and affected stress only at the level of the incisors, higher stress identified with the 0.019*0.025 stainless steel wire in setup 4.
2. Expectedly, the bone-borne expander did not result in stresses on the teeth. Among the tooth-borne setups, the least stress on teeth was observed in setup 3 that included the osteotomy and the fixed appliances with 0.016*0.022 stainless steel arch wires. This finding should not be surprising because this setup (3) reinforces the anchorage. Of interest is the fact that in common practice, teeth are not aligned and engaged in the assembly before the expansion, indicating the need to explore this model as a potential added value to maxillary expansion. Moreover, a heavier arch wire (0.019*0.025) would not be necessary as the difference between the 2 heavy wires was not significant.

5.4.3 *Tooth-borne vs bone-borne*

1. As expected, and in contrast to the tooth-borne RPE that yielded the highest expansion at the molars and gradual decrease towards the incisors, the bone-borne expansion in setup 5 did not result in stresses on the teeth and was not significant on the molars but on the incisors and premolars regions. Furthermore, the maximum amount of expansion posteriorly included the incorporation of fixed appliances (regardless of arch-wire size) in combination with the sagittal palatal osteotomy. The setup with the maximum amount of expansion anteriorly would be setup 5 with the MARPE as expander used.

This result may be assigned to the more posterior position of the RPE compared to the more anterior position of the MARPE. Concordant with this finding, the correlation between the expansion at the molars and the expansion at the incisors was negative, and the correlation between the expansion at the molars and that at the premolars was positive.

2. In all tooth-borne setups, a negative correlation was observed between the expansion at the molars, premolars and incisors with all the corresponding cortical bone thicknesses. The palatal bone thickness at the premolars had the strongest negative correlation on both expansion areas, the expansion decreasing with increasing cortical bone thickness. When the osteotomy was added, the correlation values decreased except between the expansion at the three regions with the palatal bone thickness at the incisors. This finding may be related to the extent of the palatal osteotomy short of the central incisors, starting distal to the incisive foramen.

5.4.4 Thickness

1. Thickness was a modifying factor of stress generation in the tooth-borne setups, higher stresses being associated with increased thickness. Stresses on the first premolars were mostly impacted by the buccal bone thickness at the molars. This finding along with the smaller root surface of the premolar would explain the higher stress at the premolar. The stresses on the first molars were mostly associated with the palatal bone thickness at the premolars. A thicker bone at the premolar palatal area was highly correlated with palatal bone thickness at the molars and incisors. As more resistance to expansion was correlated with thicker palatal bone, higher stress was observed at the teeth exerting the expansion.
2. In all tooth-borne setups, the low correlations between the expansion at the three regions and the buccal bone thickness at the incisors in all setups indicates that the expansion was not affected by the buccal bone thickness at the incisors. The bone-borne expanders did not result in significant correlations between expansion and cortical bone thicknesses, understandably because the bone-borne expander is unaffected with the buccal and palatal alveolar cortical bone thicknesses.

5.4.5 Regional differences

1. The stresses on the first premolars and first molars were positively correlated and their differences statistically significant across all setups. Moreover, as the expansion increased, stresses on the teeth decreased, this trend occurring within same regions: the expansion at the molars mostly affected by stresses at the first molars, and similarly for the premolars.

2. The associations among groups of teeth seemed dependent on tooth location: expansion at the molars correlated only with that at the premolars, expansion at premolar correlated with molars and incisors.

5.5 Comparison with Other Studies

Our design of expansion in adult maxillae led to more expansion posteriorly than anteriorly with setups 1,2,3 and 4, and more anteriorly with the bone-borne expander (setup 5). This difference was likely related to the load from the tooth-borne expanders was applied directly to the posterior palate that has thinner cortical bone than the anterior area. These findings mirror those of Lee et al (2009) who stated that the inclusion of the first premolars and molars in the expander would lead to more posterior displacement, in contrast to more anterior displacement with the bone-borne expanders because of the more anterior position of the expander.

Shi et al (2020) reported that a partial paramedian osteotomy with a bone-borne setup facilitated a greater expansion in the posterior part of the suture and recommended the procedure. Our findings contradict this report, having observed more an anterior expansion. The difference may be due to the more posterior or anterior position of the expander rather than the osteotomy itself. However, Koç and Bolat Gumus (2023) reported a ‘V’ shaped expansion with a bone-borne expander (“transpalatal distractor”) in conjunction with median and lateral osteotomies, whether the expander was placed at the level of the first premolar, second premolar, first molar or second molar regions. The expander screw was activated 5 mm; the maximum displacement values were measured on the central incisor region.

In a finite element study in which they used palatal osteotomies that extended beyond the incisal foramen to reach the incisors, Möhlhenrich et al (2017) simulated a posterior position of a bone-borne expander, parallel to the distal of the second premolars and distal to the first molars. They tested the response to an expansion of 1mm and measured the displacement at the marginal ridge of the alveolar bone on all the teeth. They observed more anterior displacement at the central and lateral incisors than in the posterior segment at the first molars.

Lee et al (2014) tested through finite element modelling several surgical models, one of which included a bone-borne expander placed parallel to the mesial of the first premolars and mesial to the first molars, also assisted by a surgical separation of the mid-palatal suture that extended anteriorly to separate the buccal bone completely. They measured the displacement at the lingual margin of the alveolar bone of all the teeth after a 0.5 mm expansion. More anterior than posterior displacement was reported.

The results in both previous studies join ours in setup 5, although their mid-palatal osteotomies were more extensive and invasive. This finding suggests that an extended anterior cut may not be needed, favoring our more conservative and less morbid approach.

In another FEA study in which tooth-borne and bone-borne expanders were combined with a complete LeFort 1 corticotomy and an activation of 0.5mm was performed separately along the canine, the premolar and the first molar, Tehranchi et al (2013) reported higher stresses at the PDL of the first premolars than at the first molars with the tooth-borne expanders. In addition, the Von Mises stresses with the bone-borne were ninety-five percent less than with the tooth-borne expanders. The authors

suggested that the tooth-borne Hyrax expander would result in more posterior expansion when placed nearer to the posterior segment. Their findings are concomitant with ours.

Dalband et al (2015) studied models with different Lefort 1 osteotomies in combination with both tooth-borne and bone-borne expanders that exerted an expansion force of 100N. Absent any concentration of stress around specific teeth with the bone-borne expanders, the tooth-borne expanders resulted in a maximal movement of the expander anchoring teeth, the maxillary premolars and first molars. With both types of expanders, the displacement increased with more involved osteotomies mainly in the posterior region of the maxilla. This finding is in contradiction with ours, whereby we found a difference in the displacement between the two types of expanders.

5.5. Limitations

One of our limitations was simulating the brackets as blank boxes engaged in the wire; therefore, the wire play in the bracket slots was disregarded to simplify the setup. Additionally, in the bone-borne set up, we did not model the entire length of the palatal mini-screws. However, we simulated the effect of a bone-borne expander by applying the expansion displacement force at a rectangle representing the head of the mini-screw, which is the point of force application at the level of the surface of the palatal cortical bone. In addition, we have not included different teeth morphologies of different surface areas in our models. The forementioned limitations in the method of modeling might have negligible effects on the results.

Although FEA defines effects at a timepoint rather than longitudinal, the methods has been reliable to simulate invasive procedures, particularly surgical approaches such as corticotomies, especially the SARPE method, and other evaluations

of displacement patterns and stress distributions in models involving the facial skeleton. Yet, the results of FEA analysis should be interpreted carefully for clinical practice, because of the vast variations encountered in clinical situations such as suture maturity, bone density, biologic considerations, and other anatomic structures that affect biomechanical systems of maxillary expansion. Furthermore, chewing and muscle strength, relapse, and remodeling ability typically are not considered in FEA investigations, including ours. Accordingly, the results may differ from actual clinical outcomes (Koç & Bolat Gumus, 2023).

5.6 Future Research Tracks and Recommendations

It would be ideal to simulate the full effect of the treatment under study, including the biologic factors that contribute to the reaction of the maxillofacial structure. The addition of palatal soft tissues to the model may improve simulation accuracy. Also, the addition of creep strain (viscoelastic material properties) to the FE model and the application of force cycles over time (time-dependent analysis) would better mirror the clinical setting. In addition, the evaluation of sequential, not unique activation of the expander is needed to better understand the outcome of this mechanotherapy. Parallel investigations clinically and through FEA would also be beneficial, the clinical outcomes being fed to the experimental setting for closer assessment of the biological not only the mechanical responses.

CHAPTER 6

CONCLUSIONS

1. The sagittal palatal osteotomy was minimally invasive and efficient in increasing the simulated expansion in a skeletally mature patient by decreasing the resistance to expansion at the mid-palatal suture.
2. Dental stresses were observed mainly at the teeth anchoring the tooth-borne expander, namely the first premolars and first molars. Higher stresses were calculated at the first premolars. With arch wires engaged in the maxillary teeth, the stresses were distributed on all teeth, thus decreased on the anchoring teeth.
3. The bone-borne expander led to more bony expansion anteriorly rather than posteriorly, with absent stresses on the teeth. In contrast, the tooth-borne expanders resulted in more posterior than anterior expansion.
4. As the cortical bone thickness increased, the expansion decreased and stresses on the teeth increased. As expansion increased, the stresses on the teeth decreased.
5. The amount of expansion and the cortical bone thicknesses did not correlate when using bone-borne expander, probably because the expander was anchored in the palatal bone directly and was unaffected by the thickness of the buccal and palatal alveolar cortical bone.
6. The results suggest that the optimal posterior expansion would be achieved with a tooth-borne expander combined with a sagittal palatal osteotomy and fixed rectangular arch wires engaged in the maxillary teeth. The 0.016*0.022 arch wire produced the same effect as the heavier wire (0.019*0.025). However,

anterior expansion would be accomplished with a bone-bone expander combined with a sagittal palatal osteotomy.

7. Future research is needed in more diverse facial structures, such as hyper and hypo-divergent facial patterns with variable resistance to expansion from the buttressing bones. Also, time-dependent finite element modeling should better elucidate the progressive response to expansion.

APPENDIX

Table 1: Descriptive statistics for the stress and cortical bone thickness for setup 1.

		Mean	SD	Min	Max
Setup 1	Stress at PM1	4.06	0.34	5.36	5.05
	Stress at M1	4.13	0.37	5.23	4.85
	BThickM	0.93	0.93	4.62	2.07
	BThickPM	0.60	1.46	4.31	2.41
	BThickIN	1.07	1.68	5.83	2.46
	PThickM	0.40	0.95	3.40	1.97
	PThickPM	0.63	1.14	4.28	2.40
	PThickIN	0.62	0.58	2.64	1.74

SD: Standard deviation; **Min:** minimum; **Max:** maximum; Stress in MPa; **PM1:** first premolar; **M1:** first molar. Cortical bone thickness (**Thick**) in mm; **B:** buccal; **P:** palatal; **M:** average first and second molars; **PM:** average first and second premolars; **IN:** incisors.

Table 2: Descriptive statistics of stress, expansion, and cortical bone thickness for setup 2.

		Mean	SD	Min	Max
Setup 2	Stress at PM1	4.99	0.31	4.14	5.23
	Stress at M1	4.82	0.37	4.05	5.08
	Expansion at M	0.83	0.91	0.26	2.65
	Expansion at PM	0.50	0.42	0.21	1.66
	Expansion at IN	0.18	0.11	0.09	0.48
	BThickM	2.07	0.93	0.93	4.62
	BThickPM	2.41	1.46	0.60	4.31
	BThickIN	2.46	1.68	1.07	5.83
	PThickM	1.97	0.95	0.40	3.40
	PThickPM	2.40	1.14	0.63	4.28
	PThickIN	1.74	0.58	0.62	2.64

SD: Standard deviation; **Min:** minimum; **Max:** maximum; Stress in MPa; **PM1:** first premolar; **M1:** first molar. Expansion in mm; **M:** molars; **PM:** premolars; **IN:** incisors. Cortical bone thickness (**Thick**) in mm; **B:** buccal; **P:** palatal; **M:** average first and second molars; **PM:** average first and second premolars; **IN:** incisors.

Table 3: Descriptive statistics of stress, expansion, and cortical bone thickness for setup 3.

		Mean	SD	Min	Max
Setup 3	Stress at IN1	0.43	0.05	0.31	0.50
	Stress at IN2	0.43	0.04	0.32	0.51
	Stress at C	0.70	0.08	0.45	0.79
	Stress at PM1	4.87	0.33	3.94	5.20
	Stress at PM2	0.75	0.12	0.60	0.93
	Stress at M1	4.70	0.33	4.03	5.05
	Stress at M2	0.50	1.07	0.13	4.07
	Expansion at M	0.87	0.86	0.34	2.70
	Expansion at PM	0.56	0.48	0.27	1.98
	Expansion at IN	0.22	0.11	0.12	0.50
	BThickM	2.07	0.93	0.93	4.62
	BThickPM	2.41	1.46	0.60	4.31
	BThickIN	2.46	1.68	1.07	5.83
	PThickM	1.97	0.95	0.40	3.40
	PThickPM	2.40	1.14	0.63	4.28
PThickIN	1.74	0.58	0.62	2.64	

SD: Standard deviation; **Min:** minimum; **Max:** maximum; Stress in MPa; **IN1:** central incisor; **IN2:** lateral incisor; **C:** canine; **PM1:** first premolar; **PM2:** second premolar; **M1:** first molar; **M2:** second molar. Expansion in mm: **M:** molars; **PM:** premolars; **IN:** incisors. Cortical bone thickness (**Thick**) in mm: **B:** buccal; **P:** palatal; **M:** average first and second molars; **PM:** average first and second premolars; **IN:** incisors.

Table 4: Descriptive statistics of stress, expansion, and cortical bone thickness for setup 4.

		Mean	SD	Min	Max
Setup 4	Stress at IN1	0.48	0.05	0.37	0.55
	Stress at IN2	0.49	0.04	0.4	0.55
	Stress at C	0.72	0.05	0.58	0.77
	Stress at PM1	4.89	0.35	3.81	5.22
	Stress at PM2	0.75	0.12	0.51	0.88
	Stress at M1	4.71	0.37	4.04	5.18
	Stress at M2	0.17	0.06	0.13	0.32
	Expansion at M	0.88	0.92	0.28	2.81
	Expansion at PM	0.56	0.52	0.24	2.11
	Expansion at IN	0.22	0.12	0.12	0.53
	BThickM	2.07	0.93	0.93	4.62
	BThickPM	2.41	1.46	0.6	4.31
	BThickIN	2.46	1.68	1.07	5.83
	PThickM	1.97	0.95	0.4	3.4
	PThickPM	2.40	1.14	0.63	4.28
PThickIN	1.74	0.58	0.62	2.64	

SD: Standard deviation; **Min:** minimum; **Max:** maximum; Stress in MPa; **IN1:** central incisor; **IN2:** lateral incisor; **C:** canine; **PM1:** first premolar; **PM2:** second premolar; **M1:** first molar; **M2:** second molar. Expansion in mm: **M:** molars; **PM:** premolars; **IN:** incisors. Cortical bone thickness (**Thick**) in mm: **B:** buccal; **P:** palatal; **M:** average first and second molars; **PM:** average first and second premolars; **IN:** incisors.

Table 5: Descriptive statistics of the expansion and cortical bone thickness for setup 5.

		Mean	SD	Min	Max
Setup 5	Expansion at M	0.54	0.09	0.41	0.73
	Expansion at PM	0.89	0.13	0.67	1.16
	Expansion at IN	1.01	0.19	0.8	1.32
	BThickM	2.07	0.93	0.93	4.62
	BThickPM	2.41	1.46	0.6	4.31
	BThickIN	2.46	1.68	1.07	5.83
	PThickM	1.97	0.95	0.4	3.4
	PThickPM	2.40	1.14	0.63	4.28
	PThickIN	1.74	0.58	0.62	2.64

SD: Standard deviation; **Min:** minimum; **Max:** maximum; Expansion in mm: **M:** molars; **PM:** premolars; **IN:** incisors. Cortical bone thickness (**Thick**) in mm: **B:** buccal; **P:** palatal; **M:** average first and second molars; **PM:** average first and second premolars; **IN:** incisors.

REFERENCES

- AlAsseri, N., & Swennen, G. (2018). Minimally invasive orthognathic surgery: a systematic review. *International journal of oral and maxillofacial surgery*, 47(10), 1299-1310.
- Ammoury, M. J. (2017). *Effect of cortical bone quality and quantity on two orthodontic distalization modalities: a finite element analysis study*.
- Angelieri, F., Cevidanes, L. H., Franchi, L., Gonçalves, J. R., Benavides, E., & McNamara Jr, J. A. (2013). Midpalatal suture maturation: classification method for individual assessment before rapid maxillary expansion. *American journal of orthodontics and dentofacial orthopedics*, 144(5), 759-769.
- Baik, H.-S., Kang, Y.-G., & Choi, Y. J. (2020). Miniscrew-assisted rapid palatal expansion: a review of recent reports. *Journal of the World Federation of Orthodontists*, 9(3), S54-S58.
- Baldawa, R. S., & Bhad, W. A. (2011). Stress distribution analysis during an intermaxillary dysjunction: A 3-D FEM study of an adult human skull. *Annals of maxillofacial surgery*, 1(1), 19.
- Barrabé, A., Meyer, C., Bonomi, H., Weber, E., Sigaux, N., & Louvrier, A. (2018). Surgically assisted rapid palatal expansion in class III malocclusion: Our experience. *Journal of stomatology, oral and maxillofacial surgery*, 119(5), 384-388.
- Bazargani, F., Feldmann, I., & Bondemark, L. (2013). Three-dimensional analysis of effects of rapid maxillary expansion on facial sutures and bones: a systematic review. *The Angle Orthodontist*, 83(6), 1074-1082.
- Bell, R. A. (1982). A review of maxillary expansion in relation to rate of expansion and patient's age. *American journal of orthodontics*, 81(1), 32-37.
- Bell, W. H., & Epker, B. N. (1976). Surgical-orthodontic expansion of the maxilla. *American journal of orthodontics*, 70(5), 517-528.
- Betts, N., Vanarsdall, R., Barber, H., Higgins-Barber, K., & Fonseca, R. (1995). Diagnosis and treatment of transverse maxillary deficiency. *The International journal of adult orthodontics and orthognathic surgery*, 10(2), 75-96.
- Bignotti, D., Gracco, A., Bruno, G., & De Stefani, A. (2019). Fem in orthodontics: A review of the palatal expanders clinical investigation. *Oral & Implantology*, 12(2), 161-167.
- Bishara, S. E., & Staley, R. N. (1987). Maxillary expansion: clinical implications. *American journal of orthodontics and dentofacial orthopedics*, 91(1), 3-14.
- Björk, A., & Skieller, V. (1977). Growth of the maxilla in three dimensions as revealed radiographically by the implant method. *British Journal of Orthodontics*, 4(2), 53-64.
- Brown, G. V. I. (1938). *The surgery of oral and facial diseases and malformations: their diagnosis and treatment including plastic surgical reconstruction*: Lea and Febiger.
- Bucci, R., D'antò, V., Rongo, R., Valletta, R., Martina, R., & Michelotti, A. (2016). Dental and skeletal effects of palatal expansion techniques: a systematic review of the current evidence from systematic reviews and meta-analyses. *Journal of oral rehabilitation*, 43(7), 543-564.

- Bucci, R., Montanaro, D., Rongo, R., Valletta, R., Michelotti, A., & D'Antò, V. (2019). Effects of maxillary expansion on the upper airways: Evidence from systematic reviews and meta-analyses. *Journal of oral rehabilitation*, 46(4), 377-387.
- Calvo-Henriquez, C., Sandoval-Pacheco, V., Chiesa-Estomba, C., Lechien, J., Martins-Neves, S., Esteller-More, E., . . . Capasso, R. (2022). Pediatric maxillary expansion has a positive impact on hearing? A systematic review and meta-analysis. *European Annals of Otorhinolaryngology, Head and Neck Diseases*.
- Camps-Perrepérez, I., Guijarro-Martínez, R., Peiró-Guijarro, M., & Hernández-Alfaro, F. (2017). The value of cone beam computed tomography imaging in surgically assisted rapid palatal expansion: a systematic review of the literature. *International journal of oral and maxillofacial surgery*, 46(7), 827-838.
- Carvalho, P., Moura, L., Trento, G., Holzinger, D., Gabrielli, M., Gabrielli, M., & Pereira Filho, V. (2020). Surgically assisted rapid maxillary expansion: a systematic review of complications. *International journal of oral and maxillofacial surgery*, 49(3), 325-332.
- Celenk-Koca, T., Erdinc, A. E., Hazar, S., Harris, L., English, J. D., & Akyalcin, S. (2018). Evaluation of miniscrew-supported rapid maxillary expansion in adolescents: a prospective randomized clinical trial. *The Angle Orthodontist*, 88(6), 702-709.
- Chuang, Y.-H., Chen, J.-H., Ho, K.-H., Wang, K.-L., Hsieh, S.-C., & Chang, H.-M. (2021). The role of micro-implant-assisted rapid palatal expansion (MARPE) in clinical orthodontics—A literature review. *Australasian Orthodontic Journal*, 37(2), 206-216.
- Chung, C.-H. (2019). *Diagnosis of transverse problems*. Paper presented at the Seminars in Orthodontics.
- Cortella, S., Shofer, F. S., & Ghafari, J. (1997). Transverse development of the jaws: norms for the posteroanterior cephalometric analysis. *American journal of orthodontics and dentofacial orthopedics*, 112(5), 519-522.
- Dalband, M., Kashani, J., & Hashemzahi, H. (2015). Three-dimensional finite element analysis of stress distribution and displacement of the maxilla following surgically assisted rapid maxillary expansion with tooth-and bone-borne devices. *Journal of Dentistry (Tehran, Iran)*, 12(4), 298.
- Dawson, P. E. (1995). New definition for relating occlusion to varying conditions of the temporomandibular joint. *The Journal of prosthetic dentistry*, 74(6), 619-627.
- De Assis, D., Xavier, T., Noritomi, P., Gonçalves, A., Ferreira Jr, O., De Carvalho, P., & Gonçalves, E. S. (2013). Finite element analysis of stress distribution in anchor teeth in surgically assisted rapid palatal expansion. *International journal of oral and maxillofacial surgery*, 42(9), 1093-1099.
- De Freitas, R., Gonçalves, A., Moniz, N., & Maciel, F. (2008). Surgically assisted maxillary expansion in adults: prospective study. *International journal of oral and maxillofacial surgery*, 37(9), 797-804.
- de Oliveira, C. B., Ayub, P., Ledra, I. M., Murata, W. H., Suzuki, S. S., Ravelli, D. B., & Santos-Pinto, A. (2021). Microimplant assisted rapid palatal expansion vs surgically assisted rapid palatal expansion for maxillary transverse discrepancy treatment. *American journal of orthodontics and dentofacial orthopedics*, 159(6), 733-742.

- Dergin, G., Aktop, S., Varol, A., Ugurlu, F., & Garip, H. (2015). Complications related to surgically assisted rapid palatal expansion. *Oral surgery, oral medicine, oral pathology and oral radiology*, 119(6), 601-607.
- Field, C., Ichim, I., Swain, M. V., Chan, E., Darendeliler, M. A., Li, W., & Li, Q. (2009). Mechanical responses to orthodontic loading: a 3-dimensional finite element multi-tooth model. *American journal of orthodontics and dentofacial orthopedics*, 135(2), 174-181.
- Gautam, P., Valiathan, A., & Adhikari, R. (2007). Stress and displacement patterns in the craniofacial skeleton with rapid maxillary expansion: a finite element method study. *American journal of orthodontics and dentofacial orthopedics*, 132(1), 5. e1-5. e11.
- Geran, R. G., McNamara Jr, J. A., Baccetti, T., Franchi, L., & Shapiro, L. M. (2006). A prospective long-term study on the effects of rapid maxillary expansion in the early mixed dentition. *American journal of orthodontics and dentofacial orthopedics*, 129(5), 631-640.
- Ghafari, J. G., & Ammourey, M. J. (2020). Overcoming compact bone resistance to tooth movement. *American journal of orthodontics and dentofacial orthopedics*, 158(3), 343-348.
- Ghoneima, A., Abdel-Fattah, E., Hartsfield, J., El-Bedwehi, A., Kamel, A., & Kula, K. (2011). Effects of rapid maxillary expansion on the cranial and circummaxillary sutures. *American journal of orthodontics and dentofacial orthopedics*, 140(4), 510-519.
- Gill, D., Naini, F., McNally, M., & Jones, A. (2004). The management of transverse maxillary deficiency. *Dental update*, 31(9), 516-523.
- Giudice, A. L., Spinuzza, P., Rustico, L., Messina, G., & Nucera, R. (2020). Short-term treatment effects produced by rapid maxillary expansion evaluated with computed tomography: A systematic review with meta-analysis. *Korean Journal of Orthodontics*, 50(5), 314-323.
- Gok, G. D., Topbasi, N. M., Baydas, B., Uslu, H., Ceylan, I., Yavuz, I., . . . Filik, M. (2021). Effects of Rapid Maxillary Expansion on the Temporomandibular Joint: A Bone Scintigraphy Study. *Turkish Journal of Orthodontics*, 34(3), 176.
- Grünheid, T., Larson, C. E., & Larson, B. E. (2017). Midpalatal suture density ratio: A novel predictor of skeletal response to rapid maxillary expansion. *American journal of orthodontics and dentofacial orthopedics*, 151(2), 267-276.
- Haas, A. J. (1961). Rapid expansion of the maxillary dental arch and nasal cavity by opening the midpalatal suture. *The Angle Orthodontist*, 31(2), 73-90.
- Habersack, K., Becker, J., Ristow, O., & Paulus, G. W. (2014). Dental and skeletal effects of two-piece and three-piece surgically assisted rapid maxillary expansion with complete mobilization: a retrospective cohort study. *Journal of oral and maxillofacial surgery*, 72(11), 2278-2288.
- Hernandez-Alfaro, F., Bueno, J. M., Diaz, A., & Pagés, C. M. (2010). Minimally invasive surgically assisted rapid palatal expansion with limited approach under sedation: a report of 283 consecutive cases. *Journal of oral and maxillofacial surgery*, 68(9), 2154-2158.
- Hernández-Alfaro, F., & Valls-Ontañón, A. (2021). SARPE and MARPE. *Innovative Perspectives in Oral and Maxillofacial Surgery*, 321-325.
- Huynh, T., Kennedy, D. B., Joondeph, D. R., & Bollen, A.-M. (2009). Treatment response and stability of slow maxillary expansion using Haas, hyrax, and quad-

- helix appliances: a retrospective study. *American journal of orthodontics and dentofacial orthopedics*, 136(3), 331-339.
- Isfeld, D., Lagravere, M., Leon-Salazar, V., & Flores-Mir, C. (2017). Novel methodologies and technologies to assess mid-palatal suture maturation: a systematic review. *Head & face medicine*, 13, 1-15.
- Jacobs, J. D., Bell, W. H., Williams, C. E., & Kennedy III, J. W. (1980). Control of the transverse dimension with surgery and orthodontics. *American journal of orthodontics*, 77(3), 284-306.
- Jain, V., Shyagali, T. R., Kambalyal, P., Rajpara, Y., & Doshi, J. (2017). Comparison and evaluation of stresses generated by rapid maxillary expansion and the implant-supported rapid maxillary expansion on the craniofacial structures using finite element method of stress analysis. *Progress in Orthodontics*, 18(1), 1-12.
- Jia, H., Zhuang, L., Zhang, N., Bian, Y., & Li, S. (2022). Age-dependent effects of transverse maxillary deficiency treated by microimplant-assisted rapid palatal expansion: A prospective cone-beam computed tomography study. *American journal of orthodontics and dentofacial orthopedics*, 161(4), 557-573.
- Junior, O. H., Guijarro-Martínez, R., de Sousa Gil, A., da Silva Meirelles, L., de Oliveira, R., & Hernández-Alfaro, F. (2017). Stability and surgical complications in segmental Le Fort I osteotomy: a systematic review. *International journal of oral and maxillofacial surgery*, 46(9), 1071-1087.
- Junior, O. L. H., Matje, P. R., Rosa, B. M., Rojo-Sanchis, C., Guijarro-Martínez, R., Valls-Ontañón, A., . . . de Oliveira, R. B. (2022). Minimally invasive surgical and miniscrew-assisted rapid palatal expansion (MISMARPE) in adult patients. *Journal of Cranio-Maxillofacial Surgery*, 50(3), 211-217.
- Kang, S., Lee, S.-J., Ahn, S.-J., Heo, M.-S., & Kim, T.-W. (2007). Bone thickness of the palate for orthodontic mini-implant anchorage in adults. *American journal of orthodontics and dentofacial orthopedics*, 131(4), S74-S81.
- Kapetanović, A., Theodorou, C. I., Bergé, S. J., Schols, J. G., & Xi, T. (2021). Efficacy of Miniscrew-Assisted Rapid Palatal Expansion (MARPE) in late adolescents and adults: a systematic review and meta-analysis. *European journal of orthodontics*, 43(3), 313-323.
- Knop, L., Gandini Jr, L. G., Shintcovsk, R. L., & Gandini, M. R. E. A. S. (2015). Scientific use of the finite element method in Orthodontics. *Dental press journal of orthodontics*, 20, 119-125.
- Ko, C.-C., Rocha, E. P., & Larson, M. (2012). Past, present and future of finite element analysis in dentistry. *Finite Element Analysis-From Biomedical Applications to Industrial Developments*, 1-25.
- Koç, O., & Bolat Gumus, E. (2023). Effects of different distractor positions on the formation of expansion, stress and displacement patterns in surgically assisted rapid maxillary expansion without pterygomaxillary disjunction: a finite element analysis study. *Computer Methods in Biomechanics and Biomedical Engineering*, 1-11.
- Kojima, Y., Kawamura, J., & Fukui, H. (2012). Finite element analysis of the effect of force directions on tooth movement in extraction space closure with miniscrew sliding mechanics. *American journal of orthodontics and dentofacial orthopedics*, 142(4), 501-508.
- Koudstaal, M., Wolvius, E., Schulten, A., Hop, W., & Van der Wal, K. (2009). Stability, tipping and relapse of bone-borne versus tooth-borne surgically

- assisted rapid maxillary expansion; a prospective randomized patient trial. *International journal of oral and maxillofacial surgery*, 38(4), 308-315.
- Koudstaal, M. J., Poort, L., Van der Wal, K., Wolvius, E., Prahl-Andersen, B., & Schulten, A. (2005). Surgically assisted rapid maxillary expansion (SARME): a review of the literature. *International journal of oral and maxillofacial surgery*, 34(7), 709-714.
- Kunz, F., Linz, C., Baunach, G., Böhm, H., & Meyer-Marcotty, P. (2016). Expansion patterns in surgically assisted rapid maxillary expansion. *Journal of Orofacial Orthopedics/Fortschritte der Kieferorthopädie*, 77(5).
- Kustermans, L., Van de Castele, E., Asscherickx, K., Van Hemelen, G., & Nadjmi, N. (2022). Impact of surgically assisted rapid mandibular expansion on the temporomandibular joint-A retrospective study. *Journal of Cranio-Maxillofacial Surgery*, 50(7), 590-598.
- Latham, R. (1971). The development, structure and growth pattern of the human mid-palatal suture. *Journal of anatomy*, 108(Pt 1), 31.
- Lee, H., Ting, K., Nelson, M., Sun, N., & Sung, S.-J. (2009). Maxillary expansion in customized finite element method models. *American journal of orthodontics and dentofacial orthopedics*, 136(3), 367-374.
- Lee, S. C., Park, J. H., Bayome, M., Kim, K. B., Araujo, E. A., & Kook, Y.-A. (2014). Effect of bone-borne rapid maxillary expanders with and without surgical assistance on the craniofacial structures using finite element analysis. *American journal of orthodontics and dentofacial orthopedics*, 145(5), 638-648.
- Lehman Jr, J. A., Haas, A. J., & Haas, D. G. (1984). Surgical orthodontic correction of transverse maxillary deficiency: a simplified approach. *Plastic and reconstructive surgery*, 73(1), 62-68.
- Lim, J.-W., Kim, W.-S., Kim, I.-K., Son, C.-Y., & Byun, H.-I. (2003). Three dimensional finite element method for stress distribution on the length and diameter of orthodontic miniscrew and cortical bone thickness. *The Korean Journal of Orthodontics*, 33(1), 11-20.
- Liu, S., Xu, T., & Zou, W. (2015). Effects of rapid maxillary expansion on the midpalatal suture: a systematic review. *European journal of orthodontics*, 37(6), 651-655.
- Ludwig, B., Baumgaertel, S., Zorkun, B., Bonitz, L., Glasl, B., Wilmes, B., & Lisson, J. (2013). Application of a new viscoelastic finite element method model and analysis of miniscrew-supported hybrid hyrax treatment. *American journal of orthodontics and dentofacial orthopedics*, 143(3), 426-435.
- Luxi, W., Xiaojia, S., Juan, L., Pengruofeng, L., & Jun, L. (2017). Midpalatal cortex osteotomy assisted rapid maxillary expansion for correction of maxillary transverse deficiency in young adults. *Zhejiang da xue xue bao. Yi xue ban= Journal of Zhejiang University. Medical Sciences*, 46(2), 198-205.
- Macchi, A., Carrafiello, G., Cacciafesta, V., & Norcini, A. (2006). Three-dimensional digital modeling and setup. *American journal of orthodontics and dentofacial orthopedics*, 129(5), 605-610.
- Marshall, S. D., Southard, K. A., & Southard, T. E. (2005). *Early transverse treatment*. Paper presented at the Seminars in Orthodontics.
- McNamara, J. A., Brudon, W. L., & Kokich, V. G. (2001). *Orthodontics and dentofacial orthopedics* (Vol. 3): Needham Press Ann Arbor.

- Mehta, S., Wang, D., Kuo, C.-L., Mu, J., Vich, M. L., Allareddy, V., . . . Yadav, S. (2021). Long-term effects of mini-screw–assisted rapid palatal expansion on airway: A three-dimensional cone-beam computed tomography study. *The Angle Orthodontist*, *91*(2), 195-205.
- Melsen, B. (1975). Palatal growth studied on human autopsy material: a histologic microradiographic study. *American journal of orthodontics*, *68*(1), 42-54.
- Middleton, J., Jones, M., & Wilson, A. (1996). The role of the periodontal ligament in bone modeling: the initial development of a time-dependent finite element model. *American journal of orthodontics and dentofacial orthopedics*, *109*(2), 155-162.
- Möhlhenrich, S., Ernst, K., Peters, F., Kniha, K., Chhatwani, S., Prescher, A., . . . Modabber, A. (2021). Immediate dental and skeletal influence of distractor position on surgically assisted rapid palatal expansion with or without pterygomaxillary disjunction. *International journal of oral and maxillofacial surgery*, *50*(5), 649-656.
- Möhlhenrich, S., Modabber, A., Kniha, K., Peters, F., Steiner, T., Hölzle, F., . . . Raith, S. (2017). Simulation of three surgical techniques combined with two different bone-borne forces for surgically assisted rapid palatal expansion of the maxillofacial complex: a finite element analysis. *International journal of oral and maxillofacial surgery*, *46*(10), 1306-1314.
- Möhlhenrich, S. C., Heeg, J., Raith, S., Kniha, K., Hölzle, F., Wolf, M., . . . Modabber, A. (2020). Effect of the pterygomaxillary disjunction on surgically assisted rapid palatal expansion in context of orthodontic treatment. *Oral surgery, oral medicine, oral pathology and oral radiology*, *130*(3), 241-251.
- Morselli, P. (1997). Surgical maxillary expansion: a new minimally invasive technique. *Journal of Cranio-Maxillofacial Surgery*, *25*(2), 80-84.
- Moyers, R. E. (1976). *Standards of human occlusal development*.
- Naoum, S., Goonewardene, M., Abbott, P. V., Karunanayake, K., & Budgeon, C. (2019). Changes in pulp blood flow and pulp sensibility resulting from surgically assisted rapid maxillary expansion: a clinical study. *American journal of orthodontics and dentofacial orthopedics*, *155*(5), 632-641.
- Niu, X., Di Carlo, G., Cornelis, M. A., & Cattaneo, P. M. (2020). Three-dimensional analyses of short-and long-term effects of rapid maxillary expansion on nasal cavity and upper airway: A systematic review and meta-analysis. *Orthodontics & craniofacial research*, *23*(3), 250-276.
- Nowak, R., Olejnik, A., Gerber, H., Frątczak, R., & Zawiślak, E. (2021). Comparison of Tooth-and Bone-Borne Appliances on the Stress Distributions and Displacement Patterns in the Facial Skeleton in Surgically Assisted Rapid Maxillary Expansion—A Finite Element Analysis (FEA) Study. *Materials*, *14*(5), 1152.
- Oliveira, C. B., Ayub, P., Angelieri, F., Murata, W. H., Suzuki, S. S., Ravelli, D. B., & Santos-Pinto, A. (2021). Evaluation of factors related to the success of miniscrew-assisted rapid palatal expansion. *The Angle Orthodontist*, *91*(2), 187-194.
- Park, J. J., Park, Y.-C., Lee, K.-J., Cha, J.-Y., Tahk, J. H., & Choi, Y. J. (2017). Skeletal and dentoalveolar changes after miniscrew-assisted rapid palatal expansion in young adults: a cone-beam computed tomography study. *The Korean Journal of Orthodontics*, *47*(2), 77-86.

- Patil, G. V., Lakhe, P., & Niranjane, P. (2023). Maxillary Expansion and Its Effects on Circummaxillary Structures: A Review. *Cureus*, 15(1).
- Priyadarshini, J., Mahesh, C., Chandrashekar, B., Sundara, A., Arun, A., & Reddy, V. P. (2017). Stress and displacement patterns in the craniofacial skeleton with rapid maxillary expansion—a finite element method study. *Progress in Orthodontics*, 18(1), 1-8.
- Proffit, W. R., Fields, H. W., Larson, B., & Sarver, D. M. (2018). *Contemporary orthodontics-e-book*: Elsevier Health Sciences.
- Revelo, B., & Fishman, L. S. (1994). Maturational evaluation of ossification of the midpalatal suture. *American journal of orthodontics and dentofacial orthopedics*, 105(3), 288-292.
- Ricketts, R. M. (1981). Perspectives in the clinical application of cephalometrics: the first fifty years. *The Angle Orthodontist*, 51(2), 115-150.
- Ricketts, R. M., & Grummons, D. (2003). Frontal Cephalometrics: Practical Applications, Part I. *World Journal of Orthodontics*, 4(4).
- Ricketts, R. M., Roth, R., Chaconas, S., Schulhof, R., & Engel, G. (1982). Rocky Mountain Data Systems. *Orthodontic diagnosis and planning: their roles in preventive and rehabilitative dentistry. Rocky Mountain/Orthodontics, Denver*, 1-267.
- Romanyk, D. L., Collins, C. R., Lagravere, M. O., Toogood, R. W., Major, P. W., & Carey, J. P. (2013). Role of the midpalatal suture in FEA simulations of maxillary expansion treatment for adolescents: a review. *International Orthodontics*, 11(2), 119-138.
- Sangsari, A. H., Sadr-Eshkevari, P., Al-Dam, A., Friedrich, R. E., Freymiller, E., & Rashad, A. (2016). Surgically assisted rapid palatomaxillary expansion with or without pterygomaxillary disjunction: a systematic review and meta-analysis. *Journal of oral and maxillofacial surgery*, 74(2), 338-348.
- Sankar, S. G., Prashanth, B., Rajasekhar, G., Prasad, M., Reddy, G. V., & Priyanka, J. Y. (2021). A comparison of different osteotomy techniques with and without pterygomaxillary disjunction in surgically assisted maxillary expansion utilizing modified hybrid rapid maxillary expansion device with posterior implants: A finite element study. *National Journal of Maxillofacial Surgery*, 12(2), 171.
- Sant'Ana, L., Pinzan-Vercelino, C., Gurgel, J., & Carvalho, P. S. P. d. (2016). Evaluation of surgically assisted rapid maxillary expansion with and without midpalatal split. *International journal of oral and maxillofacial surgery*, 45(8), 997-1001.
- Sawchuk, D., Currie, K., Vich, M. L., Palomo, J. M., & Flores-Mir, C. (2016). Diagnostic methods for assessing maxillary skeletal and dental transverse deficiencies: A systematic review. *The Korean Journal of Orthodontics*, 46(5), 331-342.
- Shi, Y., Zhu, C.-n., & Xie, Z. (2020). Displacement and stress distribution of the maxilla under different surgical conditions in three typical models with bone-borne distraction: a three-dimensional finite element analysis. *Journal of Orofacial Orthopedics/Fortschritte der Kieferorthopädie*, 81(6).
- Shin, H., Hwang, C.-J., Lee, K.-J., Choi, Y. J., Han, S.-S., & Yu, H. S. (2019). Predictors of midpalatal suture expansion by miniscrew-assisted rapid palatal expansion in young adults: A preliminary study. *The Korean Journal of Orthodontics*, 49(6), 360-371.

- Sinelnikov, R., Sinelnikov, A., & Sinelnikov, Y. (1996). Atlas of human anatomy. In 4 volumes. *Medicine*, 82-85.
- Singaraju, G. S., Chembeti, D., Mandava, P., Reddy, V. K., Shetty, S. K., & George, S. A. (2015). A comparative study of three types of rapid maxillary expansion devices in surgically assisted maxillary expansion: A finite element study. *Journal of International Oral Health: JIOH*, 7(9), 40.
- Singh, J. R., Kambalyal, P., Jain, M., & Khandelwal, P. (2016). Revolution in Orthodontics: Finite element analysis. *Journal of International Society of Preventive & Community Dentistry*, 6(2), 110.
- Siqueira, D. F., Cardoso, M. d. A., Capelozza Filho, L., Goldenberg, D. C., & Fernandes, M. d. S. (2015). Periodontal and dental effects of surgically assisted rapid maxillary expansion, assessed by using digital study models. *Dental press journal of orthodontics*, 20, 58-63.
- Sousa, R. V. d., Ribeiro, G. L. A., Firmino, R. T., Martins, C. C., Granville-Garcia, A. F., & Paiva, S. M. (2014). Prevalence and associated factors for the development of anterior open bite and posterior crossbite in the primary dentition. *Brazilian dental journal*, 25, 336-342.
- Suri, L., & Taneja, P. (2008). Surgically assisted rapid palatal expansion: a literature review. *American journal of orthodontics and dentofacial orthopedics*, 133(2), 290-302.
- Suzuki, S. S., Braga, L. F. S., Fujii, D. N., Moon, W., & Suzuki, H. (2018). Corticopuncture facilitated microimplant-assisted rapid palatal expansion. *Case reports in dentistry*, 2018.
- Sygouros, A., Motro, M., Ugurlu, F., & Acar, A. (2014). Surgically assisted rapid maxillary expansion: cone-beam computed tomography evaluation of different surgical techniques and their effects on the maxillary dentoskeletal complex. *American journal of orthodontics and dentofacial orthopedics*, 146(6), 748-757.
- Tehranchi, A., Ameli, N., Najirad, Z., & Mirhashemi, F. S. (2013). Comparison of the skeletal and dental changes of tooth-borne vs. bone-borne expansion devices in surgically assisted rapid palatal expansion: A finite element study. *Dental research journal*, 10(6), 777.
- Thakkar, S. (2021). A comprehensive Review of Rapid Palatal Expansion and MiniScrew Assisted Rapid Palatal Expansion. *Journal of Dental and Medical Sciences*, 20(4), 34-38.
- Torres, D., Lopes, J., Magno, M. B., Cople Maia, L., Normando, D., & Leão, P. B. (2020). Effects of rapid maxillary expansion on temporomandibular joints: A systematic review. *The Angle Orthodontist*, 90(3), 442-456.
- Trojan, L. C., González-Torres, L. A., Melo, A. C. M., & de Las Casas, E. B. (2017). Stresses and strains analysis using different palatal expander appliances in upper jaw and midpalatal suture. *Artificial Organs*, 6(41), E41-E51.
- Vanarsdall Jr, R. L. (1999). *Transverse dimension and long-term stability*. Paper presented at the Seminars in orthodontics.
- Vanarsdall Jr, R. L., & Blasi Jr, I. (2017). APPLYING NEW KNOWLEDGE TO THE CORRECTION OF THE TRANSVERSE DIMENSION. *Anecdote, Expertise and Evidence: Applying New Knowledge to Everyday Orthodontics*, 53, 167.
- Verstraaten, J., Kuijpers-Jagtman, A. M., Mommaerts, M. Y., Bergé, S. J., Nada, R. M., & Schols, J. G. (2010). A systematic review of the effects of bone-borne surgical

- assisted rapid maxillary expansion. *Journal of Cranio-Maxillofacial Surgery*, 38(3), 166-174.
- Vidalón, J. A., Louí-Gómez, I., Quiñe, A., Diaz, K. T., Liñan Duran, C., & Lagravère, M. O. (2021). Periodontal effects of maxillary expansion in adults using non-surgical expanders with skeletal anchorage vs. surgically assisted maxillary expansion: a systematic review. *Head & face medicine*, 17(1), 1-12.
- Wagner, D. M., & Chung, C.-H. (2005). Transverse growth of the maxilla and mandible in untreated girls with low, average, and high MP-SN angles: a longitudinal study. *American journal of orthodontics and dentofacial orthopedics*, 128(6), 716-723.
- Weissheimer, A., de Menezes, L. M., Mezomo, M., Dias, D. M., de Lima, E. M. S., & Rizzato, S. M. D. (2011). Immediate effects of rapid maxillary expansion with Haas-type and hyrax-type expanders: a randomized clinical trial. *American journal of orthodontics and dentofacial orthopedics*, 140(3), 366-376.
- Zandi, M., Miresmaeili, A., Heidari, A., & Lamei, A. (2016). The necessity of pterygomaxillary disjunction in surgically assisted rapid maxillary expansion: a short-term, double-blind, historical controlled clinical trial. *Journal of Cranio-Maxillofacial Surgery*, 44(9), 1181-1186.
- Zawiślak, E., Gerber, H., Nowak, R., & Kubiak, M. (2020). Dental and skeletal changes after transpalatal distraction. *BioMed Research International*, 2020.
- Zeno, K. G. (2017). *Orthodontic traction of palatally impacted canines: a finite element analysis study*.
- Zong, C., Tang, B., Hua, F., He, H., & Ngan, P. (2019). *Skeletal and dentoalveolar changes in the transverse dimension using microimplant-assisted rapid palatal expansion (MARPE) appliances*. Paper presented at the Seminars in Orthodontics.